THE UNIVERSITY OF QUEENSLAND

AUSTRALIA

MOFs-based Mixed Matrix Membranes for Gas Separation

Rijia Lin

Bachelor of Engineering, Master of Science

A thesis submitted for the degree of Doctor of Philosophy at

The University of Queensland in 2016

School of Chemical Engineering

Abstract

Energy-efficient separation of gases has attracted intensive attentions both in research and in industry. The separation of gases by membranes is more effective and energy saving with lower production and equipment cost than some traditional gas separation methods, such as adsorption or distillation. However, most of the polymeric membranes suffer from the trade-off between mass transport rates and separation efficiency. Polymeric membranes show high gas permeation flux but low selectivity, and vice versa. To overcome such weakness, mixed matrix membranes (MMMs) can provide promising potentials in high performance gas separation, by combining high separation properties of the inorganic filler with low cost and flexible of the polymers. For filler selection, metal-organic frameworks (MOFs) are promising adsorbents for gas storage and separation due to their high surface area and porosity, adjustable pore sizes and controllable surface functionality.

This thesis is focused on developing novel MOFs-based MMMs for gas separation with high permeability and selectivity, as well as good thermal and chemical stability. The studies include fabrication and optimization of MOFs-based MMMs, designing MMMs with good filler/polymer interaction and good interfacial morphology, as well as evaluating the permeation and selectivity performance of all the prepared membranes. It aims to establish the guidance for the MOF/polymer pair selection and interface manipulation in the fabrication of MMMs to greatly increase the membrane permeability and selectivity.

In the first part of the experimental chapters, novel MMM with dispersed MOF into polyimide matrix were fabricated and the derived membranes are employed for gas separation. MMMs were synthesized from 2,2-bis(3,4-anhydrodicarboxyphenyl) hexafluoropropane (6FDA) and 4,4(-diaminodiphenyl ether (oxydianiline, ODA) into which were incorporated Cd-6F MOF filler. Cd-6F was synthesized by using 4,4′-(hexafluoroisopropylidene)diphthalic anhydride (6FDA) as the organic linker which is also one of the monomers in the 6FDA-ODA synthesis. A specific interfacial interaction between MOF crystals and polymer chains was innovatively targeted with this specific MOF/polymer pair by controlling the in-situ 6FDA-ODA polymerization procedure with the existence of MOF particles. The enhanced adhesion between filler particles and polymer phase was achieved and the improved interfacial interaction between MOF and polymeric matrix was confirmed by FTIR, NMR and XPS. Moreover, it was found that the MOF/polymer interfacial morphology strongly affects the gas permeability and selectivity of the membrane. The MMM prepared by in-situ polymerization displays excellent interfaces between micron-sized Cd-6F crystals and polymer matrix as well as increased permeability and selectivity compared to pure 6FDA-ODA polymeric membrane. The interaction between MOF crystals and polymeric matrix can be controlled for the interfacial voids elimination and optimal membrane transport properties.

The second part of the experimental chapters focuses on MMMs with MOF/CNT composite. Novel MMM filler CNT-MIL was synthesized by in-situ growth of NH_2-MIL-101(Al) on the external surface of carbon nanotubes (CNT) and applied to fabricate MMMs for CO_2/CH_4 separation. Extra amino groups and active sites were introduced to the surface of CNT. Compared to pure polymeric membrane, MMMs containing synthesized MOF/CNT composite displayed significantly increased CO_2 permeance (up to 150%) and selectivity (up to 37.5%). The separation performance of derived MMMs clearly transcends the 1991 upper bound and being on the 2008 upper bound for polymeric membrane performance. MMMs for efficient C_3H_6/C_3H_8 separation were fabricated by embedding ZIF-8/CNT composite into 6FDA-durene polymer matrix. The volume of filler and voids in the polymeric matrix as well as the distribution of the fillers and their contact with the polymeric matrix were quantitatively evaluated by using the tomographic focused ion beam scanning electron microscopy (FIB-SEM). The dispersion of ZIF-8 in 6FDA-durene polymer was enhanced by growth of ZIF-8 on the CNT surfaces. Meanwhile, good adhesion between the synthesized MOF/CNT fillers and polymer matrix was observed, only 0.086% voids volume fraction is determined, even at a high filler loading. The improved ZIF-8 dispersion and filler/polymer interface lead to the efficient C_3H_6 separation in MMMs. MMMs containing synthesized MOF/CNT composite displayed significantly increased C_3H_6 permeability (up to 105%) and selectivity (up to 96%) compare to pure 6FDA-durene membrane.

The third part of the experimental chapters focuses on elimination of interfacial voids by incorporating ionic liquid (IL) as the MOFs/polymer interfacial binder into MMM. Thin layer of IL has been fabricated on CuBTC fillers for MMMs fabrication. With the aid of ionic liquid, the interfacial voids of the CuBTC-IL MMM was significantly reduced due to the favourable MOF/IL and IL/polymer adhesion, thus improving CO_2 selectivity compare to pure polymer membrane and MMMs with untreated CuBTC. The performance of 10% CuBTC-IL/6FDA-durene MMM clearly transcends the 2008 upper bound for polymer membrane. The strategy of IL decoration method can provide an effective way to eliminate interfacial voids and enhance CO_2 selectivity and can be applied in large sized fillers with better gas separation properties.

Declaration by author

This thesis is composed of my original work, and contains no material previously published or written by another person except where due reference has been made in the text. I have clearly stated the contribution by others to jointly-authored works that I have included in my thesis.

I have clearly stated the contribution of others to my thesis as a whole, including statistical assistance, survey design, data analysis, significant technical procedures, professional editorial advice, and any other original research work used or reported in my thesis. The content of my thesis is the result of work I have carried out since the commencement of my research higher degree candidature and does not include a substantial part of work that has been submitted to qualify for the award of any other degree or diploma in any university or other tertiary institution. I have clearly stated which parts of my thesis, if any, have been submitted to qualify for another award.

I acknowledge that an electronic copy of my thesis must be lodged with the University Library and, subject to the policy and procedures of The University of Queensland, the thesis be made available for research and study in accordance with the Copyright Act 1968 unless a period of embargo has been approved by the Dean of the Graduate School.

I acknowledge that copyright of all material contained in my thesis resides with the copyright holder(s) of that material. Where appropriate I have obtained copyright permission from the copyright holder to reproduce material in this thesis.

Publications during candidature

Peer-reviewed journal papers

Rijia Lin, Lei Ge, Lei Hou, Ekaterina Strounina, Victor Rudolph, Zhonghua Zhu, Mixed Matrix Membranes with Strengthened MOFs/Polymer Interfacial Interaction and Improved Membrane Performance. ACS Applied Materials & Interfaces, 2014, 6, 5609-5618.

Rijia Lin, Lei Ge, Shaomin Liu, Victor Rudolph, Zhonghua Zhu, Mixed-Matrix Membranes with Metal-Organic Framework-Decorated CNT Fillers for Efficient CO_2 Separation. ACS Applied Materials & Interfaces, 2015, 7, 14750-14757.

Rijia Lin, Lei Ge, Hui Diao, Victor Rudolph, Zhonghua Zhu, Propylene/Propane Selective Mixed Matrix Membranes with Grape-Branched MOFs/CNTs Filler. Journal of Materials Chemistry A, 2016, DOI: 10.1039/c5ta10553f.

Ying Yang, **Rijia Lin**, Lei Ge, Lei Hou, Paul Bernhardt, Thomas E. Rufford, Shaobin Wang, Victor Rudolph, Yaoyu Wang, Zhonghua Zhu, Synthesis and Characterization of Three Amino-Functionalized Metal-Organic Frameworks based on the 2-Aminoterephthalic Ligand. Dalton Transactions, 2015, 44, 8190-8197.

Conference abstracts

Rijia Lin, Lei Ge, Zhonghua Zhu, Mixed Matrix Membranes with Strengthened MOFs/Polymer Interfacial Interaction and Improved Membrane Performance. 13th International Conference on Inorganic Membranes, Brisbane, Australia, July 2014 (Oral presentation)

Rijia Lin, Lei Ge, Zhonghua Zhu, High Performance Mixed Matrix Membranes with Metal–Organic Frameworks Decorated CNTs Fillers for CO_2 Separation. International Mesostructured Materials Symposium 9, Brisbane, Australia, August 2015 (Poster presentation)

Publications included in this thesis

Rijia Lin, Lei Ge, Lei Hou, Ekaterina Strounina, Victor Rudolph, Zhonghua Zhu, Mixed Matrix Membranes with Strengthened MOFs/Polymer Interfacial Interaction and Improved Membrane Performance. ACS Applied Materials & Interfaces, 2014, 6, 5609-5618. – incorporated as Chapter 4

Contributor	Statement of contribution
Author Rijia LIN (Candidate)	Concept and designed (65%) Conducted experiment (95%) Analyzed and interpreted data (85%) Wrote and edited the paper (70%)
Author Lei Ge	Concept and designed (15%) Analyzed and interpreted data (10%) Wrote and edited paper (15%)
Author Lei Hou	Conducted experiment (5%)
Author Ekaterina Strounina	Analyzed and interpreted data (5%)
Author Victor Rudolph	Concept and designed (10%) Wrote and edited the paper (5%)
Author Zhonghua Zhu	Concept and designed (15%) Wrote and edited the paper (10%)

Rijia Lin, Lei Ge, Shaomin Liu, Victor Rudolph, Zhonghua Zhu, Mixed-Matrix Membranes with Metal-Organic Framework-Decorated CNT Fillers for Efficient CO_2 Separation. ACS Applied Materials & Interfaces, 2015, 7, 14750-14757. – incorporated as Chapter 5

Contributor	Statement of contribution
Author Rijia LIN (Candidate)	Concept and designed (60%) Conducted experiment (100%) Analyzed and interpreted data (90%) Wrote and edited the paper (60%)
Author Lei Ge	Concept and designed (15%) Analyzed and interpreted data (10%) Wrote and edited paper (15%)
Author Shaomin Liu	Wrote and edited the paper (10%)
Author Victor Rudolph	Concept and designed (10%) Wrote and edited the paper (5%)

Author Zhonghua Zhu	Concept and designed (15%) Wrote and edited the paper (10%)

Rijia Lin, Lei Ge, Hui Diao, Victor Rudolph, Zhonghua Zhu, Propylene/Propane Selective Mixed Matrix Membranes with Grape-Branched MOFs/CNTs Filler. Journal of Materials Chemistry A, 2016. DOI: 10.1039/c5ta10553f. – incorporated as Chapter 6

Contributor	Statement of contribution
Author Rijia LIN (Candidate)	Concept and designed (60%) Conducted experiment (100%) Analyzed and interpreted data (85%) Wrote and edited the paper (70%)
Author Lei Ge	Concept and designed (15 %) Analyzed and interpreted data (10%) Wrote and edited the paper (15%)
Author Hui Diao	Analyzed and interpreted data (5%)
Author Victor Rudolph	Concept and designed (10 %) Wrote and edited the paper (5%)
Author Zhonghua Zhu	Concept and designed (15 %) Wrote and edited the paper (10%)

Contributions by others to the thesis

Contributions by Prof. Zhonghua Zhu, Prof. Victor Rudolph and Dr Lei Ge in concept proposal, experiment design, research data analysis as well as interpretation, drafting, and writing in the advisory capacity.

Statement of parts of the thesis submitted to qualify for the award of another degree

None

Acknowledgements

I would like to express my sincerest gratitude to my supervisors, Prof. John Zhu, Prof. Victor Rudolph and Dr. Lei Ge for their valuable guidance, support and encouragement throughout my PhD study. I feel I can turn to them for help and suggestions in both research and life. It would not be possible for me to finish this thesis without their guidance and support.

I would also like to express my regards and blessings to all of those who supported me in any respect as follows:

Mengran Li, Prof. Lei Hou, Dr. Xiaoyong Xu, Dr. Wei Zhou, Dr. Fengli Liang, Dr. Li Wang, Dr Ying Yang, Dr. Taiwo Odedairo, Arash Arami Niya and Shuai Gao from John's Group for their useful discussion on the project and friendship.

The Centre for Microscopy and Microanalysis staff provided the training and support of using the equipment and in particular I would like to thank Anya Yago, Ying Yu and Hui Diao. Thanks to Siu Bit Iball, Anne Tan and Vicki Thompson for their administrative support.

The financial support from Australian Research Council (ARC) Discovery Project, CSC (China Scholarship Council) Scholarship and Top-Up Assistance Plan (TUAP) scholarship support from UQ are all greatly appreciated.

Many thanks to all my friends in Australia for helping me enjoy living here. Most of all I would like to thank my Dad, my Mom and my girlfriend for their long time encourage, support and love. Any step toward my dream cannot be made without you.

Keywords

mixed matrix membrane, metal-organic frameworks, gas separation, separation efficiency, eliminate interfacial voids

Australian and New Zealand Standard Research Classifications (ANZSRC)

ANZSRC code: 090404, Membrane and Separation Technologies, 60%
ANZSRC code: 091202, Composite and Hybrid Materials, 30%
ANZSRC code: 091205, Functional Materials, 10%

Fields of Research (FoR) Classification

FoR code: 0904 Chemical Engineering, 65%
FoR code: 0912 Material Engineering, 35%

Table of Contents

List of Figures

List of Tables

List of abbreviations

MOF – Metal organic frameworks

BET – Brunauer, Emmett, and Teller theory of gas adsorption

BTC-1,3,5-benzenetricarboxylate

CNTs – Carbon nanotubes

DMF – N,N-dimethylformamide

DMAc – Dimethylacetamide

Durene – 2,3,5,6-Tetramethyl-1,3-phenyldiamine

EDX – Energy-Dispersive X-ray spectroscopy

FTIR – Fourier Transform Infrared Spectroscopy

FIB-SEM – Focused ion beam scanning electron microscopy

6FDA – 4,4'-(hexafluoroisopropylidene) diphthalic anhydride

MMMs – Mixed-matrix membranes

NMP – N-methyl-2-pyrrolidone

TEM – Transmission Electron Microscopy

TGA – ThermoGravimetric Analysis

SEM – Scanning Electron Microscopy

XPS – X-ray Photoelectron Specstroscopy

XRD – X-Ray Diffraction

ZIF – Zeolite imidazolate frameworks

ODA – oxydianiline

Chapter 1 Introduction

1.1 Backgrounds

Membrane separation has emerged as a promising process for various industrial applications, especially in gas separation industries for air separation, hydrogen recovery and CO_2 removal.[1] Table 1-1 shows the major industrial applications of gas separation membrane. Compared to traditional separation methods, such as adsorption or distillation, membrane separation has some advantages, such as high energy efficient, low production and equipment cost, ease of operation and limited environmental impact.[2-4] Therefore, the development of high performance membranes for industrial use with lower cost has attracted increasing attentions from both research and industry.

Nowadays the separation of gases by polymeric membranes is becoming a commercially utilized unit operation. Ease of fabrication and low cost are the advantages of polymeric membranes that make them widely preferable in gas-separation processes.[5] However, It was recognized that most of the existing polymeric membranes suffer from the limit of trade-off between permeability and selectivity, as more permeable polymers are generally less selective and vice versa, which results in a Robeson upper bound.[6, 7] The upper bound relationship by Robeson for O_2/N_2 membrane separation for polymeric membranes is shown in Figure 1-1. In order to enhance the gas separation performance of polymeric membranes, one effective method is to introduce inorganic fillers such as zeolites,[8, 9] carbon nanotubes,[10, 11] carbon molecular sieves,[1, 12] mesoporous silica[13] and metal-organic frameworks (MOFs)[14-17] into the polymeric matrix to fabricate mixed matrix membranes (MMMs). As a result, MMMs can combine the advantages of both inorganic particles and polymer membranes, such as high separation properties of the filler particles, good process ability and mechanical properties of the polymer.

Metal–organic frameworks (MOFs), as the new inorganic-organic hybrid materials, consist of metals connected by organic linkages to create 1D, 2D and 3D microporous structures. They have been receiving widely research attentions due to their remarkable properties, such as high surface area, controllable porosity and high adsorption affinity.[18, 19] Therefore, it can provide promising opportunities of developing novel MOFs based MMMs with superior permeability and selectivity. MOF based MMMs have shown promising separation performances with the combination of molecular sieving effect of MOFs and common feature of polymers matrix, which can be an alternative approach to solve the trade-off problem of traditional polymer membranes. Moreover, the employment of MOFs in MMMs provides several potential advantages over other inorganic fillers. For instance, MOFs perform better compatibility with the polymer matrix since the organic linkers in

MOFs have stronger interaction with polymer chains.[20]

Table 1-1 Main industrial applications of membrane gas separation [21]

Separation	Process
H_2/N_2	ammonia purge gas
H_2/CO	syngas ratio adjustment
H_2/hydrocarbons	hydrogen recovery in refineries
O_2/N_2	nitrogen generation, oxygen-enriched, air production
CO_2/hydrocarbons (CH_4)	natural gas sweetening, landfill gas upgrading
H_2O/hydrocarbons (CH_4)	natural gas dehydration
H_2S/hydrocarbons	sour gas treating
He/hydrocarbons	helium separation
He/N_2	helium recovery
hydrocarbons/air	hydrocarbons recovery, pollution control
H_2O/air	air dehumidification
volatile organic species (e.g., ethylene or propylene) / light gases (e.g., nitrogen)	polyolefin purge gas purification

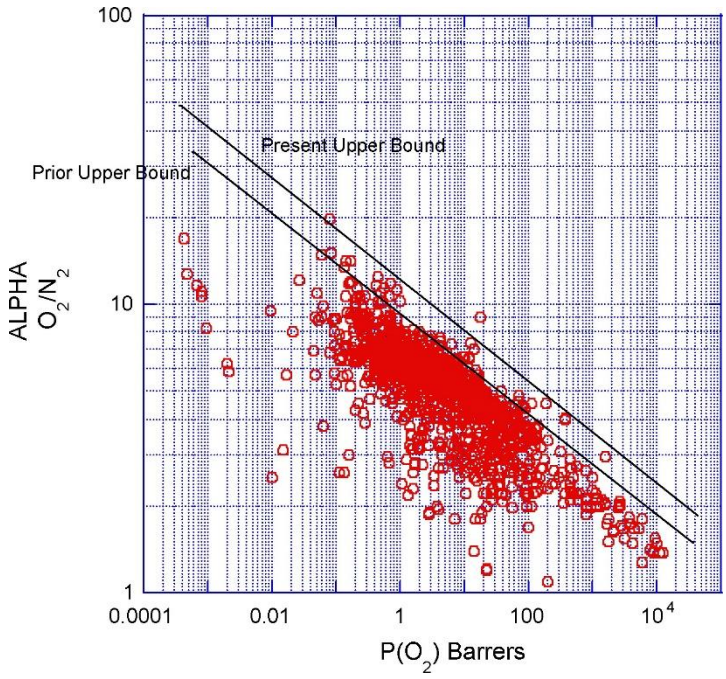

Figure 1-1 Upper bound correlation for O_2/N_2 separation [7]

1.2 Scope and research contributions

Prompted by the above descriptions, this project aims to synthesize MOFs-based MMMs with novel structure and high gas separation performance. The specific objectives are:

- To fabricate novel MOFs-based MMMs, optimize the synthesis routine to improve the gas separation performance and investigate effect of different MOFs/polymer pair on desired gas separation.
- To develop a guidance methodology for MOFs/polymer materials selection in MMMs fabrication.
- To develop a strategy to optimize MMMs interface through designing interaction between MOFs and polymer.
- To investigate the mechanism for the formation of optimal MMMs interface and MOF/polymer interaction.
- To develop systematic strategies to improve membrane performance of MOFs-based MMMs

Gas separation and purification are important but energy-consuming unit operation in industrial applications. At present, most of the existing polymeric membranes suffer from the limit of trade-off between permeability and selectivity. MOFs-based mixed matrix membranes, as new hybrid materials, combine the advantages of MOFs and polymer membranes, such as high adsorption selectivity of the

MOFs, good process ability and mechanical properties of the polymer. Even though numerous MOFs-based MMMs have been reported about gas separation in the past several years, there still exist some challenges in membrane performance optimisation and mechanism development. In this work, appropriate filler and polymer pair will be chosen for the MMMs fabrication. The ralationship between MMMs fabrication and selectivity will be investigated for improving the gas separation performance. As a whole, new membrane materials and gas separation concepts based on MOFs will be explored in the project. The knowledge collected throughout the project will enhance our technological ability and capability of the design and configuration of gas separation membranes.

1.3 Structure of thesis

Chapter 1 Introduction

This chapter introduces the background of the thesis and outlines the scope and key contributions to the field of research.

Chapter 2 Literature review

This chapter presents an overview of membrane separation area, metal-organic frameworks and metal-organic frameworks based mixed matrix membrane.

Chapter 3 Mixed matrix membranes with strengthened MOFs/polymer interfacial interaction and improved membrane performance

This chapter presents the fabrication and characterization of mixed matrix membranes with Cd-6F crystal MOF and 6FDA-ODA polymer. A specific interfacial interaction between MOF crystals and polymer chains was designed with this specific MOF/polymer pair by controlling synthesis procedures and conditions in the mixed matrix membranes fabrication. The adhesion between filler particles and polymer phase was improved. FTIR, NMR and XPS were used to confirm the interfacial interaction between MOF and polymeric matrix. The gas permeability and selectivity of the mixed matrix membranes depend on the morphology of the membranes. Mixed matrix membrane with excellent interface between micrometer-sized MOF crystals and polymeric matrix demonstrates both increased permeability and selectivity. This chapter is published in the ACS Applied Materials & Interfaces 2014, 6, 5609–5618.

Chapter 4 Mixed matrix membranes with metal-organic framework-decorated CNT fillers for efficient CO_2 separation

In this chapter, a novel MMM filler derived from in-situ growth of metal–organic frameworks (MOFs) on the surface of the CNTs was synthesized and applied to improve the separation performance. Through MOF decoration, sufficient amino groups and active sites were introduced to external surface of CNTs. The good adhesion between the synthesized CNT-MIL fillers and polymer phase was observed. Mixed matrix membranes containing synthesized MOF/CNT composite displayed significantly improved CO_2 permeance and selectivity compared to pure polymeric membrane and unmodified CNT MMMs. The separation performance of derived MMMs clearly transcends the 1991 upper bound and being on the 2008 upper bound for polymeric membrane performance. This chapter is published in the ACS Applied Materials & Interfaces 2015, 67, 14750–14757.

Chapter 5 Propylene/propane selective mixed matrix membranes with grape-branched MOFs/CNTs filler

In this chapter, a novel carbon nanotube/metal–organic frameworks (MOFs) filler was applied to fabricate mixed matrix membranes (MMMs) for efficient propylene/propane separation. Compared to pure polymeric membrane, mixed matrix membranes containing synthesized MOF/CNT composite displayed significantly enhanced C_3H_6 permeance and selectivity. Tomographic focused ion beam scanning electron microscopy was applied to quantitatively evaluate the filler dispersion and filler/polymer interfacial voids ratio, 3D surface-rendered image of MMM was provide by the segmentation of the individual phases (e.g. polymer, filler and voids). By confining growth of MOF on the carbon nanotube external surface, improved dispersion of MOF in polymeric matrix has been realized. Good adhesion between the synthesized MOF/CNT fillers and the polymer matrix was achieved even at a high filler loading. This chapter is published in the Journal of Chemistry Materials A, DOI: 10.1039/C5TA10553F.

Chapter 6 Ionic liquids as the MOFs/polymer interfacial binder for efficient membrane separation

In this chapter, ionic liquid (IL) functionalized CuBTC has been synthesized by decoration of a thin IL [Emim][Tf_2N] layer on CuBTC and was used to fabricate MMMs with 6FDA-durene polyimide. The ionic liquid behaves like a binding material and eliminates the non-selective defects between MOF/polymer due to the favourable MOF/IL and IL/polymer interaction. With introduction of IL, the interfacial voids in CuBTC MMM were significantly reduced with comparison to the MMM with untreated CuBTC, resulting in the significant increase in CO_2 selectivity. This chapter is in preparation for submitting to ACS Applied Materials & Interfaces.

Chapter 7 Conclusions and recommendations

This chapter presents the overall conclusions and recommendations for future work.

1.4 References

(1) Vu, D. Q., Koros, W. J., Miller, S. J., Mixed Matrix Membranes Using Carbon Molecular Sieves: I. Preparation and Experimental Results. Journal of Membrane Science, 2003, 211, 311-334.

(2) Koros, B., Three Hundred Volumes. Journal of Membrane Science, 2007, 300, 1-1.

(3) Alexander Stern, S., Polymers for Gas Separations: the Next Decade. Journal of Membrane Science, 1994, 94, 1-65.

(4) Nasir, R., Mukhtar, H., Man, Z., Mohshim, D. F., Material Advancements in Fabrication of Mixed-Matrix Membranes. Chemical Engineering & Technology, 2013, 36, 717-727.

(5) Erucar, I., Yilmaz, G., Keskin, S., Recent Advances in Metal-Organic Framework-based Mixed Matrix Membranes. Chemistry an Asian Journal, 2013, 8, 1692-1704.

(6) Robeson, L. M., Correlation of Separation Factor versus Permeability for Polymeric Membranes. Journal of Membrane Science, 1991, 62, 165-185.

(7) Robeson, L. M., The Upper Bound Revisited. Journal of Membrane Science, 2008, 320, 390-400.

(8) Bastani, D., Esmaeili, N., Asadollahi, M., Polymeric Mixed Matrix Membranes Containing Zeolites as a Filler for Gas Separation Applications: A Review. Journal Of Industrial And Engineering Chemistry, 2013, 19, 375-393.

(9) Pechar, T. W., Kim, S., Vaughan, B., Marand, E., Tsapatsis, M., Jeong, H. K., Cornelius, C. J., Fabrication and Characterization of Polyimide–Zeolite L Mixed Matrix Membranes for Gas Separations. Journal of Membrane Science, 2006, 277, 195-202.

(10) Ge, L., Zhu, Z., Rudolph, V., Enhanced Gas Permeability by Fabricating Functionalized Multi-Walled Carbon Nanotubes and Polyethersulfone Nanocomposite Membrane. Separation and Purification Technology, 2011, 78, 76-82.

(11) Ge, L., Zhu, Z., Li, F., Liu, S., Wang, L., Tang, X., Rudolph, V., Investigation of Gas Permeability in Carbon Nanotube (CNT)−Polymer Matrix Membranes via Modifying CNTs with Functional Groups/Metals and Controlling Modification Location. The Journal of Physical Chemistry C, 2011, 115, 6661-6670.

(12) Weng, T.-H., Tseng, H.-H., Wey, M.-Y., Fabrication and Characterization of Poly(phenylene oxide)/SBA-15/Carbon Molecule Sieve Multilayer Mixed Matrix Membrane for Gas Separation. International Journal Of Hydrogen Energy, 2010, 35, 6971-6983.

(13) Zornoza, B., Irusta, S., Téllez, C., Coronas, J. n., Mesoporous Silica Sphere−Polysulfone Mixed Matrix Membranes for Gas Separation. Langmuir, 2009, 25, 5903-5909.

(14) Yang, T., Xiao, Y., Chung, T.-S., Poly-/Metal-Benzimidazole Nano-Composite Membranes for Hydrogen Purification. Energy & Environmental Science, 2011, 4, 4171-4180.

(15) Adams, R., Carson, C., Ward, J., Tannenbaum, R., Koros, W., Metal Organic Framework Mixed Matrix Membranes for Gas Separations. Microporous and Mesoporous Materials, 2010, 131, 13-20.

(16) Sumida, K., Rogow, D. L., Mason, J. A., McDonald, T. M., Bloch, E. D., Herm, Z. R., Bae, T. H., Long, J. R., Carbon Dioxide Capture in Metal-Organic Frameworks. Chemical Reviews, 2012, 112, 724-781.

(17) Jeazet, H. B. T., Staudt, C., Janiak, C., A Method for Increasing Permeability in O_2/N_2 Separation with Mixed-Matrix Membranes Made of Water-Stable MIL-101 and Polysulfone. Chemical Communications, 2011, 48, 2140-2142.

(18) Ferey, G., Hybrid Porous Solids: Past, Present, Future. Chemical Society Reviews, 2008, 37, 191-214.

(19) Li, J.-R., Sculley, J., Zhou, H.-C., Metal–Organic Frameworks for Separations. Chemical Reviews, 2012, 112, 869-932.

(20) Perez, E. V., Balkus Jr, K. J., Ferraris, J. P., Musselman, I. H., Mixed-Matrix Membranes Containing MOF-5 for Gas Separations. Journal of Membrane Science, 2009, 328, 165-173.

(21) Bernardo, P., Drioli, E., Golemme, G., Membrane Gas Separation: A Review/State of the Art. Industrial & Engineering Chemistry Research, 2009, 48, 4638-4663.

Chapter 2 Literature Review

This chapter reviews the existing literatures of metal-organic frameworks based mixed matrix membranes for gas separation. It begins with an introduction to mixed matrix membranes (preparation, testing and modelling) in section 2.1. Then the trade-off effect of current membranes is outlined and the metal-organic frameworks are proposed to be promising membrane materials. The background of metal-organic frameworks will be overviewed in section 2.2. Several types of MOFs that are extensively investigated for MOF-based membranes will also be introduced in this section. Section 2.3 focuses on the review of MOFs-based mixed matrix membranes in gas application. Section 2.4 introduces three main factors that affect structure and performance of mixed matrix membranes. Section 2.5 introduces various techniques about MMM materials modification. Finally, the conclusion is given in section 2.6, some future trends on these MOFs-based mixed matrix membranes are proposed.

2.1 Mixed matrix membranes (MMMs)

Membrane separation has emerged as a promising process for various industrial applications, especially in gas separation and purification.[1, 2] Nonetheless, it was recognized that most of the existing polymeric membranes suffer from the limit of trade-off between permeability and selectivity, as more permeable polymers are generally less selective and vice versa, which results in a Robeson upper bound.[3, 4] To overcome this limitation, an alternative route is to introduce inorganic fillers into polymeric matrix to obtain mixed matrix membranes (MMMs). Schematic diagram of mixed matrix membrane is shown in Figure 2-1. As a result, mixed matrix membranes combine the advantages of both inorganic particles and polymer membranes, including high permeability and selectivity of filler particles, good process ability and mechanical properties of the polymer.[5, 6]

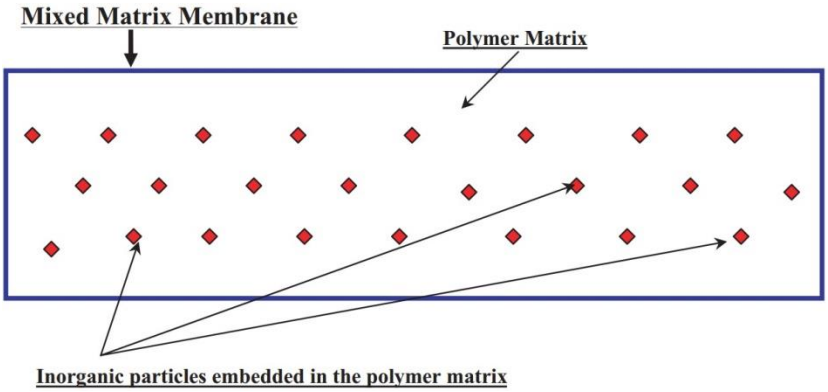

Figure 2-1 A schematic diagram of mixed matrix membrane with inorganic dispersed phase embedded in the polymeric matrix [7]

2.1.1 Preparation of mixed matrix membranes

Fabrication of MMMs is regarded as a potentially solution to the trade-off problem of the polymeric membranes.[6] The synthesis of MMMs is analogous to that of normal polymer membranes, which can be developed to fabricate MMMs in industrial scale by applying the current technology of polymer membranes preparation. There are three main methods to prepare MMMs: (1) disperse filler particles into solvent before adding polymer, (2) dissolve polymer into solvent before addition of the filler particles to the polymer solution, (3) dissolve polymer into solvent and disperse filler particles into solvent separately, then mix them.[7, 8] It is noted that the first and third methods are able to better disperse inorganic particles in the suspension. The second method is usually used for nanoparticles dispersion in the polymer matrix. Figure 2-2 shows the different methods for mixed matrix dope preparation.[7] After obtaining polymer solution with well-dispersed fillers, this mixture is cast on a flat surface and the solvent evaporates. The membranes are dried in a vacuum oven at a specific temperature (depending on the glass transition temperature of the polymer) to remove the remaining solvent.

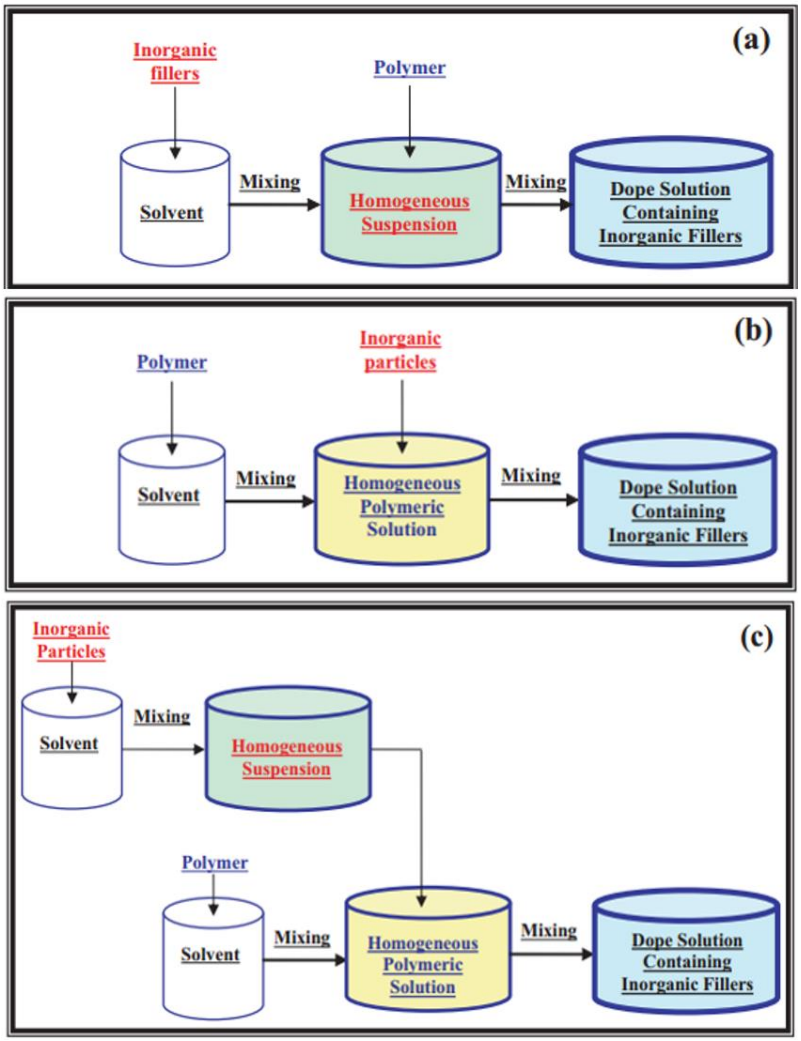

Figure 2-2 Different methods for mixed matrix dope preparation [7]

2.1.2 Testing of mixed matrix membranes

Permeability and separation factor are the two key parameters used in polymeric membranes characterization. Permeability is the rate at which penetrant permeate through the membrane. It equals the diffusive flux of penetrant A ($Flux_A$) through the membrane normalized by the change in partial pressure across the membrane, Δp_A (cmHg), per unit thickness of the membrane, l (cm):

$$P_A = \frac{Flux_A \cdot l}{\Delta pA} \quad (2\text{-}1)$$

Gas permeability values of polymer membraen are typically reported in Barrer units (1 Barrer = 1×10^{-10} cm^3 (STP) cm cm^{-2} s^{-1} cm Hg^{-1} = 3.348×10^{-16} mol m m^{-2} Pa^{-1} s^{-1}).

The ideal selectivity of a membrane for a gas pair A and B is the ratio of the permeability of gas A over the permeability of gas B:

$$\alpha = \frac{P_A}{P_B} \quad (2\text{-}2)$$

For permeation of gas mixture, the separation factor α_{ab} shows the ability of a membrane to separate binary gas mixture, and it is defined as:

$$\alpha_{a,b} = \frac{y_{a,permeate} / y_{b,permeate}}{y_{a,retentate} / y_{b,retentate}} \quad (2\text{-}3)$$

where $y_{a,permeate}$ and $y_{b,permeate}$ are the molar ratios of the components A and B in permeate, $y_{a,retentate}$ and $y_{b,\ retentate}$ are the molar ratio of components A and B in retentate.[9]

2.1.3 Models to describe transport in mixed matrix membranes

Gas separation in membranes can take place by different mechanisms.[10, 11] The gas separation in dense polymeric membranes is based on the diffusion-solution mechanism, which can be divided into three steps: absorption, diffusion and desorption (Figure 2-3). Therefore, the permeability coefficient also can be viewed as the product of a solubility coefficient and a diffusion coefficient. Gas diffusion in polymers is primarily based on the free volume of the polymer, pressure/concentration gradients. As gaps between polymer chains, called the free volumes, is much larger in amorphous polymers than crystalline polymers. The selectivity of a polymer membrane depends on the leap channels, segment motions can permit unrestricted passage of all gas particles resulting in low selectivity, whereas limited motions allow smaller species pass through much more frequently than larger species. In this chapter, most of the MOFs-based mixed matrix membranes mainly follow the diffusion-solution mechanism and the effect of MOFs will be discussed.

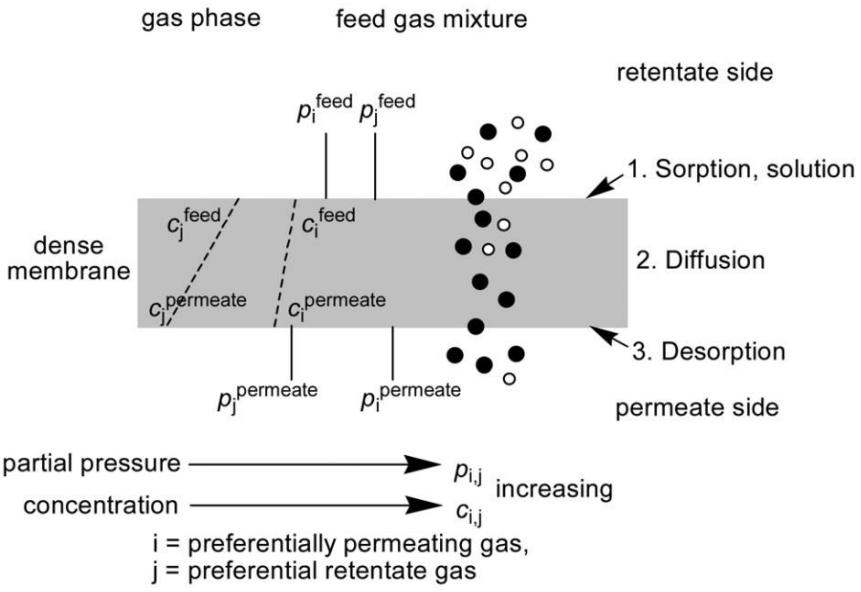

Figure 2-3 Gas separation mechanism in dense membranes by solution–diffusion [12]

2.1.4 Membrane materials

In mixed matrix membranes, the polymer is the continuous phase while the filler particle is the dispersed phase. The selections of both matrix and inorganic particles are crucial for the MMMs fabrication. Generally, polymers with higher selectivity result in mixed matrix membranes with better separation performance. Consequently, glassy polymers with high selectivity are preferred than rubbery polymers which have high permeability however low selectivity.[13-15] Table 2-1 shows CO_2 permeability and CO_2/CH_4 selectivity of some common-used polymeric membranes. Normally glassy polymers have rigid structures, adhesion between inorganic phase and polymeric matrix is still a problem in the mixed matrix membranes preparation, for voids forms due to poor interaction between fillers and polymer. Gas separation performance and interaction with inorganic filler are two factors that should be considered when choosing the polymer matrix.

Table 2-1 CO_2 permeability and CO_2/CH_4 selectivity of some polymeric membranes [16-18]

Polymer	P_{CO_2} (Barrer)	α_{CO_2/CH_4}
Polyethersulfone	2.8	28
Polysulfone	3.7	23
Cellulose acetate	6.0	29
Matrimid 5218	6.5	34
Polyimide (6FDA-ODA)	14.4	44.1
Polyimide (6FDA-DAF)	24.1	51
Polyimide (6FDA-6FpDA)	63.9	39.9
Poly(4-methyl-1-pentene)	63.5	5.7
PPO	90	16.7
Polyimide (6FDA-DAM)	370	21
Poly(tert-butylacetylene)	1020	8.5
Silicone rubber (PDMS)	4553	3.4

Table 2-2 outlines advantages and limitations of inorganic materials used in MMMs fabrications. The selection of inorganic fillers in mixed matrix membranes mainly bases on several factors, such as adsorption performance for the desired gas, particle size, surface chemistry and functional groups. A large number of studies have reported that incorporating inorganic particles such as zeolites,[19, 20] carbon nanotubes,[21, 22] carbon molecular sieves,[23, 24] silica[25] into polymers to fabricate mixed matrix membranes. It is an effective route to enhance the separation performance of polymeric membranes with the potential to meet the Robeson upper bound.

Table 2-2 Different filler particles and their properties[2]

Filler particles	Properties
Zeolite	High diffusivity and selectivity as compared to polymer material, but difficult to fabricate MMMs of void-free.
Carbon molecular sieve (CMS)	High adsorption performance for gas separation. Good adsorptivity for some particular gases. Narrow pore size.
Mesoporous silica	Different pore diameter, shape and particle size; pore size in the range of 2–50 nm. Excellent mechanical and thermal stability and good adhesion. The large pore size is the reason of better wetting and dispersion of particles. Common types of this molecular sieve: MCM-41, MCM-48, SBA-15. Limitations: the large pores may be blocked with polymer chains. Chemical modification of pores is necessary to achieve selective adsorption.
Nonporous silica	Addition of this filler can modify the molecular packing of polymer chains; permeability and selectivity can be improved.
Metal oxide	Nano size, high specific area; good particle distribution can be achieved, able to reduce voids formation
Carbon nanotubes (CNTs)	Super high flux of gas diffusion in CNT tunnels as well as enhanced tensile modulus and break stress. Able to meet the Robeson upper bound, but expensive. Uniform dispersion difficult.

2.1.4.1 Zeolite

Numerous studies have been reported about the use of zeolites in the fabrication of MMMs for their thermal stability and outstanding adsorption and permeation properties.[19, 26] Zeolite are aluminosilicate with opened 3D framework structures and uniform cavities and channels.[6] Embedding zeolites into polymer matrix have been indicated as an alternative method to enhance the permeability and selectivity of polymeric membranes.[20, 27-29] Introducing zeolites into glassy polymers shows higher mechanical stability and more desirable gas separation behaviours compared with rubbery polymers. However, the MMMs prepared by glassy polymers and zeolites are inclined to form voids between the zeolite and polymer. The interfacial voids, which is called ‘‘sieve-in-a-cage’’ morphology, appear because of the poor adhesion at the zeolite-polymer interface, as shown in Figure 2-4. This morphology results in a reduction of the selectivity and increase of permeability of the mixed matrix membranes. In order to solve the poor adhesion problem between zeolites and glassy polymers, a wide range of modification has been involved, such as coating of a diluted solution of a highly permeable silicone rubber, surface modification of zeolites and adding a plasticizer to increase the flexibility of the polymeric matrix.[30, 31]

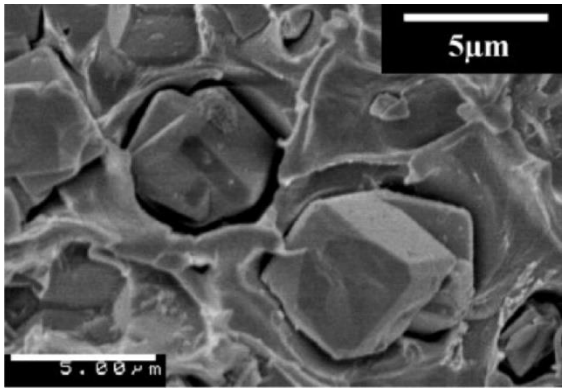

Figure 2-4 “Sieve-in-cage” SEM morphology exhibited by zeolite particles when incorporated in polymer matrix [32]

2.1.4.2 Silica

Silica is another class of filler materials in MMMs fabrication which received much attention. Silica can be further categorized into mesoporous silica and nonporous silica. These particles are usually incorporated into the polymeric matrix to form heterogeneous MMMs through a sol−gel reaction with hydrolyzation of the silica precursors, which helps to develop nanoscale particles and disperse nanoparticles into polymeric matrix.[33, 34] By adding of these fillers, the molecular packing of polymer chains can be modified, which resulting in enhanced permeability and selectivity. Ahn *et al*.[35]

introduced 20 % nonporous fumed silica nanoparticles into polysulfone. The addition of silica resulted in an increase in free volume for the insufficient polymer chain packing. The increase in free volume significantly enhanced the diffusion and solubility coefficients of MMM and improved the permeability of all test gases. However, the permeability of large gases was more enhanced by the addition of silica, resulted in a reduction in selectivity.

2.1.4.3 Carbon Molecular Sieve

Carbon molecular sieves (CMS) are carbonaceous porous solids that contain constricted apertures that approach the molecular dimensions of the diffusing gas molecules.[36] CMS has attracted attentions on its well-defined micropores and excellent permeation behaviors as potential filler in the synthesis of MMMs.[37, 38] Some of CMS show excellent affinity to glassy polymers, which can contribute to good interfacial adhesion. Several methods have been reported about improving both permeability and selectivity of CMS MMMs and prevent the formations of voids.[39] Vu *et al*.[23] introduced CMS into Matrimid and Ultem. It was found that the selectivities of CO_2/CH_4 and O_2/N_2 had significantly improved with 45% and 20%, respectively.

2.1.4.4 Metal Oxide

Metal oxide nanoparticles such as MgO and TiO_2 are also emerged as filler particles in the preparation of mixed matrix membranes. These nanoparticles with high specific surface area are able to improve the filler dispersion and prevent the non-selective voids formation at filler/polymer interface during the fabrication of mixed matrix membranes.[40-43] For instance, Matteucci *et al*.[42] investigated the influence of TiO_2 particle surface chemistry on the gas separation performance of the MMM. The dispersion of TiO_2 nanoparticles was depending on the amount of TiO_2 loading in the MMM. The MMMs were defect-free at low particle loading, while at high filler loading, it was found that some nanoparticles formed micron-sized aggregates and the defects presented. The gas separation performance was also found to be depended on the particle loadings: the selectivity increased with increasing particle loading.

2.1.4.5 Carbon Nanotubes

In recent years, carbon nanotubes (CNTs) have been recognized as novel filler materials in the fabrication of MMMs due to its desired physical and chemical properties. Carbon nanotubes with diameters in the nanometer range and atomically smooth surface, can offer a promising opportunity to make membranes with high flux and selectivity. As other inorganic fillers, there exist same problems to introduce CNTs into polymer matrix, such as the incompatibility of CNTs and polymer matrix and agglomeration of CNTs. For the CNTs MMMS, the voids caused by the agglomeration of

CNTs can weaken the separation performance. Therefore, improve the dispersion of CNTs in polymeric matrix is important. The most common method is to introduce functional groups (such as hydroxyl and carboxyl groups) to the CNT surface through surface modification by strong inorganic acids.[21, 22] For example, Weng *et al*.[44] prepared MWCNTs/PBNPI membrane with acid treated CNTs. The high loading of acid-treated CNTs (15%) in PBNPI polymer still shows high dispersion. As a result, both the permeabilities and the selectivities of H_2, CO_2 and CH_4 enhanced significantly at high MWCNTs loading (>5 wt.%).

2.1.5 Conclusions

The limitation expressed by the Robeson's upper bound is hard to be broke through with pure polymer membranes. Development of mixed matrix membrane by introducing inorganic fillers into polymer matrix is regarded as an effective approach to enhance the gas separation performance of the membrane. However, the inorganic materials reviewed above still have their limitations in MMMs fabrications. Materials with high surface area, adsorption properties, controllable cage dimension, modifiable external surface and special interaction with polymer matrix are more attractive. The development of novel fillers for high performance MMMs is still on the way.

2.2 Metal-organic Frameworks (MOFs)

2.2.1 MOFs structure, properties and utilizations

Metal–organic frameworks (MOFs), novel class of hybrid materials, consist of inorganic metal centre or cluster linked by organic linkers forming flexible frameworks and one-, two-, and three-dimensional porous structures.[8] They can be synthesized relatively easily, in high purity and crystallinity. MOFs have the several unique structural properties and advantages: high surface area and porosity,[45] adjustable pore sizes and fine tunable pore surface property,[46] rigid and flexible framework,[47] low densities (0.2–1 g/cm^3), reasonable thermal and chemical stability.[48] The surface area and porosity of MOFs are generally higher than those of zeolites, silica, and activated carbons.[49] The most important advantage of MOFs over traditional porous materials is that the pore structure and pore size can be tailored to specific applications through simply changing combination of metals and organic ligands. Due to these physical and chemical properties of MOFs, MOFs have shown great potential in wide range of applications, including gas adsorption and separation,[50, 51] gas storage,[52] catalysist,[53, 54] drug delivery,[55] chemical sensor,[56] and biological application.[57]

2.2.2 MOFs used in MMMs

Due to structural properties and advantages of MOFs, it provides opportunities to develop novel MOFs MMMs with outstanding gas separation performance. MOFs also perform better compatibility with the polymer matrix since the organic linkers in MOFs can provide stronger interaction with polymer chains. In the past decade, more than 20,000 structures of MOF have been reported and studied.[46] However, only a small number of MOF types were used for MOFs-based MMMs fabrication so far because of the requirements on stability, pore size, gas selectivity, solubility and diffusivity for membrane fillers. In this study, several MOFs which extensively used in MMMs fabrication will be introduced.

2.2.2.1 MOF-5

MOF-5 (or IRMOF-1) is one of the most well studied MOFs with impressive properties.[58, 59] Figure 2-5 shows the structure of MOF-5, where the red secondary building unit is composed of Zn_4O tetrahedra that are coordinated to terephthalate ion ligands. The resulting MOF-5 structure has pores 1.2 nm in diameter with 0.8 nm windows. Functionalized of the MOF-5 structure type can be prepared by using other linear dicarboxylate linkers. This family of materials are referred as isoreticular metal organic frameworks (IRMOFs), which have a wide range of different pore sizes and pore functionalities.[60]

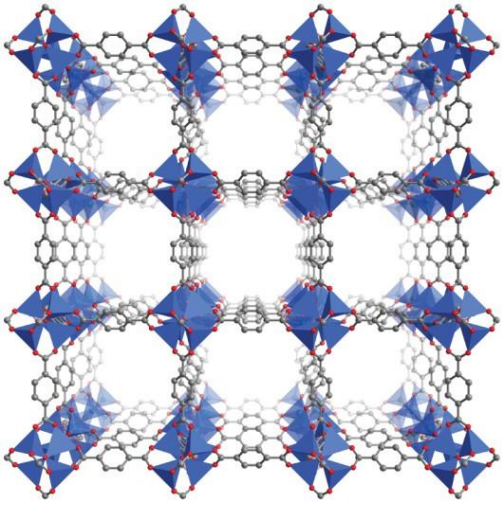

Figure 2-5 Crystal structure of $Zn_4O(BDC)_3$ (MOF-5) [50]

2.2.2.2 HKUST-1

HKUST-1 [$Cu_3(BTC)_2$, BTC =1,3,5-benzenetricarboxylate] is well-known to its excellent adsorption and separation properties for different gases. Figure 2-6 shows the crystal structure of HKUST-1. HKUST-1 has a unique cubic structure with multiple pore and adsorption sites for promoting adsorption. The crystal cell consists of large central cavities (diameter 9.0 Å) and surrounded small cavities (diameter 5.0 Å).[61] The as-synthesized HKUST-1 contains weakly bonded solvent molecule on the axial coordination sites of each Cu^{2+} ion, which can be removed by heated under vacuum and create open binding sites. The generation of these exposed metal ion sites can provide high selectivity to specific gas molecules, therefore, HKUST-1 presents promising performance in gas separation.[62]

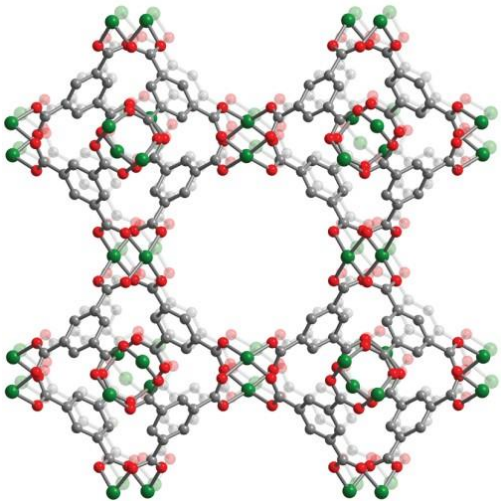

Figure 2-6 Crystal structure of HKUST-1 [63]

2.2.2.3 Zeolite Imidazolate Frameworks

Zeolite imidazolate frameworks (ZIFs) are a subclass of MOFs based on transition metals and imidazolate ligands. The crystal structure of ZIF-8 is shown in Figure 2-7. The structures of ZIFs are similar to zeolite topologies which has been proved to be higher thermally stable as well as more stable to moisture compared with other MOFs. This is cause by the full saturation of the metal and the use of imidazole ligands, which also result in the formation of small pores (e.g. ZIF-8 has pores of 3.4 Å in diameter).

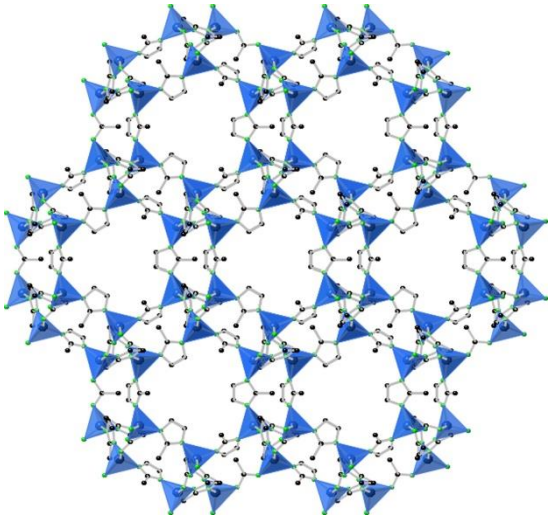

Figure 2-7 ZIF-8 structure looking down the [111] direction [64]

2.2.2.4 Flexible MOFs

Flexible MOFs is a special type that can change their framework reversibly when the specific molecules are introduced. A most common example of MOFs with breathing effect is the MIL-53 series. MIL-53 contains $MO_4(OH)_2$ octahedra (M = Al^{3+}, Cr^{3+}, Fe^{3+}, Ga^{3+}, In^{3+} or Sc^{3+}) and terephthalate ligands. MIL-53 has 1D diamond shaped pores with a diameter of 8.6 Å.[65, 66] It displays a flexible framework during the adsorption and desorption processes. The framework of MIL-53 change reversibly when specific molecules such as CO_2 or H_2O is introduced by contracting and opening the pores. For MIL-53(Al) or MIL-53(Cr), the pores in the frameworks contract when the adsorption is carried out, show the narrow pore form (np form), after removing the guest molecules, the pores open and transfer to the large pore form (lp form), as shown in Figure 2-8.

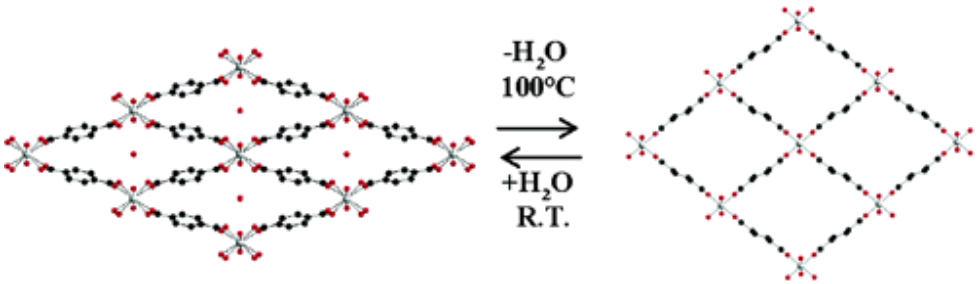

Figure 2-8 Hydration and dehydration process occurring in MIL-53 (Al, Cr). (Left) MIL-53 hydrated. (Right) MIL-53 dehydrated [67]

2.2.3 Conclusions

MOFs have attracted considerable attentions for their controllable porosity, high surface area and high adsorption affinity. Additionally, their pore size and chemical functionalities can be directly

manipulated during synthesis with different metal and ligands. The large number of MOFs is both an opportunity and challenge for using MOFs as the filler in the fabrication of MMMs. The large numbers of metal/organic linker pairs offer potentially in synthesizing large variety of structures with different adsorpability and selectivity for specific gases. It provides opportunities of developing novel MOF-based MMMs with outstanding permeability and selectivity. Meanwhile, the proper selection of MOFs among such large numbers of them will be very important for the preparation of MMMs with high gas separation performance.

2.3 MOFs-based MMMs in Gas Separation Application

Increasing number of studies has been reported about using MOFs as filler particles in MMMs fabrications to improve the gas separation performance over pure polymers. Experimental data of gas permeation with MOFs-based MMMs were summarized in Table 2-3. Compared with other inorganic porous materials, MOF-based MMMs show two signifacant advantages, (i) Better compatibility between MOF and polymer matrix can be achieved due to the stronger interaction between organic linkers of MOFs and corresponding polymer chains. (ii) Pore size and functionalities can be tailored by choosing particular association with metal and ligands. Figure 2-9 compares the CO_2/CH_4 separation performance of MOF-based MMMs with other MMMs using zeolite, mesoporous silica, alumina and CMS as filler particles.[8] MOF-based MMMs show outstanding gas separation performances over pure polymeric membranes, expected to exceed the upper bound.

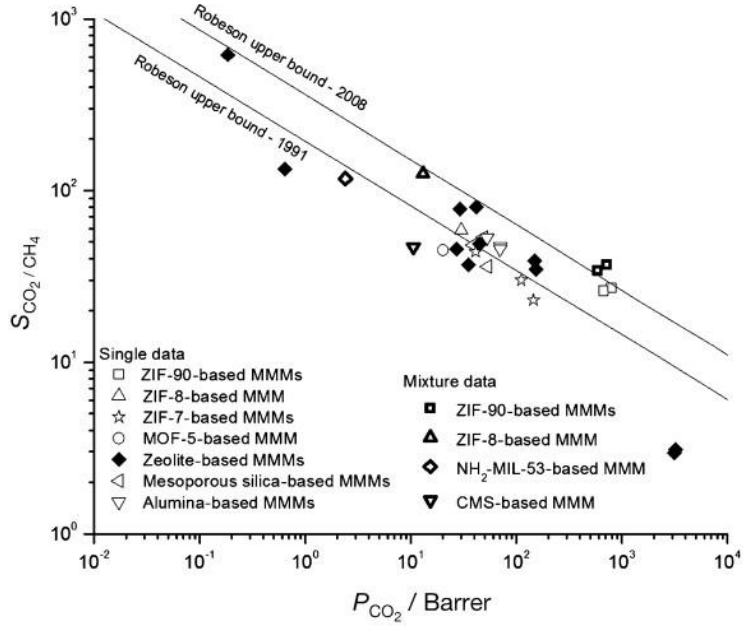

Figure 2-9 CO_2/CH_4 separation performance of various MMMs[8]

Table 2-3 Gas separation performance data for MOFs-based MMMs.

MOFs/Polymer	Loading (wt. %)	Test condition		Permeability (*P*)				Ideal selectivity (*S*)			Ref.
		T (°C)	Δ*P* (bar)	CO_2	CH_4	N_2	H_2	CO_2/N_2	CO_2/CH_4	H_2/CH_4	
CuBPDC–TED/ PAET	30	25	2	1.4					18		[68]
[$Cu_2(PF_6)(NO_3)$(4,4'-bpy)$_4$] -$(PF_6)_2(H_2O)_2$/PSF	3.75				0.08	0.1	9.6			123.1	[69]
HKUST-1/PSF	10			7.9	1.1	0.9	14.9	8.8	7.2	13.5	[70]
HKUST-1/ PMDA-ODA	6	25	10	37.2	5.3	7.8	1270	4.8	7.0	240	[71]
HKUST-1/ PPO	10	30		86	3.8	4.1	94	24	28	27	[72]
HKUST-1/6FDA-ODA	25	35	10	21.8	0.43				51.2		[18]
NH_2-HKUST-1/6FDA-ODA	25	35	10	26.6	0.45				59.6		[18]
UiO-66/6FDA-ODA	25	35	10	50.4	1.10				46.1		[18]
NH_2-UiO-66/6FDA-ODA	25	35	10	13.7	0.27				51.6		[18]
MIL-53/6FDA-ODA	25	35	10	20.5	0.47				44		[73]
NH_2-MIL-53/6FDA-ODA	25	35	10	14	0.21				66		[73]
NH_2-MIL-53/ Matrimid	25	35	3	14.7	0.42				35		[74]
NH_2-MIL-53/ PSF	25	-10	10	2.4	0.02				117		[75]
CAU-1-NH_2/ PMMA	15	25	5	846			11000				[76]
MIL-68/PSF	8	35	3	4.7	0.13		12.3		36.5	77	[77]
MOF-5/ Matrimid	20	35	2	13.8	0.3	0.4	38.3	34.5	40.6	112.7	[78]
ZIF-90/6FDA-DAM	15	25	2	803	29.5				27.0		[79]
ZIF-7/ PBI	25	35	3.5	1.3			15.4				[80]

ZIF-8/ Matrimid	30	35	2	14.2	0.4	0.6	47.2	24.1	37.4	124	[81]
ZIF-8/ Matrimid	20	22	4	16.6	0.46	0.88	63.5	19.0	35.8	137	[82]
ZIF-8/ PSF	16	35	2	12.1	0.61	0.60	39.8	20	19.8	118	[83]
ZIF-8/6FDA-Durene	20	35	10	487	27.2				17.91		[84]
ZIF-8/6FDA-Durene-DABA	20	35	10	276	10.5				26.29		[84]
ZIF-8/6FDA-Durene cross-linked	33.3	35	3.5	23.7	1.4	2.0	283.5	16.9	11.9	203.3	[85]

2.3.1 MOFs in Glassy Polymers

2.3.1.1 Classical MOFs for MMMs

Some common MOFs are first considered to be embedded into polymer matrix. The First MOF-based MMM was synthesized by Yehia *et al*.[68] through incorporation of copper (II) biphenyl dicarboxylate triethylenediamine (CuBPDC–TED) into poly(3-acetoxyethylthiophene) (PAET). The MMM showed an enhancement in CH_4 permeability and selectivity compared with the pure polymeric membrane.

Won *et al*.[69] introduced MOF $[Cu_2(PF_6)(NO_3)(4,4'\text{-bpy})_4](PF_6)_2(H_2O)_2$ into amorphous glassy polysulfone (PSF) to prepare a MMM. The He, H_2, O_2, N_2 and CH_4 gas separation abilities of the MMM and pure PSF membrane were compared. It was found that the MMM with 5 wt.% MOF loading exhibited improved selectivity for H_2. More importantly, the permeability of CH_4 significantly decrease with the increase of MOF loading which is thought to be due to molecular sieving effect of MOF, and the small pores of the MOF resisted the permeation of CH_4.

MOF-5 nanocrystals with high surface area and high thermalstability was synthesized by Perez *et al*.[86] and dispersed into Martimid matrix to form a MMM. It was found that remarkable increase of H_2, O_2, CO_2, N_2 and CH_4 with almost constant ideal selectivity from the neat polymer. In mixture gas permeation test, slight improvements in CH_4 selectivity for CO_2/CH_4 and N_2/CH_4 mixtures owing to the larger solubility of CO_2 and N_2 in the polymer matrix.

Adams *et al*.[87] synthesized Cu-BDC from copper nitrate trihydrate and terephthalic acid (TPA) and incorporated MOF into PVAc matrix for MMM analysis. MMMs with a 15 wt.% of loading showed improvements in gas permeabilities and selectivities over pure PVAc membrane. This improvement

can be due to both molecular sieving effect from small pores of MOF framework and enhanced contact between MOF and polymer.

Car *et al*.[88] were first to embedded HKUST-1 into PSF to form MMM for gas permeation test. The gas separation performance of MMM are compared with similar ones made using $Mg(HCOO)_2$. The HKUST-1 MMM showed higher permeability of CO_2 and H_2. The use of $Mg(HCOO)_2$ only resulted in an increase in H_2 permeability.

Hu *et al*.[71] incorporated HKUST-1 into PI (PMDA-ODA) to prepare MMMs for gas separations. The MMM hollow fiber was obtained by the dry/wet-spinning method. The hollow fiber morphology is illustrated in Figure 2-10. It was showed that the MMM has good compatibility between PI and HKUST-1. The HKUST-1 MMM hollow fiber at 6 wt.% MOF loading showed increased H_2 permeability by 45% and the ideal selectivity increased by a factor of 2-3 compared to the corresponding values of pure PI.

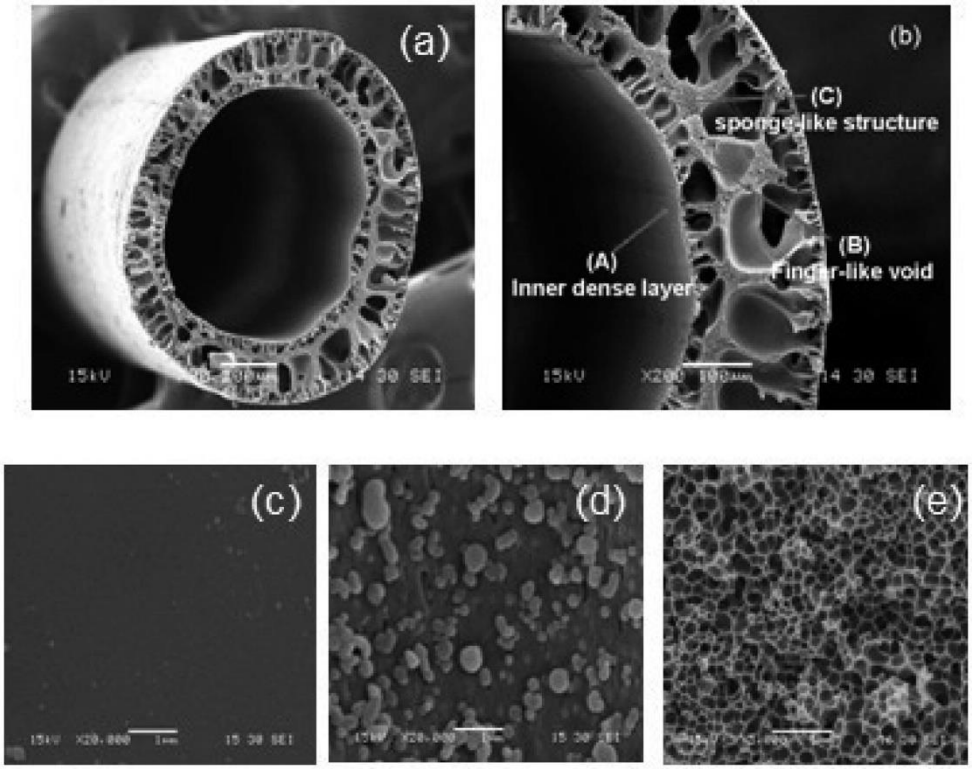

Figure 2-10 SEM images of hollow-fiber PI-$Cu_3(BTC)_2$MMMs: (a, b) cross section, (c) outer surface, (d) surface of fingerlike void, and (e) spongelike structure [71]

2.3.1.2 ZIF Containing MMMs

ZIF series materials were used as filler particles in most of the recent MOF-based MMMs fabrications.

Ordonez *et al*.[89] introduced ZIF-8 into Matrimid and tested the permeability of H_2, CO_2, O_2, N_2, CH_4 and C_3H_8. The permeability values of gases increased as the ZIF-8 loading increased to 40%, owing to addition of ZIF-8 increase the polymer free volume. When the MMMs at higher loadings (50% and 60% wt.%), the permeability decreased for all gases, the selectivities increased with the increased loading of the ZIF-8 particles, showing a transition from polymer-driven to ZIF-8-controlled gas transport process.

Diaz *et al*.[90] reported the permeability of H_2, N_2, O_2, CO_2, CH_4, C_2H_6 and C_2H_2 across ZIF-8/poly(1,4-phenylen ether-ether-sulfone) membranes containing 0-30 wt.% of ZIF-8. It was found that permeability and diffusion coefficient of all gases increase as the ZIF-8 loading increases, due to the formation of extra free volume in the membrane by the MOF addition. The MMM with a 30 wt.% ZIF-8 loading showed selectivities for O_2/N_2 and H_2/N_2 close to the Robeson upper bound.

Recently, mixed matrix asymmetric dual layer hollow fiber membranes were spun through a jet-wet process containing ZIF-8 in Ultem polymer matrix by Dai *et al*..[91] Increase in separation performance of the CO_2/N_2 was observed, Good adhesion between ZIF-8 and polymer matrix was observed. As expected, increase in separation performance of the CO_2/N_2 was achieved.

Yang *et al*.[80] mixed the as-synthesized ZIF-7 nanoparticles without the traditional drying process with polybenzimidazole (PBI) and obtained MMM containing highly dispersed nano-size ZIF-7. The MMM showed higher H_2 permeability and H_2/CO_2 selectivity than both neat PBI and ZIF-7 membranes. The addition of ZIF-7 helps to create extra free volume and slightly larger pores as sub-nano interphase channels for gas transport. The improved performance should be result of strong chemical interactions between the ZIF-7 surface and PBI and minimal non-selective voids.

Zhang *et al*.[92] embedded ZIF-8 into 6FDA-DAM to form MMMs for propylene/propane separations. SEM images showed good adhesion between ZIF-8 and 6FDA-DAM without the ‘‘sieve-in-a-cage’’ morphology. Gas separation test showed significant increase in C_3H_6/C_3H_8 selectivity over the pure 6FDA-DAM membrane. C_3H_6 permeability of 56 Barrer and C_3H_6/C_3H_8 selectivity of 31 were achieved when the ZIF-8 loading was 48 wt.%.

A high-performance gas-separation MMM containing ZIF-90 filler particles in 6FDA-DAM polymeric matrix was fabricated by Bae *et al*..[79] The ZIF-90 fillers showed well dispersed in the polymeric matrix as well as good adhesion with polymer (Figure 2-11 a-d). Both pure and mixed gas permeabilities of CO_2 and CH_4 were tested. At a 15 wt.% loading of ZIF-90, 6FDA-DAM-based MMM showed enhancement in both CO_2 permeability and CO_2/CH_4 ideal selectivity. In mixed-gas permeation test, CO_2 permeability coefficient of 720 Barrer and CO_2/CH_4 selectivity of 34 were

observed, which are both significantly higher than pure 6FDA-DAM. ZIF-90/6FDA-DAM MMMs show potential in exceeding the upper bound (Figure 2-11 e).

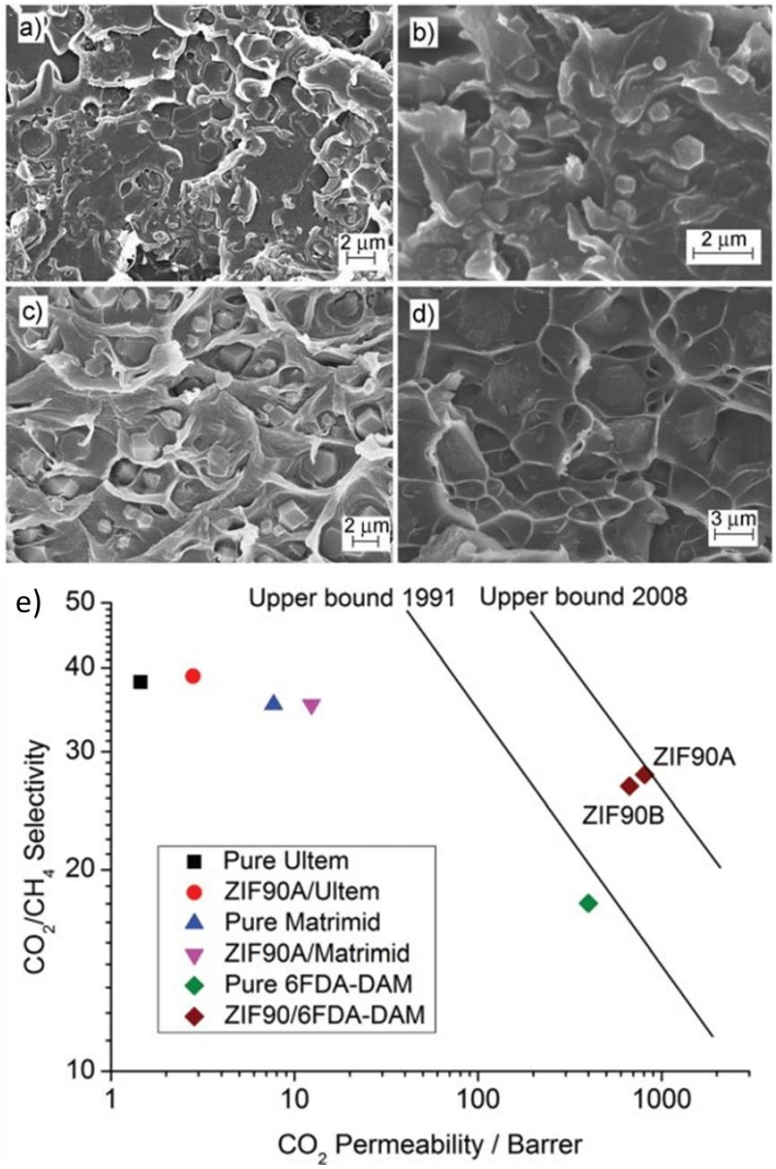

Figure 2-11 (a-d) SEM images of cross-sections of mixed-matrix membranes containing ZIF-90 crystals; a) ZIF-90A/Ultem, b) ZIF-90A/Matrimid, c) ZIF-90A/6FDA-DAM, and d) ZIF-90B/6FDA-DAM. (e) gas permeation properties of mixed-matrix membranes containing 15 wt% of ZIF-90 crystals measured with pure gases.[79]

2.3.1.3 Flexible MOFs Containing MMMs

The first MMMs containing flexible MOFs were reported by Basu *et al*..[93] They introduced MIL-47 and MIL-53 into PDMS for nanofiltration application. They also reported MMMs containing HKUST-1, ZIF-8 and MIL-53(Al) for CO_2 separation over N_2 and CH_4.[94] Dense membranes and

asymmetric membranes using Matrimid as polymeric matrix with this three MOFs all showed improvement in permeability and CO_2/CH_4, CO_2/N_2 selectivity as compared to the unfilled reference membrane. HKUST-1 and MIL-53(Al) showed higher selectivities than ZIF-8. For MIL-53(Al), the breathing behaviour was claimed to enhance the CO_2/MOF interaction.

Zornoza *et al.*[75] introduced amino functionalized MIL-53 [NH_2-MIL-53(Al)] into polysulfone (PSF) to fabricate nanocomposite membranes. The morphology of MMMs cross-sections is shown in Figure 2-12. The NH_2-MIL-53(Al) showed excellent adhesion with the PSF in MMMs due to hydrogen bonding interactions between the surface amine moieties of the MOF and the sulfonic groups of the polymer at a high NH_2-MIL-53(Al) loading of 40 wt.% (Figure 2-12 d). More interesting, the CO_2/CH_4 selectivity increased with pressure, owing to the flexibility of the NH_2-MIL-53(Al).

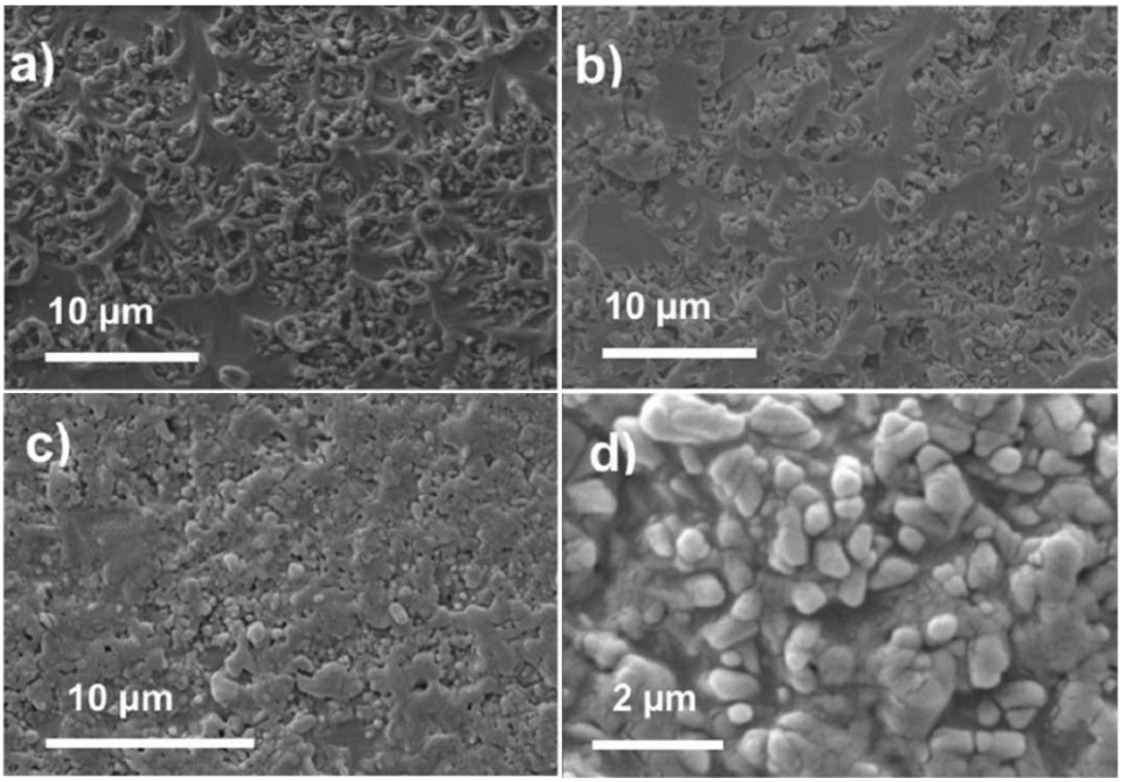

Figure 2-12 SEM micrographs of mixed matrix membrane cross-sections containing 8 (a), 16 (b), 25 (c) and 40 (d) wt% NH_2-MIL-53(Al) crystals.[75]

2.3.1.4 Mixed Types of Fillers or Polymers

Dual inorganic fillers or dual polymer matrix is also proposed in MOFs MMMs fabrication for improving membrane performances. Basu *et al.*[95] prepared MMMs through embedding HKUST-1 into Matrimid/polysulfone for gas mixtures separation. Higher CO_2 permeability and selectivity of CO_2/N_2 and CO_2/CH_4 over unfilled polymers were obtained with the HKUST-1/ Matrimid /PSF

membranes.

Zornoza *et al*.[83] used HKUST-1 and silicate-1 together as filler particles to form MMMs of PSF matrix. With the combination of HKUST-1 and silicate-1, the MMMs with good dispersion and dis-aggregation of the fillers are achieved. The HKUST-1-silicalite-1 MMM showed CO_2/CH_4 and CO_2/N_2 separation factors of 22 and 38, respectively. The results achieved pointed out a new strategy in preparing MMMs by using MOF–zeolite, MOF–MOF or other combinations for the enhancement in gas separation applications.

2.3.2 MOFs in Rubbery Polymers

Rubbery polymer is an important class of flexible elastomer well-known for their elastic property, which can regain its shape when stretching or deforming force is removed. The corresponding rubbery polymer membranes are of high permeance but low selectivity.[96]

Car *et al*.[88] reported the first MOF-based MMM using a high flux rubbery polymer. HKUST-1 was introduced into polydimethylsiloxane (PDMS) with a loading 0-40 wt.%. The MMM showed higher fluxes for all gases compared with pure polymer. Increase in selectivity of CO_2/N_2 and CO_2/CH_4 were observed by MMM with 10 wt% HKUST-1 loading.

Liu *et al*.[97] incorporated ZIF-8 nanoparticles into silicon rubber poly-methylphenylsiloxane (PMPS) and coated on the inside surface of alumina capillary substrates for the efficient recovery of bio-alcohols by pervaporation. May be due to the apertures and hydrophobic surfaces of ZIF-8, permeability and selectivity (dilute aqueous solutions, 1.0 wt.%) of ethanol, n-propanol, n-buta-nol and n-pentanol alcohols increased as the addition of ZIF-8.

2.3.3 Conclusions

Experimental results proved that MOFs based MMMs show higher gas separation performance than pure polymer membranes. They are highly expected to exceed the trade-off of pure polymer membranes. MOFs based MMMs also offer significant potential in the separation of desired gases by selecting MOFs with proper topologies and pore structures. For the polymer matrix, glassy polymers have high selectivity due to their strong size-sieving ability while their permeability is not high. Rubbery polymers have high permeability along with low selectivity because of their flexible elastic properties. In most cases, improvement of selectivity is more challenging to achieve than permeability after introducing MOF into the polymer matrix. So recently, most of the studies prefer to use glassy polymer rather than rubbery polymer for the high selectivity of glassy polymer in gas separation.

2.4 Factors affecting MMMs structure and performance

Despite of the promising perspectives of MOFs-based membranes, there exist some challenges for MMMs fabrication to obtain optimized performance and desired morphology: (1) the selection of the proper MOF/polymer pair needs to be fundamentally considered for the MMMs fabrication. (2) the uniform dispersion of inorganic phase in the polymeric phase should be achieved. (3) the interfacial interaction between inorganic phase and continuous phase should be considered to favour the generation of a void-free MMMs.

2.4.1 Selection of filler and polymer pair

Amongst them, pair-wise selection is fundamentally important for MMMs fabrication which is associated with affinity and compatibility between filler particles and polymer. Both polymer properties and filler properties can affect the morphology and separation performance of the MMMs. In a defect-free mixed matrix membrane, the polymer phase determines the minimum separation performance and the filler determines the improvement of the membrane permeability and selectivity.[98, 99] When MOF is used as filler in polymer matrix, its chemical structure, surface chemistry, pore size distribution and functional groups must be matched with the desired gas. One of the key issue for prepare high performance MMMs is the compatibility between filler phase and polymer matrix. To overcome this issue, an appropriate approach is to use MOFs which contain similar functional groups in polymer chains.

For instance, reports showed that MOFs containing amino groups may improve the interaction between the filler and polymer, especially with specific polymer such as polysulfone and polyimide.[18, 73-75, 100-103] Nik *et al*.[18] reported the preparation and CO_2/CH_4 gas separation properties of MMMs made from five different MOFs: UiO-66, NH_2-UiO-66, UiO-67, MOF-199, and NH_2-MOF-199 fillers and 6FDA-ODA polyimide in order to investigate the amino group effect on the CO_2/CH_4 gas separation performance of the MMMs. It was found that embedding fillers in the MMMs lead to an increase in perm-selectivity except for the UiO-67 filler. The presence of amine groups in as-synthesized MOFs increased both the CO_2 permeability and ideal selectivity.

ZIFs are regarded as good candidates to obtain good compatibility and interaction with specific polymer matrix such as polybenzimidazole (PBI) because of the similar linkers in ZIF and PBI structure.[80, 104, 105] Yang *et al*.[80] fabricated MMMs containing fully dispersed ZIF-7 by mixing as-synthesized ZIF-7 nano-particles without the traditional drying process. The final MMMs achieved a high ZIF-7 loading up to 50 wt% together with improved H_2 permeability and H_2/CO_2 ideal selectivity.

2.4.2 Filler dispersion

The distribution of filler particles in polymer matrix continuous phase is another important factor that affects the performance of MMMs. Aggregation of filler particles is an important issue need to be solved while increasing the filler particle loading. The aggregation of filler particles can lead to the formation of non-selective interfacial voids which can cause the decline of gas selectivity of membrane because filler aggregates cannot contact with polymer.

There are different methods for dispersing particles during dope preparation.[106, 107] Generally, filler particles are first dispersed into the solvent followed by adding a small portion of polymer in order to be coated with a thin layer of polymer, after that the remaining polymer is added to the filler suspension gradually with repeated stirring and sonication.[108]

To avoid the agglomeration of filler particles, an appropriate approach was carried out by Yang *et al*.[80] to prepare ZIF-7/PBI MMMs by synthesizing ZIF-7 with excess benzimidazole and mixing this as-synthesized ZIF-7 nano-particles with PBI which containing reactive hydrogen atoms without the traditional drying step. The excellent dispersion of ZIF nanoparticles with minimal agglomeration was achieved. Recently, Sanchez-Lainez *et al*.[109] prepared a nano-size ZIF-11 through one-step crystallization and applied it in MMMs fabrication. The nano-size ZIF-11 was suspended in chloroform, and the MMMs were prepared by direct addition of polymer to this ZIF-11 colloidal suspension, thus avoiding particle agglomeration resulting from drying.

2.4.3 Filler/polymer interface morphology

The filler/polymer interface morphology is another critical factor that affects the gas transport properties of MMMs. Because of the difference between the inorganic phase and polymer phase, it is challenging to fabricate ideal MMMs which shown in Figure 2-13. Poor adhesion between filler and polymer lead to the formation of defects at the filler/polymer interface. Generally poor interface morphology includes three major type: interfacial voids, rigidification of polymer around the filler and blocking of the filler pores.[32]

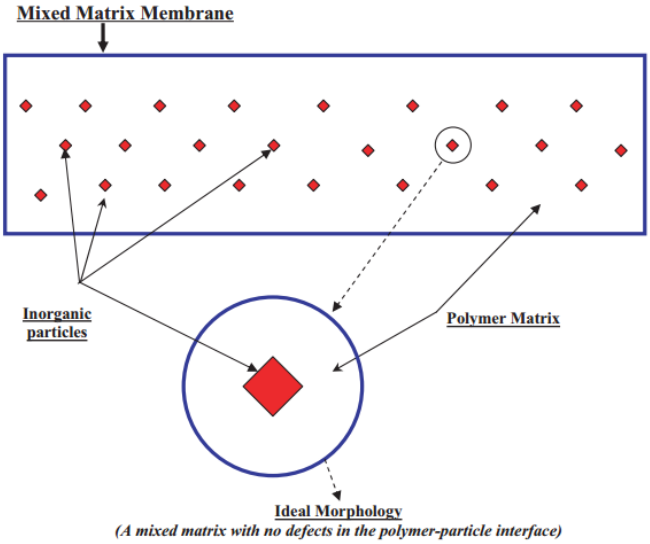

Figure 2-13 Schematic diagram of an ideal MMM [7]

Low interfacial adhesion creates interfacial voids at the filler/polymer interface region, which is known as "sieve-in-a-cage" morphology. These voids will act as extra channels to allow gas molecules to transport through, thus reducing the selectivity of the whole membrane. Rigidification of polymer layer around the filler caused by the immobilization of polymer chains at the filler/polymer interface, which can influence the gas transport behaviour around the fillers. Although the interfacial adhesion between filler/polymer is good, permeability decreases and the selectivity enhancement is not significant.[32] Figure 2-14 displays the interface voids (a) and the rigidified polymer layer (b) in the polymer–particles interface.[7] Pore blockage of the filler could decrease membrane permeability with no help for selectivity enhancement. Particle pores can be blocked by sorbent, solvent, agents or polymer chains during the membrane fabrication.[13, 29, 110]

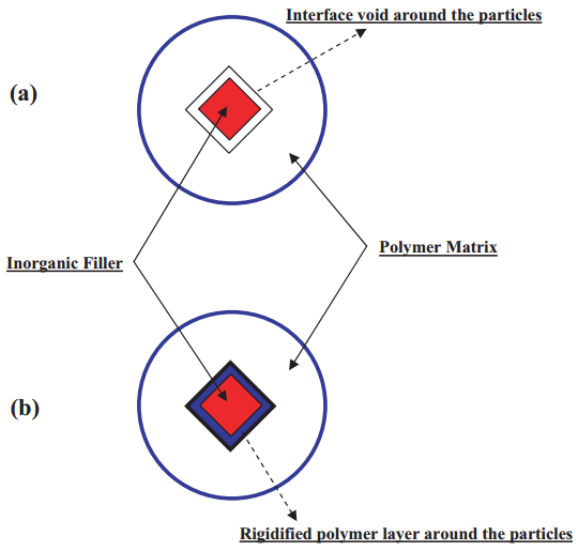

Figure 2-14 Interface void (a) and rigidified polymer layer (b) in the polymer–particles interface [7]

2.4.4 Conclusions

To achieve desirable mixed matrix membranes, there are some issues need to be addressed. The appropriate selection of MOF/polymer pair is the basis for MMMs fabrication. The affinity and compatibility between filler particles and polymer are important factors need to be considered in the preparation of MMMs. Dispersion of filler particle in the polymer matrix and the interfacial morphology inorganic phase and continuous phase can dramatically affect the membrane integrity and overall gas transport performance. Enhancing the filler dispersion to avoid aggregation of particles and improving the filler/polymer adhesion to eliminate the interface voids are critical for increasing the separation performance of MMMs.

2.5 Potential MMMs modification methods

To achieve high performance MMMs, the important factors mentioned before must be considered during the fabrication of MMMs. Poor affinity between MOFs and polymer may cause the deterioration of gas selectivity and integrity of membrane structure.[18, 23, 111] In order to obtain MMMs with good interfacial properties and break through the Robeson upper bound, various approaches have been applied to enhance the MOFs/polymer compatibility and interaction, as well as improve the membrane interfacial morphology.

2.5.1 Filler size and shape

Applying the nano or sub-micrometer sized MOFs particles as fillers into polymer matrix can be one promising method to obtain MMMs with favourable interfacial property, such as ZIF-8 and MIL-53. In most cases, smaller sizes of MOFs show stronger interaction with the polymeric matrix as well as good dispersion because smaller particles can provide more polymer/particle interfacial area.[73, 74, 78, 79, 82, 92, 112] Bae *et al*.[79] decreased the size of ZIF-90 by a nonsolvent-induced crystallization method and fabricated a MMM with the as-synthesized submicrometer-sized ZIF-90 and 6FDA-DAM polyimide. An interfacial void-free MMM with high gas separation performance was achieved. An interfacial void-free MMM with high gas separation performance was achieved. The ZIF-90/6FDA-DAM MMM showed a CO_2 permeability of 720 Barrer with CO_2/CH_4 selectivity of 37 at 25 ºC, which transcends the 1991 upper bound for polymer membrane. Compared to nano-sized MOFs, it is very challenging for some micron-sized MOFs to reach excellent compatibility and affinity with the polymeric matrix. One feasible way is tailoring MOFs by physical treatment. Lei *et al*.[72] reduced the size of Cu-BTC by using a facial sonication post-treatment and improve the poorly attached interface between MOF/polymer.

Adjust the shape of MOF is another approach that can alter membrane interface morphology and improve membrane performance. Rodenas *et al*.[113] reported the synthesis of CuBDC nanosheets and their application in MMMs. MMMs were prepared by incorporating CuBDC nanosheets into polyimide. The same procedure was employed to prepare comparative MMMs incorporating either bulk-type or sub-micron sized CuBDC crystals as fillers. The internal structure of the MMMs was studied with FIB-SEM, as shown in Figure 2-15. It was found that the MMMs with CuBDC nanosheets showed much better filler dispersion and selectivity than the MMMs with bulk-type or sub-micron sized CuBDC crystals. Hwang *et al*.[114] reported the preparation of hollow ZIF-8 nanoparticles by solvothermal surface coating of ZIF-8 shell on a polystyrene core and upon selective removal of the polystyrene core. MMMs were prepared by dispersing hollow ZIF-8 filler in poly(vinyl chloride)-g-poly(oxyethylene methacrylate) (PVC-g-POEM) graft copolymer matrix and exhibited significantly enhanced CO_2 permeability relative to pure PVC-g-POEM membranes: an 8.9-fold increase in permeability from 70.0 to 623 Barrer.

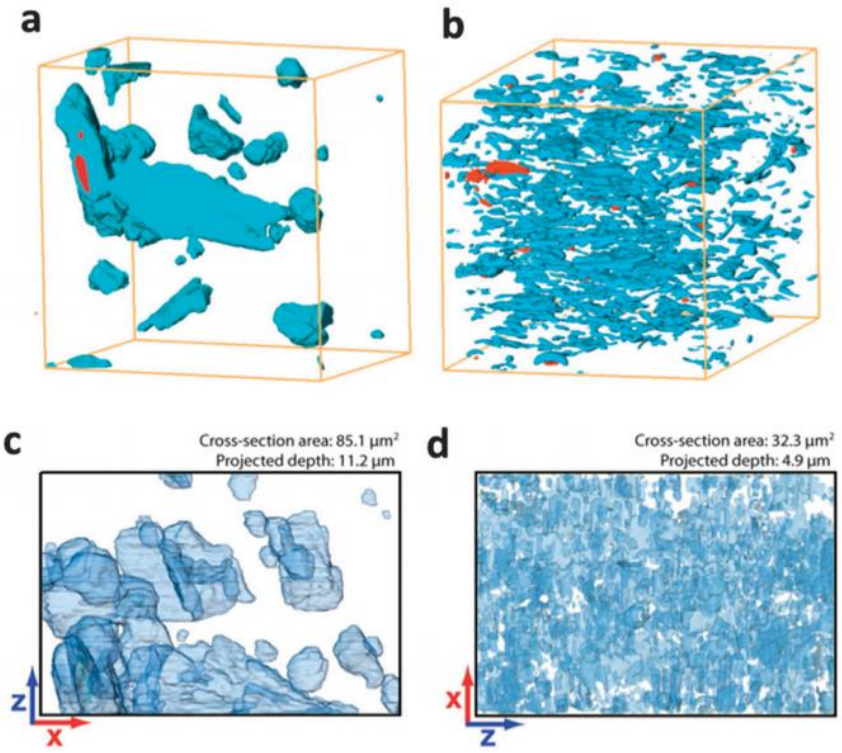

Figure 2-15 Surface-rendered views of the segmented FIB-SEM tomograms for composite membranes containing bulk-type (a) and nanosheet (b) CuBDC metal–organic-framework embedded in polyimide. Full projections along the y-direction of the reconstructed volumes (c, d).[113]

2.5.2 Surface modification of filler

Another route to achieve enhanced adhesion is through the modification of MOFs. The functionalization of MOFs can improve the affinity between MOF linkers and polymer chains, eliminate the formation of non-selective interfacial voids.[18, 111]

Xin *et al.*[115] prepared a polyethylenimine decorated MOF through immobilizing MIL-101(Cr) with polyethylenimine (PEI). The obtained PEI@MIL-101(Cr) was incorporated into sulfonated poly(ether ether ketone) (SPEEK) to fabricate MMMs. The PEI in the pore channels and on the surface of MIL-101(Cr) improved the filler/polymer interface compatibility due to the electrostatic interaction and hydrogen bond between sulfonic acid groups and PEI. The as-synthesized SPEEK/PEI@MIL-101(Cr) MMMs showed high CO_2 permeability of 2490 Barrer with CO_2/CH_4 and CO_2/N_2 ideal selectivities up to 71.8 and 80.0.

Venna *et al.*[116] modified and optimized the surface of MOF UiO-66-NH_2 with phenyl acetyl group to improve its interaction with Matrimid® in the MMMs. MMMs containing surface modified MOF UiO-66-NH_2 displayed improved thermal and mechanical properties. The MMMs show significantly enhanced CO_2 permeability by 200% and CO_2/N_2 ideal selectivity by 25%. Interactions between MOF and polymer are expected through the π–π stacking of the aromatic ring from the modified MOF and polymer chains, as well as hydrogen bonding between the amide groups from the modified MOF and the imide groups from the polymer. Xin *et al.*[115] decorated MIL-101(Cr) with polyethylenimine (PEI) through a facile vacuum-assisted method and applied the derived MOF into poly(ether ether ketone)(SPEEK). The PEI both in the pore channels and on the surface of MOF improved the MOF/polymer interface compatibility via the electrostatic interaction and hydrogen bond between sulfonic acid groups from SPEEK and amine groups from PEI.

2.5.3 Crosslinking

Moreover, some studies are focused on polymeric matrix modifications through using cross-linkable polymer (*e.g.* copolyimides) and cross-linking them after the cast of MMMs,[84] or surface cross-linking the MMMs by a cross-linking agent.[85]

Askari *et al.*[84] developed MMMs with ZIF-8 loading as high as 40 wt% by directly mixing ZIF-8 suspension into the cross-linkable co-polyimides 6FDA-Durene/DABA (9/1) or 6FDA-Durene/DABA (7/3) solution. Results showed that the plasticization resistance and gas selectivity of MMMs are strongly depend on the amount of cross-linkable moiety and annealing temperature. MMMs prepared from cross-linkable co-polyimides showed significant improvements in CO_2/CH_4 and C_3H_6/C_3H_8 selectivity after annealing at 400 °C because of the cross-linking reaction of the

carboxyl acid (COOH) in the DABA moiety. Surface cross-linking was performed on MMMs which containing 33.3 wt% ZIF-8 filler in 6FDA-durene by exposure to ethylenediamine (EDA) vapor (Figure 2-16) to improve gas selectivity.[85] After the MMM reacted with EDA vapor, the MMM obtained a 10-fold increase in H_2/CO_2, H_2/N_2, and H_2/CH_4 selectivities with compare to 6FDA-durene. The permselective properties of the cross-linked MMM fall above the 2008 Robeson upper bounds trade-off lines for H_2/CO_2, H_2/N_2, and H_2/CH_4 separations.

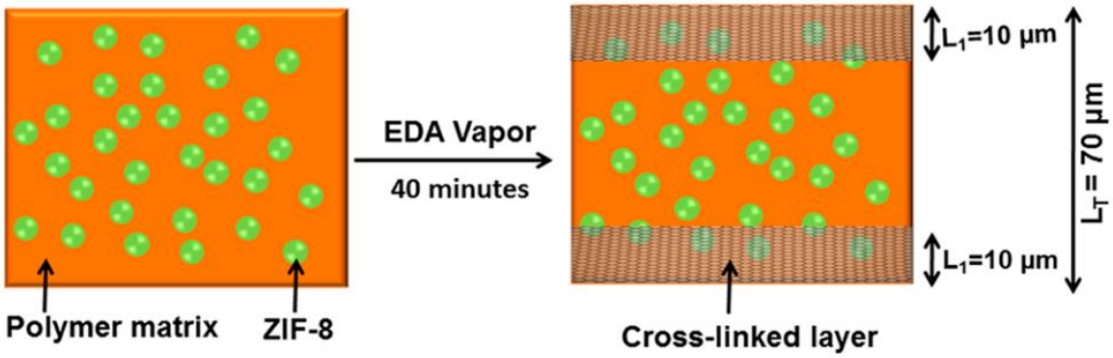

Figure 2-16 Schematic representation of the formation of the crosslinked skin in 33.3 wt % ZIF-8/6FDA-durene MMM upon reaction with EDA vapour [85]

2.5.4"One-pot" synthesis of MMMs

One way to well dispersed MOFs nanoparticle and restrain agglomeration is to synthesize MOFs and solution-casting in the same solution, which is known as "one-pot synthesis". Seoane *et al.*[77] synthesized MIL-68(Al) in THF solvent to prepare MOF/polysulfone (PSF) MMMs, as THF can dissolve PSF, which make it possible to one-pot process of both MIL-68(Al) and PSF, without the stages of crystal separation and drying from the mother liquor. Figure 2-17 shows the cross-section images of MMMs fabricated in one-pot. It is clearly to find that the dispersions of MOFs and the filler/polymer contact in one-pot-synthesized MMMs are much better than those of conventional MMM.

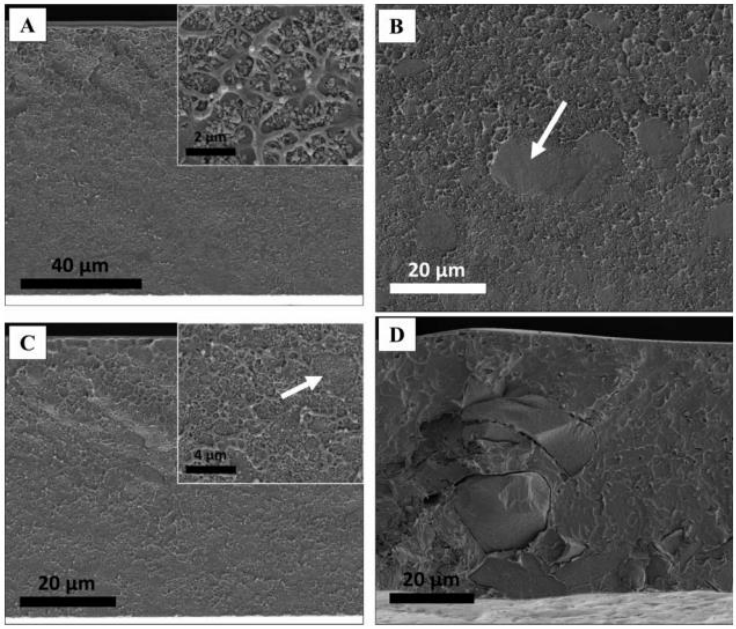

Figure 2-17 SEM images of MMMs: a) membrane M2 (8 wt% MIL-68@PSF MMM); b) membrane M3 (16 wt% MIL-68@PSF MMM); c) membrane M4 (8 wt% MIL-68@PSF MMM by priming); and d) membrane M5 (conventional 8 wt% MIL-68@PSF MMM).[77]

2.5.5 Adding third component

Ionic liquid offers a new possibility of improving the filler/polymer interface and separation performance of MMMs, since ionic liquid can behave like a wetting agent and eliminate the non-selective defects between MOF/polymer. Hao et al.[117] incorporated ZIF-8 into miscible ionic liquid blend systems for natural gas sweetening and post-combustion CO_2 capture. The miscible blend system consists of a polymerizable room temperature ionic liquid (poly(RTIL)) and a ‘‘free’’ room temperature ionic liquids (RTILs). Results showed that the free ionic liquids were miscible with poly(RTIL) and ZIF-8 are uniformly dispersed in the MMMs. ZIF-8-incorporated membranes exhibited significantly enhanced permeability for CO_2 than in PIL/IL membranes, while the CO_2/N_2 and CO_2/CH_4 selectivity were only slightly reduced.

2.5.6 Conclusions

In the fabrication of MOFs based MMMs, proper selection of MOFs particles and good interfacial interaction between MOFs and polymer are necessary for membrane with high gas separation performance. In order to overcome the trade-off of polymer membrane and obtain defect-free MMMs, the MMM materials need to be modified. Several methods have been conducted on prevention or elimination of the interfacial voids between the inorganic phase and polymer phase, such as adjusting

filler size or shape, surface modification of filler, crosslinking of polymer and 'one pot' synthesis. These modifications can dramatically improve the gas transport performance of the membranes if they are correctly applied.

2.6 Summary

Mixed matrix membranes offer an alternative route to the next generation membranes for gas separation due to their impressive advantages. Mixed matrix membranes combine the easy process ability, low cost and flexibility of polymer with high permeability and selectivity of inorganic particles. The fabrication methods for MMMS are similar to that of polymer membranes, the established fabrication techniques can be easily extended to MMMs for industrial scale-up. Among MMMs, MOF-based MMMs show promising performance in gas separation application. In the above review, many previous studies have been presented and discussed on MOFs-based MMMs synthesis and their gas separation performance. Although a lot of reports have been published in this area, the permeability and selectivity of these MMMs still need to be improved. Novel MMM materials with high performance are required for industry use. The mechanism of gas diffusion in MOF based MMMs needs to be further investigated and the rate-limiting step of the gas separation process need to be identified. The impact of water vapour in the gas separation process of MMMs need to be studied. Only a few of studies consider the MOFs/polymer interactions and focus on the interfacial morphology control. How to design and control the interfacial morphology including the elimination of the non-selective defect and the improvement in gas selectivity need further investigation.

2.7 References

(1) Koros, B., Three Hundred Volumes. Journal of Membrane Science, 2007, 300, 1-1.

(2) Nasir, R., Mukhtar, H., Man, Z., Mohshim, D. F., Material Advancements in Fabrication of Mixed-Matrix Membranes. Chemical Engineering & Technology, 2013, 36, 717-727.

(3) Robeson, L. M., Correlation of Separation Factor versus Permeability for Polymeric Membranes. Journal of Membrane Science, 1991, 62, 165-185.

(4) Robeson, L. M., The Upper Bound Revisited. Journal of Membrane Science, 2008, 320, 390-400.

(5) Dong, G. X., Li, H. Y., Chen, V. K., Challenges and Opportunities for Mixed-Matrix Membranes for Gas Separation. Journal of Materials Chemistry A, 2013, 1, 4610-4630.

(6) Goh, P. S., Ismail, A. F., Sanip, S. M., Ng, B. C., Aziz, M., Recent Advances of Inorganic Fillers in Mixed Matrix Membrane for Gas Separation. Separation and Purification Technology, 2011, 81,

243-264.

(7) Aroon, M. A., Ismail, A. F., Matsuura, T., Montazer-Rahmati, M. M., Performance Studies of Mixed Matrix Membranes for Gas Separation: A review. Separation and Purification Technology, 2010, 75, 229-242.

(8) Erucar, I., Yilmaz, G., Keskin, S., Recent Advances in Metal-Organic Framework-based Mixed Matrix Membranes. Chemistry an Asian Journal, 2013, 8, 1692-1704.

(9) Koros, W., Ma, Y., Shimidzu, T., Terminology for Membranes and Membrane Processes. Journal of Membrane Science, 1996, 120, 149-159.

(10) Koros, W. J., Fleming, G. K., Membrane-based Gas Separation. Journal of Membrane Science, 1993, 83, 1-80.

(11) Lei, G., Carbon Nanotube-based Membranes for Gas Separation, in, University of Queensland, 2012.

(12) Tanh Jeazet, H. B., Staudt, C., Janiak, C., Metal-Organic Frameworks in Mixed-Matrix Membranes for Gas Separation. Dalton Transactions, 2012, 41, 14003-14027.

(13) Mahajan, R., Koros, W. J., Factors Controlling Successful Formation of Mixed-Matrix Gas Separation Materials. Industrial & Engineering Chemistry Research, 2000, 39, 2692-2696.

(14) Mahajan, R., Koros, W. J., Mixed Matrix Membrane Materials with Glassy Polymers. Part 1. Polymer Engineering & Science, 2002, 42, 1420-1431.

(15) Mahajan, R., Koros, W. J., Mixed Matrix Membrane Materials with Glassy Polymers. Part 2. Polymer Engineering & Science, 2002, 42, 1432-1441.

(16) Scholes, C. A., Stevens, G. W., Kentish, S. E., Membrane Gas Separation Applications in Natural Gas Processing. Fuel, 2012, 96, 15-28.

(17) Sridhar, S., Smitha, B., Aminabhavi, T. M., Separation of Carbon Dioxide from Natural Gas Mixtures through Polymeric Membranes—A Review. Separation & Purification Reviews, 2007, 36, 113-174.

(18) Nik, O. G., Chen, X. Y., Kaliaguine, S., Functionalized Metal Organic Framework-Polyimide Mixed Matrix Membranes for CO_2/CH_4 Separation. Journal of Membrane Science, 2012, 413-414, 48-61.

(19) Bastani, D., Esmaeili, N., Asadollahi, M., Polymeric Mixed Matrix Membranes Containing Zeolites as a Filler for Gas Separation Applications: A Review. Journal Of Industrial And Engineering Chemistry, 2013, 19, 375-393.

(20) Pechar, T. W., Kim, S., Vaughan, B., Marand, E., Tsapatsis, M., Jeong, H. K., Cornelius, C. J., Fabrication and Characterization of Polyimide–Zeolite L Mixed Matrix Membranes for Gas Separations. Journal of Membrane Science, 2006, 277, 195-202.

(21) Ge, L., Zhu, Z., Rudolph, V., Enhanced Gas Permeability by Fabricating Functionalized Multi-Walled Carbon Nanotubes and Polyethersulfone Nanocomposite Membrane. Separation and Purification Technology, 2011, 78, 76-82.

(22) Ge, L., Zhu, Z., Li, F., Liu, S., Wang, L., Tang, X., Rudolph, V., Investigation of Gas Permeability in Carbon Nanotube (CNT)−Polymer Matrix Membranes via Modifying CNTs with Functional Groups/Metals and Controlling Modification Location. The Journal of Physical Chemistry C, 2011, 115, 6661-6670.

(23) Vu, D. Q., Koros, W. J., Miller, S. J., Mixed Matrix Membranes Using Carbon Molecular Sieves: I. Preparation and Experimental Results. Journal of Membrane Science, 2003, 211, 311-334.

(24) Weng, T.-H., Tseng, H.-H., Wey, M.-Y., Fabrication and Characterization of Poly(phenylene oxide)/SBA-15/Carbon Molecule Sieve Multilayer Mixed Matrix Membrane for Gas Separation. International Journal Of Hydrogen Energy, 2010, 35, 6971-6983.

(25) Zornoza, B., Irusta, S., Téllez, C., Coronas, J. n., Mesoporous Silica Sphere−Polysulfone Mixed Matrix Membranes for Gas Separation. Langmuir, 2009, 25, 5903-5909.

(26) Nik, O. G., Chen, X. Y., Kaliaguine, S., Amine-Functionalized Zeolite FAU/EMT-Polyimide Mixed Matrix Membranes for CO_2/CH_4 Separation. Journal of Membrane Science, 2011, 379, 468-478.

(27) Sen, D., Kalipcilar, H., Yilmaz, L., Development of Zeolite Filled Polycarbonate Mixed Matrix Gas Separation Membranes. Desalination, 2006, 200, 222-224.

(28) Zeng, C., Zhang, L., Cheng, X., Wang, H., Xu, N., Preparation and Gas Permeation of Nano-Sized Zeolite NaA-Filled Carbon Membranes. Separation and Purification Technology, 2008, 63, 628-633.

(29) Li, Y., Chung, T.-S., Cao, C., Kulprathipanja, S., The Effects of Polymer Chain Rigidification, Zeolite Pore Size and Pore Blockage on Polyethersulfone (PES)-Zeolite A Mixed Matrix Membranes. Journal of Membrane Science, 2005, 260, 45-55.

(30) Hillock, A. M. W., Miller, S. J., Koros, W. J., Crosslinked Mixed Matrix Membranes for the Purification of Natural Gas: Effects of Sieve Surface Modification. Journal of Membrane Science, 2008, 314, 193-199.

(31) Şen, D., Kalıpçılar, H., Yilmaz, L., Development of Polycarbonate based Zeolite 4A Filled Mixed Matrix Gas Separation Membranes. Journal of Membrane Science, 2007, 303, 194-203.

(32) Moore, T. T., Koros, W. J., Non-Ideal Effects in Organic–Inorganic Materials for Gas Separation Membranes. Journal Of Molecular Structure, 2005, 739, 87-98.

(33) Ahn, J., Chung, W.-J., Pinnau, I., Song, J., Du, N., Robertson, G. P., Guiver, M. D., Gas Transport Behavior of Mixed-Matrix Membranes Composed of Silica Nanoparticles in a Polymer of Intrinsic

Microporosity (PIM-1). Journal of Membrane Science, 2010, 346, 280-287.
(34) Jadav, G. L., Singh, P. S., Synthesis of Novel Silica-Polyamide Nanocomposite Membrane with Enhanced Properties. Journal of Membrane Science, 2009, 328, 257-267.
(35) Ahn, J., Chung, W.-J., Pinnau, I., Guiver, M. D., Polysulfone/Silica Nanoparticle Mixed-Matrix Membranes for Gas Separation. Journal of Membrane Science, 2008, 314, 123-133.
(36) Ismail, A. F., David, L. I. B., A Review on the Latest Development of Carbon Membranes for Gas Separation. Journal of Membrane Science, 2001, 193, 1-18.
(37) Liu, J., Wang, H., Zhang, L., Highly Dispersible Molecular Sieve Carbon Nanoparticles. Chemistry of Materials, 2004, 16, 4205-4207.
(38) Xu, L., Rungta, M., Koros, W. J., Matrimid® Derived Carbon Molecular Sieve Hollow Fiber Membranes for Ethylene/Ethane Separation. Journal of Membrane Science, 2011, 380, 138-147.
(39) Rafizah, W. A. W., Ismail, A. F., Effect of Carbon Molecular Sieve Sizing with Poly(Vinyl Pyrrolidone) K-15 on Carbon Molecular Sieve–Polysulfone Mixed Matrix Membrane. Journal of Membrane Science, 2008, 307, 53-61.
(40) Hosseini, S. S., Li, Y., Chung, T.-S., Liu, Y., Enhanced Gas Separation Performance of Nanocomposite Membranes Using MgO Nanoparticles. Journal of Membrane Science, 2007, 302, 207-217.
(41) Matteucci, S., Kusuma, V. A., Kelman, S. D., Freeman, B. D., Gas Transport Properties of MgO Filled Poly(1-Trimethylsilyl-1-Propyne) Nanocomposites. Polymer, 2008, 49, 1659-1675.
(42) Matteucci, S., Kusuma, V. A., Sanders, D., Swinnea, S., Freeman, B. D., Gas Transport in TiO_2 Nanoparticle-Filled Poly(1-Trimethylsilyl-1-Propyne). Journal of Membrane Science, 2008, 307, 196-217.
(43) Liang, C.-Y., Uchytil, P., Petrychkovych, R., Lai, Y.-C., Friess, K., Sipek, M., Mohan Reddy, M., Suen, S.-Y., A Comparison on Gas Separation between PES (Polyethersulfone)/MMT (Na-Montmorillonite) and PES/TiO_2 Mixed Matrix Membranes. Separation and Purification Technology, 2012, 92, 57-63.
(44) Weng, T.-H., Tseng, H.-H., Wey, M.-Y., Preparation and Characterization of Multi-Walled Carbon Nanotube/PBNPI Nanocomposite Membrane for H_2/CH_4 Separation. International Journal Of Hydrogen Energy, 2009, 34, 8707-8715.
(45) Furukawa, H., Ko, N., Go, Y. B., Aratani, N., Choi, S. B., Choi, E., Yazaydin, A. Ö., Snurr, R. Q., O'Keeffe, M., Kim, J., Yaghi, O. M., Ultrahigh Porosity in Metal-Organic Frameworks. Science, 2010, 329, 424-428.
(46) Furukawa, H., Cordova, K. E., O'Keeffe, M., Yaghi, O. M., The Chemistry and Applications of Metal-Organic Frameworks. Science, 2013, 341.

(47) Kitagawa, S., Kitaura, R., Noro, S.-i., Functional Porous Coordination Polymers. Angewandte Chemie International Edition, 2004, 43, 2334-2375.

(48) Park, K. S., Ni, Z., Cote, A. P., Choi, J. Y., Huang, R., Uribe-Romo, F. J., Chae, H. K., O'Keeffe, M., Yaghi, O. M., Exceptional Chemical and Thermal Stability of Zeolitic Imidazolate Frameworks. Proceedings of the National Academy of Sciences of the United States of America, 2006, 103, 10186-10191.

(49) Adatoz, E., Avci, A. K., Keskin, S., Opportunities and Challenges of MOF-based Membranes in Gas Separations. Separation and Purification Technology, 2015, 152, 207-237.

(50) Sumida, K., Rogow, D. L., Mason, J. A., McDonald, T. M., Bloch, E. D., Herm, Z. R., Bae, T. H., Long, J. R., Carbon Dioxide Capture in Metal-Organic Frameworks. Chemical Reviews, 2012, 112, 724-781.

(51) Li, J.-R., Sculley, J., Zhou, H.-C., Metal–Organic Frameworks for Separations. Chemical Reviews, 2012, 112, 869-932.

(52) Murray, L. J., Dinca, M., Long, J. R., Hydrogen Storage in Metal-Organic Frameworks. Chemical Society Reviews, 2009, 38, 1294-1314.

(53) Ranocchiari, M., Bokhoven, J. A. v., Catalysis by Metal-Organic Frameworks: Fundamentals and Opportunities. Physical Chemistry Chemical Physics, 2011, 13, 6388-6396.

(54) Ma, L., Falkowski, J. M., Abney, C., Lin, W., A Series of Isoreticular Chiral Metal–Organic Frameworks as a Tunable Platform for Asymmetric Catalysis. Nature Chemistry, 2010, 2, 838-846.

(55) Horcajada, P., Chalati, T., Serre, C., Gillet, B., Sebrie, C., Baati, T., Eubank, J. F., Heurtaux, D., Clayette, P., Kreuz, C., Chang, J.-S., Hwang, Y. K., Marsaud, V., Bories, P.-N., Cynober, L., Gil, S., Ferey, G., Couvreur, P., Gref, R., Porous Metal-Organic-Framework Nanoscale Carriers as a Potential Platform for Drug Delivery and Imaging. Nature Materials, 2010, 9, 172-178.

(56) Kreno, L. E., Leong, K., Farha, O. K., Allendorf, M., Van Duyne, R. P., Hupp, J. T., Metal–Organic Framework Materials as Chemical Sensors. Chemical Reviews, 2012, 112, 1105-1125.

(57) Horcajada, P., Gref, R., Baati, T., Allan, P. K., Maurin, G., Couvreur, P., Férey, G., Morris, R. E., Serre, C., Metal–Organic Frameworks in Biomedicine. Chemical Reviews, 2012, 112, 1232-1268.

(58) Zhao, Z., Li, Z., Lin, Y. S., Adsorption and Diffusion of Carbon Dioxide on Metal−Organic Framework (MOF-5). Industrial & Engineering Chemistry Research, 2009, 48, 10015-10020.

(59) Venkataramanan, N. S., Sahara, R., Mizuseki, H., Kawazoe, Y., Probing the Structure, Stability and Hydrogen Adsorption of Lithium Functionalized Isoreticular MOF-5 (Fe, Cu, Co, Ni and Zn) by Density Functional Theory. International Journal of Molecular Sciences, 2009, 10, 1601-1608.

(60) Eddaoudi, M., Kim, J., Rosi, N., Vodak, D., Wachter, J., O'Keeffe, M., Yaghi, O. M., Systematic Design of Pore Size and Functionality in Isoreticular MOFs and Their Application in Methane Storage.

Science, 2002, 295, 469-472.

(61) Bordiga, S., Regli, L., Bonino, F., Groppo, E., Lamberti, C., Xiao, B., Wheatley, P. S., Morris, R. E., Zecchina, A., Adsorption Properties of HKUST-1 toward Hydrogen and other Small Molecules Monitored by IR. Physical Chemistry Chemical Physics, 2007, 9, 2676-2685.

(62) Yang, Y., Shukla, P., Wang, S., Rudolph, V., Chen, X.-M., Zhu, Z., Significant Improvement of Surface Area and CO_2 Adsorption of Cu–BTC via Solvent Exchange Activation. RSC Advances, 2013, 3, 17065.

(63) Chui, S. S.-Y., Lo, S. M.-F., Charmant, J. P. H., Orpen, A. G., Williams, I. D., A Chemically Functionalizable Nanoporous Material $[Cu_3(TMA)_2(H_2O)_3]n$. Science, 1999, 283, 1148-1150.

(64) Bushell, A. F., Attfield, M. P., Mason, C. R., Budd, P. M., Yampolskii, Y., Starannikova, L., Rebrov, A., Bazzarelli, F., Bernardo, P., Carolus Jansen, J., Lanč, M., Friess, K., Shantarovich, V., Gustov, V., Isaeva, V., Gas Permeation Parameters of Mixed Matrix Membranes based on the Polymer of Intrinsic Microporosity PIM-1 and the Zeolitic Imidazolate Framework ZIF-8. Journal of Membrane Science, 2013, 427, 48-62.

(65) Ferey, G., Latroche, M., Serre, C., Millange, F., Loiseau, T., Percheron-Guegan, A., Hydrogen Adsorption in the Nanoporous Metal-Benzenedicarboxylate $M(OH)(O_2C\text{-}C_6H_4\text{-}CO_2)$ ($M = Al^{3+}$, Cr^{3+}), MIL-53. Chemical Communications, 2003, 2976-2977.

(66) Llewellyn, P. L., Bourrelly, S., Serre, C., Filinchuk, Y., Férey, G., How Hydration Drastically Improves Adsorption Selectivity for CO_2 over CH_4 in the Flexible Chromium Terephthalate MIL-53. Angewandte Chemie International Edition, 2006, 45, 7751-7754.

(67) Bourrelly, S., Llewellyn, P. L., Serre, C., Millange, F., Loiseau, T., Férey, G., Different Adsorption Behaviors of Methane and Carbon Dioxide in the Isotypic Nanoporous Metal Terephthalates MIL-53 and MIL-47. Journal Of The American Chemical Society, 2005, 127, 13519-13521.

(68) Yehia, H., Pisklak, T. J., Ferraris, J. P., Balkus, K. J., Musselman, I. H., Methane Facilitated Transport Using Copper(II) Biphenyl Dicarboxylatetriethylenediamine/Poly(3-Acetoxyethylthiophene) Mixed Matrix Membranes. Polymer Preprint, 2004, 45, 35-36.

(69) Won, J., Seo, J. S., Kim, J. H., Kim, H. S., Kang, Y. S., Kim, S. J., Kim, Y., Jegal, J., Coordination Compound Molecular Sieve Membranes. Advanced Materials, 2005, 17, 80-84.

(70) Car, A., Stropnik, C., Peinemann, K.-V., Hybrid Membrane Materials with Different Metal-Organic Frameworks (MOFs) for Gas Separation. Desalination, 2006, 200, 424-426.

(71) Hu, J., Cai, H., Ren, H., Wei, Y., Xu, Z., Liu, H., Hu, Y., Mixed-Matrix Membrane Hollow Fibers of $Cu_3(BTC)_2$ MOF and Polyimide for Gas Separation and Adsorption. Industrial & Engineering Chemistry Research, 2010, 49, 12605-12612.

(72) Ge, L., Zhou, W., Rudolph, V., Zhu, Z. H., Mixed Matrix Membranes Incorporated with Size-Reduced Cu-BTC for Improved Gas Separation. Journal of Materials Chemistry A, 2013, 1, 6350-6358.

(73) Chen, X. Y., Vinh-Thang, H., Rodrigue, D., Kaliaguine, S., Amine-Functionalized MIL-53 Metal-Organic Framework in Polyimide Mixed Matrix Membranes for CO_2/CH_4 Separation. Industrial & Engineering Chemistry Research, 2012, 51, 6895-6906.

(74) Rodenas, T., van Dalen, M., García-Pérez, E., Serra-Crespo, P., Zornoza, B., Kapteijn, F., Gascon, J., Visualizing MOF Mixed Matrix Membranes at the Nanoscale: Towards Structure-Performance Relationships in CO_2/CH_4 Separation Over NH_2-MIL-53(Al)@PI. Advanced Functional Materials, 2014, 24, 249-256.

(75) Zornoza, B., Martinez-Joaristi, A., Serra-Crespo, P., Tellez, C., Coronas, J., Gascon, J., Kapteijn, F., Functionalized Flexible MOFs as Fillers in Mixed Matrix Membranes for Highly Selective Separation of CO_2 from CH_4 at Elevated Pressures. Chemical Communications, 2011, 47, 9522-9524.

(76) Cao, L., Tao, K., Huang, A., Kong, C., Chen, L., A Highly Permeable Mixed Matrix Membrane Containing CAU-1-NH_2 for H_2 and CO_2 separation. Chemical Communications, 2013, 49, 8513-8515.

(77) Seoane, B., Sebastian, V., Tellez, C., Coronas, J., Crystallization in THF: the Possibility of One-Pot Synthesis of Mixed Matrix Membranes Containing MOF MIL-68(Al). CrystEngComm, 2013.

(78) Perez, E. V., Balkus Jr, K. J., Ferraris, J. P., Musselman, I. H., Mixed-Matrix Membranes Containing MOF-5 for Gas Separations. Journal of Membrane Science, 2009, 328, 165-173.

(79) Bae, T.-H., Lee, J. S., Qiu, W., Koros, W. J., Jones, C. W., Nair, S., A High-Performance Gas-Separation Membrane Containing Submicrometer-Sized Metal–Organic Framework Crystals. Angewandte Chemie International Edition, 2010, 49, 9863-9866.

(80) Yang, T., Xiao, Y., Chung, T.-S., Poly-/Metal-Benzimidazole Nano-Composite Membranes for Hydrogen Purification. Energy & Environmental Science, 2011, 4, 4171-4180.

(81) Ordonez, M. J. C., Balkus Jr, K. J., Ferraris, J. P., Musselman, I. H., Molecular Sieving Realized with ZIF-8/Matrimid Mixed-Matrix Membranes. Journal of Membrane Science, 2010, 361, 28-37.

(82) Song, Q. L., Nataraj, S. K., Roussenova, M. V., Tan, J. C., Hughes, D. J., Li, W., Bourgoin, P., Alam, M. A., Cheetham, A. K., Al-Muhtaseb, S. A., Sivaniah, E., Zeolitic Imidazolate Framework (ZIF-8) based Polymer Nanocomposite Membranes for Gas Separation. Energy & Environmental Science, 2012, 5, 8359-8369.

(83) Zornoza, B., Seoane, B., Zamaro, J. M., Téllez, C., Coronas, J., Combination of MOFs and Zeolites for Mixed-Matrix Membranes. ChemPhysChem, 2011, 12, 2781-2785.

(84) Askari, M., Chung, T.-S., Natural Gas Purification and Olefin/Paraffin Separation Using Thermal Cross-Linkable Co-Polyimide/ZIF-8 Mixed Matrix Membranes. Journal of Membrane Science, 2013,

444, 173-183.

(85) Wijenayake, S. N., Panapitiya, N. P., Versteeg, S. H., Nguyen, C. N., Goel, S., Balkus, K. J., Musselman, I. H., Ferraris, J. P., Surface Cross-Linking of ZIF-8/Polyimide Mixed Matrix Membranes (MMMs) for Gas Separation. Industrial & Engineering Chemistry Research, 2013, 52, 6991-7001.

(86) Perez, E. V., Balkus Jr, K. J., Ferraris, J. P., Musselman, I. H., Mixed-Matrix Membranes Containing MOF-5 for Gas Separations. Journal of Membrane Science, 2009, 328, 165-173.

(87) Adams, R., Carson, C., Ward, J., Tannenbaum, R., Koros, W., Metal Organic Framework Mixed Matrix Membranes for Gas Separations. Microporous and Mesoporous Materials, 2010, 131, 13-20.

(88) Car, A., Stropnik, C., Peinemann, K.-V., Hybrid Membrane Materials with Different Metal-Organic Frameworks (MOFs) for Gas Separation. Desalination, 2006, 200, 424-426.

(89) Ordoñez, M. J. C., Balkus Jr, K. J., Ferraris, J. P., Musselman, I. H., Molecular Sieving Realized with ZIF-8/Matrimid® Mixed-Matrix Membranes. Journal of Membrane Science, 2010, 361, 28-37.

(90) Díaz, K., López-González, M., del Castillo, L. F., Riande, E., Effect of Zeolitic Imidazolate Frameworks on the Gas Transport Performance of ZIF8-Poly(1,4-Phenylene Ether-Ether-Sulfone) Hybrid Membranes. Journal of Membrane Science, 2011, 383, 206-213.

(91) Dai, Y., Johnson, J. R., Karvan, O., Sholl, D. S., Koros, W. J., Ultem®/ZIF-8 mixed matrix hollow fiber membranes for CO_2/N_2 separations. Journal Of Membrane Science, 2012, 401–402, 76-82.

(92) Zhang, C., Dai, Y., Johnson, J. R., Karvan, O., Koros, W. J., High Performance ZIF-8/6FDA-DAM Mixed Matrix Membrane for Propylene/Propane Separations. Journal of Membrane Science, 2012, 389, 34-42.

(93) Basu, S., Maes, M., Cano-Odena, A., Alaerts, L., De Vos, D. E., Vankelecom, I. F. J., Solvent Resistant Nanofiltration (SRNF) Membranes based on Metal-Organic Frameworks. Journal of Membrane Science, 2009, 344, 190-198.

(94) Basu, S., Cano-Odena, A., Vankelecom, I. F. J., MOF-Containing Mixed-Matrix Membranes for CO_2/CH_4 and CO_2/N_2 Binary Gas Mixture Separations. Separation and Purification Technology, 2011, 81, 31-40.

(95) Basu, S., Cano-Odena, A., Vankelecom, I. F. J., Asymmetric Matrimid®/$[Cu_3(BTC)_2]$ Mixed-Matrix Membranes for Gas Separations. Journal of Membrane Science, 2010, 362, 478-487.

(96) Zornoza, B., Tellez, C., Coronas, J., Gascon, J., Kapteijn, F., Metal Organic Framework based Mixed Matrix Membranes: An Increasingly Important Field of Research with a Large Application Potential. Microporous and Mesoporous Materials, 2013, 166, 67-78.

(97) Liu, X.-L., Li, Y.-S., Zhu, G.-Q., Ban, Y.-J., Xu, L.-Y., Yang, W.-S., An Organophilic

Pervaporation Membrane Derived from Metal–Organic Framework Nanoparticles for Efficient Recovery of Bio-Alcohols. Angewandte Chemie International Edition, 2011, 50, 10636-10639.

(98) Kim, S., Lee, Y. M., Rigid and Microporous Polymers for Gas Separation Membranes. Progress In Polymer Science, 2015, 43, 1-32.

(99) Rezakazemi, M., Amooghin, A. E., Montazer-Rahmati, M. M., Ismail, A. F., Matsuura, T., State-of-the-Art Membrane based CO_2 Separation Using Mixed Matrix Membranes: An Overview on Current Status and Future Directions. Progress In Polymer Science, 2014.

(100) Seoane, B., Téllez, C., Coronas, J., Staudt, C., NH_2-MIL-53(Al) and NH_2-MIL-101(Al) in Sulfur-Containing Copolyimide Mixed Matrix Membranes for Gas Separation. Separation and Purification Technology, 2013, 111, 72-81.

(101) Rodenas, T., van Dalen, M., Serra-Crespo, P., Kapteijn, F., Gascon, J., Mixed Matrix Membranes based on NH_2-Functionalized MIL-Type MOFs: Influence of Structural and Operational Parameters on the CO_2/CH_4 Separation Performance. Microporous and Mesoporous Materials, 2014, 192, 35-42.

(102) Valero, M., Zornoza, B., Téllez, C., Coronas, J., Mixed Matrix Membranes for Gas Separation by Combination of Silica MCM-41 and MOF NH_2-MIL-53(Al) in Glassy Polymers. Microporous and Mesoporous Materials, 2013.

(103) Guo, X., Huang, H., Ban, Y., Yang, Q., Xiao, Y., Li, Y., Yang, W., Zhong, C., Mixed Matrix Membranes Incorporated with Amine-Functionalized Titanium-based Metal-Organic Framework for CO_2/CH_4 separation. Journal of Membrane Science, 2015, 478, 130-139.

(104) <Metal–organic framework based mixed matrix.pdf>. 2015.

(105) Yang, T., Chung, T.-S., Room-Temperature Synthesis of ZIF-90 Nanocrystals and the Derived Nano-Composite Membranes for Hydrogen Separation. Journal of Materials Chemistry A, 2013, 1, 6081.

(106) Xiao, Y., Guo, X., Huang, H., Yang, Q., Huang, A., Zhong, C., Synthesis of MIL-88B(Fe)/Matrimid Mixed-Matrix Membranes with High Hydrogen Permselectivity. RSC Advances, 2015, 5, 7253-7259.

(107) Zhang, C., Zhang, K., Xu, L., Labreche, Y., Kraftschik, B., Koros, W. J., Highly Scalable ZIF-based Mixed-Matrix Hollow Fiber Membranes for Advanced Hydrocarbon Separations. Aiche Journal, 2014, 60, 2625-2635.

(108) Kusworo, T. D., Ismail, A. F., Mustafa, A., Matsuura, T., Dependence of Membrane Morphology and Performance on Preparation Conditions: The Shear Rate Effect in Membrane Casting. Separation and Purification Technology, 2008, 61, 249-257.

(109) Sanchez-Lainez, J., Zornoza, B., Mayoral, A., Berenguer-Murcia, A., Cazorla-Amoros, D.,

Tellez, C., Coronas, J., Beyond the H_2/CO_2 Upper Bound: One-Step Crystallization and Separation of Nano-sized ZIF-11 by Centrifugation and its Application in Mixed Matrix Membranes. Journal of Materials Chemistry A, 2015, 3, 6549-6556.

(110) Chung, T.-S., Jiang, L. Y., Li, Y., Kulprathipanja, S., Mixed Matrix Membranes (MMMs) Comprising Organic Polymers with Dispersed Inorganic Fillers for Gas Separation. Progress In Polymer Science, 2007, 32, 483-507.

(111) Ren, H., Jin, J., Hu, J., Liu, H., Affinity between Metal-organic Frameworks and Polyimides in Asymmetric Mixed Matrix Membranes for Gas Separations. Industrial & Engineering Chemistry Research, 2012, 51, 10156-10164.

(112) Shi, G. M., Yang, T. X., Chung, T. S., Polybenzimidazole (PBI)/Zeolitic Imidazolate Frameworks (ZIF-8) Mixed Matrix Membranes for Pervaporation Dehydration of Alcohols. Journal of Membrane Science, 2012, 415, 577-586.

(113) Rodenas, T., Luz, I., Prieto, G., Seoane, B., Miro, H., Corma, A., Kapteijn, F., Llabrés i Xamena, F. X., Gascon, J., Metal–Organic Framework Nanosheets in Polymer Composite Materials for Gas Separation. Nature Materials, 2015, 14, 48-55.

(114) Hwang, S., Chi, W. S., Lee, S. J., Im, S. H., Kim, J. H., Kim, J., Hollow ZIF-8 Nanoparticles Improve the Permeability of Mixed Matrix Membranes for CO_2/CH_4 Gas Separation, in: Journal of Membrane Science, 2015, pp. 11-19.

(115) Xin, Q., Ouyang, J., Liu, T., Li, Z., Li, Z., Liu, Y., Wang, S., Wu, H., Jiang, Z., Cao, X., Enhanced Interfacial Interaction and CO_2 Separation Performance of Mixed Matrix Membrane by Incorporating Polyethylenimine-Decorated Metal-Organic Frameworks. ACS Applied Materials & Interfaces, 2015, 7, 1065-1077.

(116) Venna, S. R., Lartey, M., Li, T., Spore, A., Kumar, S., Nulwala, H. B., Luebke, D. R., Rosi, N. L., Albenze, E., Fabrication of MMMs with Improved Gas Separation Properties Using Externally-Functionalized MOF Particles. Journal of Materials Chemistry A, 2015, 3, 5014-5022.

(117) Hao, L., Li, P., Yang, T., Chung, T.-S., Room Temperature Ionic Liquid/ZIF-8 Mixed-Matrix Membranes for Natural Gas Sweetening and Post-Combustion CO_2 Capture. Journal of Membrane Science, 2013, 436, 221-231.

Chapter 3 Mixed matrix membranes with strengthened MOFs/polymer interfacial interaction and improved membrane performance

Introduction

As mention in 2.4.1, selection of the MOF/polymer pair is fundamentally important for MMMs fabrication because it is associated with the affinity and compatibility between MOF and polymer. However, most of the studies were performed without consideration of the difference between interactions of the MOFs with polymer matrix. This nature of interactions between organic linkers in MOFs and polymer chains can be used to improve the adhesion between MOFs and polymer of target MMMs by intentionally selecting the appropriate MOFs/polymer couple. Likewise, other achievements can be reached through designing and controlling the interface interaction including the elimination of the non-selective defect and the improvement in gas selectivity. The aim of the Chapter 3 is to develop novel mixed matrix membrane by selecting proper MOF/polymer pair for targeting MOF/polymer interfacial controls. The specific interfacial interaction between MOF and polymer chains are studied and the MOFs MMMs morphology and membrane gas separation were also comprehensively investigated.

Contributions

This chapter presents the fabrication and characterizations of MMMs with selected MOF/polymer couple, in an attempt to optimize the MOF/polymer interface by a specific interfacial interaction between MOF and polymer chains. Cd-6F synthesized with 6FDA ligand and in-situ polymerization of 6FDA-ODA were used to tailor the interfacial interaction in this Cd-6F/6FDA-ODA MMMs. A specific interaction between the uncoordinated $–COO^-$ on the surface of Cd-6F and the $–NH_2$ groups of ODA monomer at the terminal of poly (6FDA-ODA) chains has been achieved. Cd-6F in MMM derived from in-situ polymerization of 6FDA-ODA with the existence of Cd-6F shows the good adhesion with the 6FDA-ODA matrix. Both gas CO_2 permeability and selectivity of the MMM are significantly increased compared to the pure 6FDA-ODA polymer membrane. The strategy shown here may lead to the development of MOF/polymer pair selection and the interface manipulation in the fabrication of high performance MMMs. This chapter has been published in the ACS Applied Materials & Interfaces 2014, 6, 5609–5618.

Mixed Matrix Membranes with Strengthened MOFs/polymer Interfacial Interaction and Improved Membrane Performance

Rijia Lin[1], Lei Ge[1]*, Lei Hou[1,2], Ekaterina Strounina[3], Victor Rudolph[1], Zhonghua Zhu[1]*

[1]School of Chemical Engineering, The University of Queensland, Brisbane 4072 Australia

[2] Key Laboratory of Synthetic and Natural Functional Molecule Chemistry of the Ministry of Education, Northwest University, Xi'an 710069, P.R. China

[3]Centre for Advanced Imaging, The University of Queensland, Brisbane 4072 Australia

Abstract

MOFs-based mixed matrix membranes (MMMs) have attracted extensive attention in recent years due to their potential high separation performance, the low cost and good mechanical properties. However, it is still very challenging to achieve defect-free interface between micron-sized MOFs and polymer matrix. In this study, $[Cd_2L(H_2O)]_2 \cdot 5H_2O$ (Cd-6F) synthesized using 4,4'-(hexafluoroisopropylidene) diphthalic anhydride (6FDA) as organic ligand was introduced into the 6FDA-ODA polyimide matrix to achieve novel MOF MMMs. A specific interfacial interaction between MOF crystals and polymer chains was innovatively targeted and achieved through in-situ polymerization procedure. The enhanced adhesion between MOF particles and polymer phase was observed, and the improved interfacial interaction between Cd-6F and 6FDA-ODA polyimide matrix was confirmed by detailed characterisations including FTIR and NMR. In the meantime, the gas permeance and selectivity of the MMMs are strongly dependent on their morphology. The MMM derived from in-situ polymerization presents excellent interfaces between micron-sized MOF crystals and polymer matrix, resulting in increased permeability and selectivity. The strategy shown here can be further utilized to select MOF/polymer pair, eliminate interfacial voids and improve membrane separation performance of MOFs-based MMMs.

3.1 Introduction

Gas separation continues to be an active area of research and membrane technology has been found far superior to conventional separation method, for its high energy efficiency, low production cost and inappreciable environmental impact.[1-3] Nonetheless, most of the conventional polymer membranes are restricted to the limit of trade-off between permeability and selectivity,[4, 5] for instance, high selectivity is always achieved at the cost of low permeability. One effective treatment is to introduce inorganic fillers such as zeolites,[6, 7] carbon nanotubes,[8, 9] carbon molecular sieves,[10, 11] and mesoporous silica[12] into polymer matrix to obtain mixed matrix membranes (MMMs). The selection of inorganic fillers is commensurate with the importance of polymer matrix, which depends not only on the separation performance of inorganic particles but also on the compatibility with the polymer matrix.

Metal organic frameworks (MOFs), a novel hybrid materials consisting of organic and inorganic moieties in crystalline lattices, have many characteristics favourable towards use as filler embeded in MMMs.[13-16] Due to their large surface area, controllable porosity and high adsorption affinity, [17, 18] it provides promising opportunities of developing novel MOF MMMs with outstanding permeability and selectivity. MOF MMMs show impressive separation performance with the combination of molecular sieving effect of MOFs and common feature of polymers matrix, which can be an alternative approach to solve the trade-off problem of traditional polymer membranes. Moreover, the employment of MOFs in MMMs provides several potential advantages over other inorganic fillers, MOFs perform better compatibility with the polymer matrix since the organic linkers in MOFs can provide stronger interaction with polymer chains.[19]

Despite of the promising perspectives, the production of MOFs-based membranes is still an on-going area of investigation. As the structure is heterogeneous, defects can be observed between MOFs and polymer matrix which may be the underlying reason for the deterioration of gas selectivity and integrity of membrane structure.[10, 20, 21] To achieve good interficial mophology, the followings need to be considered: (1) proper selection of the MOF/polymer pair, (2) sufficient dispersion of inorganic phase in the polymer phase to avoid aggregation of particle and (3) enhancement of interfacial interaction between inorganic phase and continuous phase. Amongst them, pair-wise selection is the basis for MMMs fabrication which is associated with affinity and compatibility between filler particles and polymer. Several experimental approaches have been proposed to produce MMMs with favourable interfacial property.[22-27] In general, the size of MOFs particles is preferable to be nano or sub-micrometer (eg. ZIF-8 and NH_2-MIL-5) in order to achieve strong interaction with the polymer matrix as well as good dispersion.[22-24, 28-31] A void-free MMM with high gas separation performance

was prepared by Bae *et al* by applying as-synthesized submicrometer-sized ZIF-90 in fabrication of ZIF-90/6FDA-DAM.[28] On the other hand, the implement of micron-sized MOFs as fillets requires stronger interfacial adhesion which can be achieved through modification of MOFs and/or polymers. Functionalization of MOFs can improve the affinity between MOF linkers and polymer chains, and also eliminate the formation of non-selective interfacial voids.[20, 21] Another feasible way is tailoring MOFs by physical treatment. In our previous work, the size of Cu-BTC was reduced by using a facial sonication post-treatment and the affinity between MOF and polymer is largely improved.[27] Compared to modification of MOFs, polymer matrix can be improved by introducing cross-linkable polymer (*e.g.* copolyimides) and solidifying it after the cast of MMMs,[26] or surface cross-linking the MMMs with a cross-linking agent.[25]

Although numerous research has been conducted on MOF-based MMMs, the studies on the selection of the appropriate MOFs/polymer couples for targeting MOF/polymer interfacial controls are still limited. In this study, a specific MOF/polymer pair was chosen for the MMM fabrication with targeted interfacial interaction. For polymer selection, 4,4'-(hexafluoroisopropylidene)diphthalic anhydride-4,4'-oxydianiline (6FDA-ODA) polyimide was selected in this work due to its good combination of selectivity and permeability coefficients for CO_2/CH_4 separation.[29, 30] As to the MOFs, $[Cd_2L(H_2O)]_2 \cdot 5H_2O$ (Cd-6F)[31, 32] with high sorption selectivity of CO_2 over N_2 and CH_4 was chosen here to embed into the 6FDA-ODA polymer matrix. Particularly, Cd-6F was synthesized by using 4,4'-(hexafluoroisopropylidene)diphthalic anhydride (6FDA) as the organic linker which is also one of the monomers in the 6FDA-ODA synthesis. Targeted interfacial interaction was studied by controlling the in-situ polymerization synthesis procedure. The MOFs MMMs morphology and membrane gas separation were also comprehensively investigated.

3.2 Experimental section

3.2.1 Materials synthesis

3.2.1.1 Materials

4, 4'-(Hexafluoroisopropylidene) diphthalic anhydride (6FDA), oxydianiline (ODA), cadmium nitrate tetrahydrate, dimethylformamide (DMF), triethylamine, ethanol, methyl ethyl ketone (MEK) were supplied by Sigma-Aldrich.

3.2.1.2 Cd-6F crystals synthesis

Cd-6F was synthesized based on a manner reported elsewhere.[31] 0.868 g $Cd(NO_3)_2 \cdot 4H_2O$ and 0. 616 g 6FDA were mixed into 70 mL of a 50 vol.% : 50 vol.% ethanol-water. Then the mixture was

transferred into a Teflon-line stainless steel autoclave and heated at 140 ºC for 72 h, and cooled to room temperature at a rate of 0.1 ºC/min. The colorless crystals product was filtered, washed with DMF and dried at 80 ºC in vacuum for 24 h.

3.2.1.3 Membrane preparation

The procedures of pure 6FDA-ODA polyimide membrane preparation are shown in Figure 3-1. 6FDA-ODA polyimide was prepared by a three-step method similar to a work reported elsewhere.[33] **In the step 1**, 1.00 g of ODA was dissolved into 10 mL of DMF. Once the ODA was fully dissolved, 2.22 g of 6FDA powder was added, followed by 5 mL of DMF. The mixture was stirred under nitrogen at room temperature for 3 h to form poly amic acid (PAA). **In the step 2**, 1.7 mL of triethylamine and 3 mL of DMF were added slowly to the reaction mixture, which was stirred under nitrogen at room temperature for additional 3 h. After that, poly(amic acid) tertiary amine salt (PAAS) was recovered by precipitating with a large amount of MEK, then washed by MEK and dried at 50 ºC for 24 h. **In the step 3**, the polyimide film was obtained by thermal imidization of its PAAS. PAAS was dissolved in DMF (15 wt. %) at room temperature and stirred for 6 h. The solution was cast onto a clean glass plate, followed by drying at 150 ºC for 24 h in a vacuum oven. Figure 3-2 shows the casting knife applied in this study.

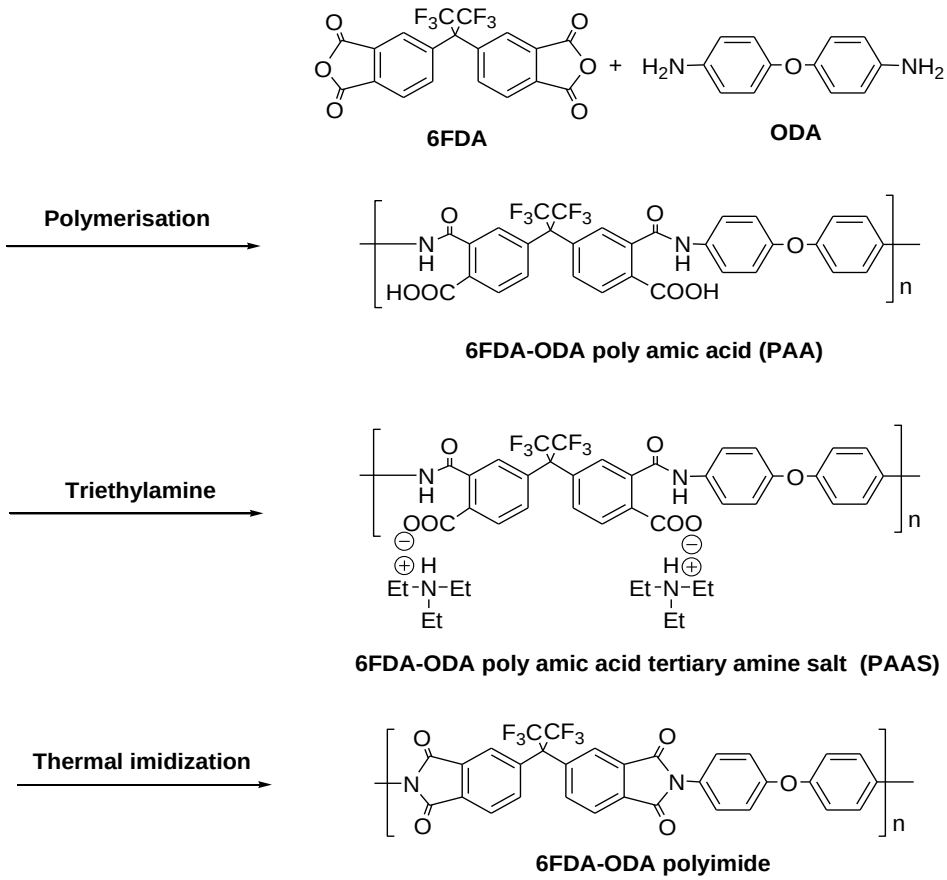

Figure 3-1 Multi-staged of 6FDA-ODA poly (amic acid) salt and polyimide synthesis

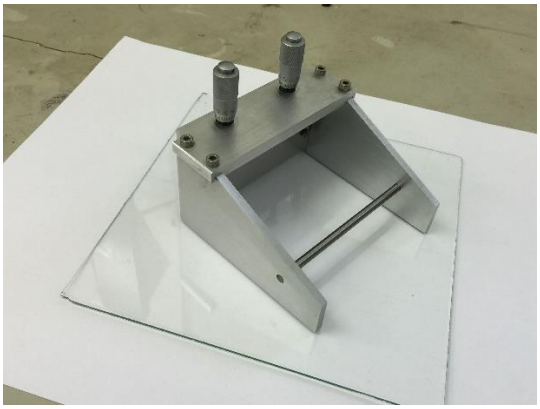

Figure 3-2 The casting knife applied in this study

Cd-6F based MMMs were prepared by incorporation of Cd-6F at each stages of polyimide synthesis, as shown in Figure 3-3. The derived MMMs from three different synthesis routes were marked as MMM-A, MMM-B and MMM-C, respectively. Before embedding in mixed matrix membranes, the as-synthesised Cd-6F was grinded into smaller and more uniform particles by ball milling (Fritsch, Pulverisette, Germany) for 15 min at a rotational speed of 750 rpm. For the films of type MMM-A, Cd-6F filler was dispersed in DMF and sonicated for 1-2 min before the step 1 of the pure 6FDA-ODA membrane fabrication. Then the polymerization was carried on in the presence of MOF filler following the step 1 and step 2 described above. After reacting with triethylamine, the filler suspension was directly cast onto a glass plate and heated at 150 ºC for 24 h under vacuum to form the final product. In the route B, Cd-6F was added into DMF and the suspension was sonicated for 1-2 min before adding the PAAS obtained in the step 2. The mixture was further stirred for 6 h and was cast onto a glass plate. MMM-B was obtained by thermal imidization of PAAS in the presence of Cd-6F at 150 ºC for 24 h under vacuum. In the route C, the solid PAAS was heated at 150 ºC to prepare the 6FDA-ODA polyimide. Cd-6F was also dispersed in DMF and sonicated for 1-2 min. The 6FDA-ODA polyimide obtained by thermal imidization of PAAS was added followed by an additional 6 h stir. The resulting mixture was cast and dried at 150 ºC for 24 h under vacuum to form MMM-C. The selected thickness for casting procedure was 40 μm for all the membranes. The thickness of pure 6FDA-ODA and MMMs were measured using a micrometer within the range of 30–40 μm.

The loadings of Cd-6F in composite membranes were calculated by Eq. (3-1):

$$\phi = \frac{m_{\text{Cd-6F}}}{m_{\text{Cd-6F}} + m_{\text{6FDA-ODA polyimide}}} \quad (3\text{-}1)$$

where $m_{\text{Cd-6F}}$ and $m_{\text{6FDA-ODA polyimide}}$ are the mass of Cd-6F and 6FDA-ODA after imidization in the

MMMs, respectively.

In order to investigate the interaction between Cd-6F and the polymer matrix, Cd-6F and ODA were mixed into DMF and the suspension was stirred for 1 h and 6 h separately. The resulting Cd-6F was recovered by centrifugation, and then washed by ethanol for several times to remove the remained DMF. The resulting Cd-6F was dried at 80 ºC in a vacuum oven.

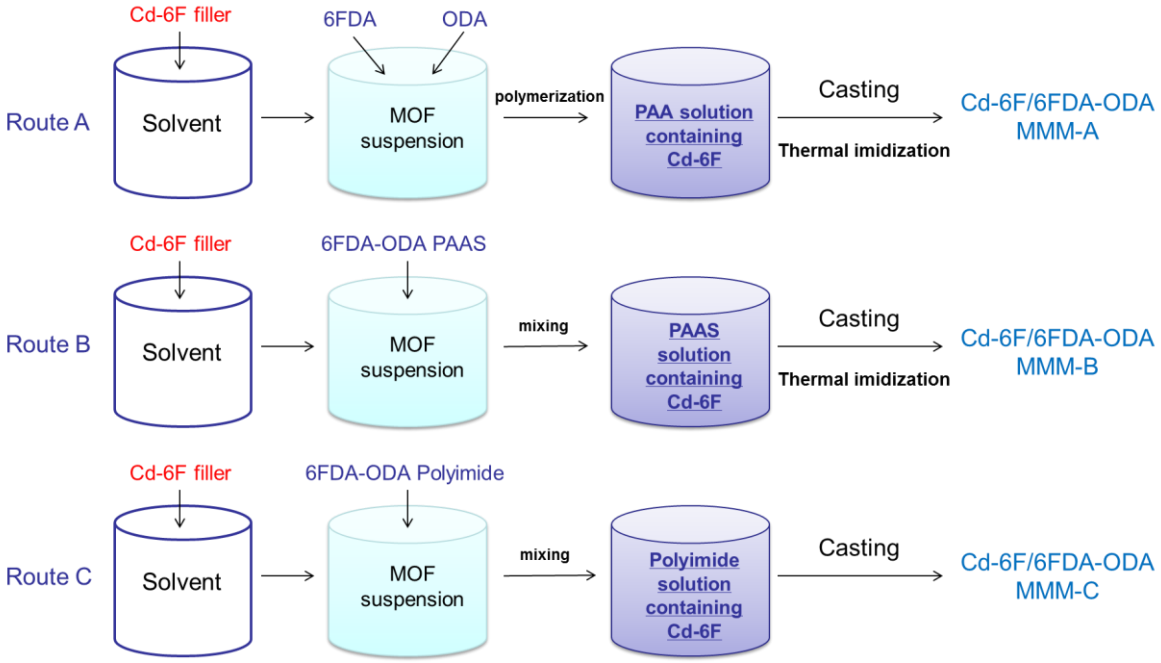

Figure 3-3 Schematic diagram of three different synthesis routes for Cd-6F based MMMs

3.2.2 Characterization

The X-ray diffraction spectra (XRD) of Cd-6F and mixed matrix membranes were obtained with a Brucker Advanced X-ray Diffractometer (40 kV, 30 mA) with Cu Kα (λ= 0.15406 nm) radiation at a scanning rate of 1º min^{-1} from 5º to 50º. Infrared spectra were obtained with a PerkinElmer Spectrum 100 spectrometer equipped with an attenuated total reflection (ATR) objective. All spectra were collected from 650 to 4000 cm^{-1} wavenumbers. The thermal stability of MMMs and the Cd-F loadings were measured by a Perkin Elmer Instruments STA 6000 Thermo Gravimetric Analyser. All samples were heated under an air atmosphere at a uniform heating rate of 5 ºC min^{-1} from 40 to 800 ºC. The N_2 adsorption isotherms of Cd-6F were obtained with a Micromeritics TriStar II 3020 at 77 K, after degassing the sample at 150 ºC for 24 h and 200 ºC for 2 h. The corresponding specific surface area was analysed using the Langmuir and BET theories at relative pressure (p/p^0) between 0.005 and 0.05. After N_2 adsorption, the samples were regenerated at 150 ºC under a pressure of 10 mTorr until no further pressure drop was observed. Then, the adsorption isotherms of CO_2 and N_2 at 273 K and 298

K were measured using the same instrument. The desorption isotherms of CO_2 and N_2 were obtained by gradually decreasing the system pressure. The adsorption selectivity of CO_2 to N_2 (S) is calculated according equation:

$$S = \frac{q_{CO2} / q_{N2}}{p_{CO2} / p_{N2}} \quad (3\text{-}2)$$

where S is the relative selectivity value, q is the amount of adsorbed gas ($cm^3\ g^{-1}$), p is the exact gas pressure (kPa).

The high pressure sorption of CO_2 and N_2 was tested in BEL-BG using a magnetic suspension balance (Rubotherm) with high accuracies. About 0.7 g of pure 6FDA-ODA or MMMs was degassed at 80 ^oC under vacuum for 2 to 4 h before adsorption. The particle size distributions of the Cd-6F after ball milling was measured by a Malvern Zetasizer with 0.2% Cd-6F in ethanol at 25 ^oC. The analysis was done using a general purpose model. The morphologies of the samples were obtained with a JEOL JSM6300 scanning electron microscope (SEM) at 5 kV. Solid-state NMR was performed on the Avance III spectrometer (Bruker), operating at 300.13 MHz for ^1H and 75.47 MHz for ^{13}C. Powdered material was placed in the 4 mm zirconium rotor with Kel-F cap and rotated at 7kHz. CPMAS technique with 1ms cross-polarization time was employed. Usual parameters included 42ms acquisition time with sweep width of 40 kHz and recycling delay 3s; 2K data points were collected. High-power decoupling was applied using tppm15 scheme. X-ray photoelectron spectroscopy (XPS) was performed on a PHI-560 ESCA (Perkin Elmer) using a non-monochromatic Mg Kα excitation source at 15 kV. The C 1s peak position was set to 284.6 eV and taken as an internal standard.

3.2.3 Permeation test

The variable feed pressure and the constant volume permeation system was used to measure the gas permeation of pure 6FDA-ODA and MMMs, as described elsewhere.[9] The membranes were held under vacuum for approximately 5 min to achieve a steady state before the exposing to the selected gas at a specific pressure. Before switching to the feed gas, the membrane has to be degassed for some time to ensure the complete desorb of initial permeate gas. The permeation coefficient is calculated using the following equation:

$$P = \frac{273.15 \times 10^{10}}{760\mathrm{AT}} \frac{VL}{\frac{P_0 \times 76}{14.7}} \frac{\mathrm{d}p}{\mathrm{d}t} \quad (3\text{-}3)$$

where P is the permeation coefficient in barrer (1 barrer $=1\times10^{-10}$ cm^3 (STP) cm cm^{-2} s^{-1} cm Hg^{-1}), A is the effective area of the membrane (cm^2), T is the absolute temperature (K), V is the dead-volume

of the downstream chamber (cm^3), L is the membrane thickness (cm), P_0 is the feed pressure (psi), and dp/dt is the steady rate of pressure increase in the downstream side (mm Hg s^{-1}).

The ideal selectivity for two gases is determined as:

$$\alpha = \frac{P_A}{P_B} \quad (3\text{-}4)$$

where P_A and P_B are the permeation coefficients of pure gas A and B, respectively.

3. 3 Results and discussions

3.3.1 Synthesis and characterization of Cd-6F

Figure 3-4 presents the XRD spectra Cd-6F and simulated structure diagram of Cd-6F. Based on the Cd-6F structural data,[31, 32] the observed pattern shows high similarity to the simulated pattern, which confirm the formation of well-crystallined pure Cd-6F. Figure 3-5 shows the crystal morphology of the as-synthesized Cd-6F samples. The as-synthesized Cd-6F crystals consist of heterogeneous hexagonal-shaped crystals with various dimensions up to several mm long. In order to achieve more uniform distribution particles for the MMM fabrication, ball milling was used to reduce the size of the as-synthesized Cd-6F. After the ball mill treatment, the size of Cd-6F crystals becomes smaller (shown in Figure 3-6a). The particle size distributions of ball mill-treated Cd-6F is also shown in Figure 3-6b. The particles tend to be smaller and more homogeneously distributed compared to the as-synthesized sample Cd-6F, which matches well with the SEM observation (Figure 3-6a).

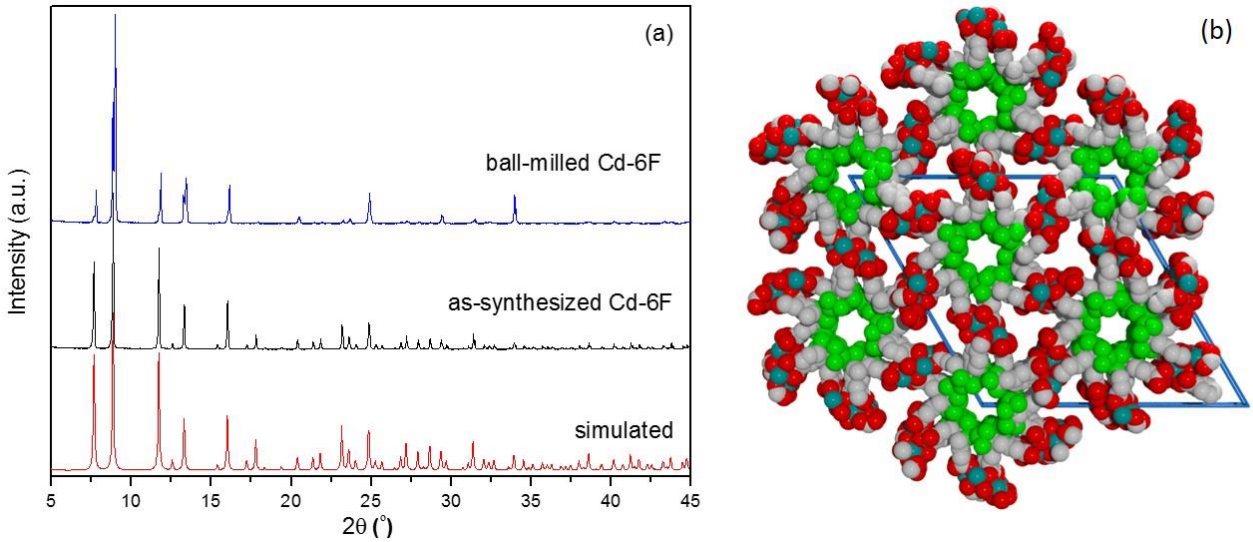

Figure 3-4 (a) XRDs spectra of as-synthesized Cd-6F and ball-milled Cd-6F (b) Projection view of the Cd-6F framework along the *c*-axis (red: O, white: C, green: F, cyan: Cd)

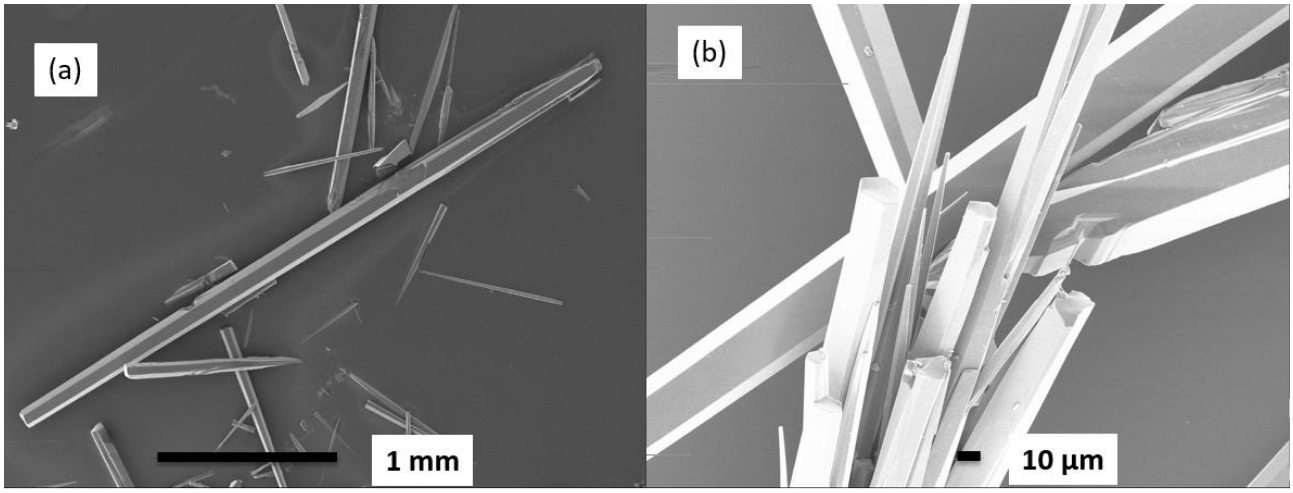

Figure 3-5 SEM images of as-synthesized Cd-6F crystals

(a: low magnification; b: high magnification)

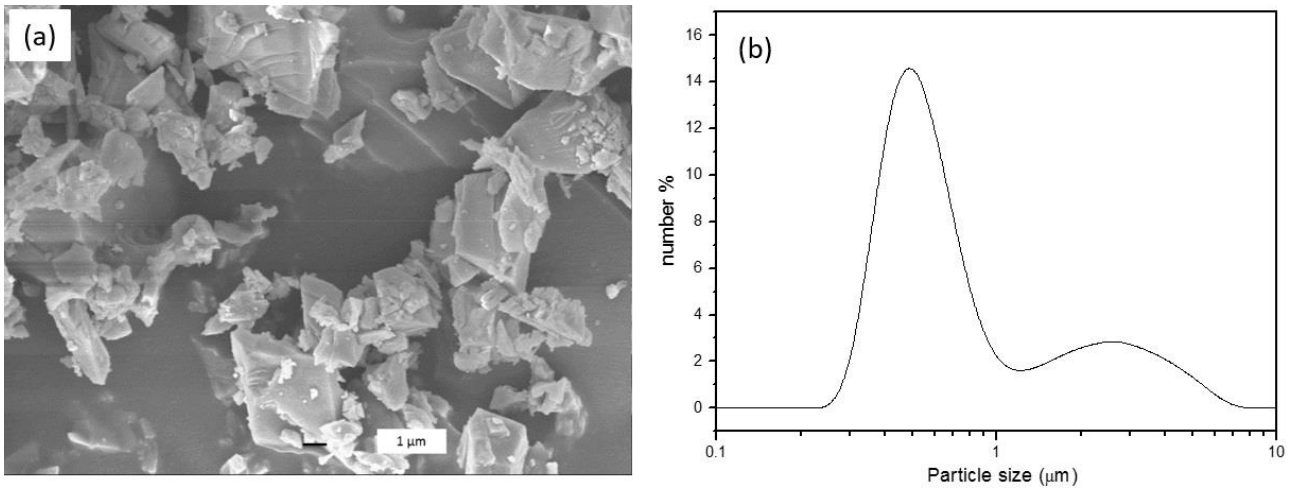

Figure 3-6 SEM image of ball mill-treated Cd-6F; (b) Particle size distribution of ball mill-treated Cd-6F

Thermal gravimetric analysis (TGA) shows that Cd-6F remains stable below 250 ºC, the weight loss can be assigned to the evacuation of solvent and coordinated H_2O (Figure 3-7) and the curve matches well with the previous report.[31] Noteworthy, the excellent thermal stability of Cd-6F can meet the requirement of membrane fabrication at the temperature of thermal imidization of polymer (~150 ºC). The nitrogen sorption isotherm of Cd-6F performed at 77 K is presented in Figure 3-8a. The BET surface area and pore volume were summarized in Table 3-1. The results are consistent with the previous study.[31] The CO_2 and N_2 adsorption capacities of Cd-6F are depicted in Figure 3-8b. The adsorption quantities of CO_2 and N_2 on the Cd-6F add up to 42.0 $cm^3\ g^{-1}$ and 5.11 $cm^3\ g^{-1}$, respectively, at 111 kPa and 273 K. Adsorption capacity of CO_2 and N_2 decreases when the temperature increases to 298 K, which is similar to the previous work of Cd-6F.[34] The influence of temperature on the

adsorption capability can be attributed to the decrease of maximum pore density (or pore capacity) with the increased molecular mobility during heating. More importantly, Cd-6F exhibits almost no uptake of N_2 (0.72 cm^3 g^{-1}) but a CO_2 uptake of up to 30.9 cm^3 g^{-1} at 298 K and ambient pressure. The relative CO_2/N_2 adsorption selectivity is as high as 42.89 at 298 K, 101 kPa, which is higher than that of most MOFs which are usually used in MMMs fabrication, such as Cu-BTC and MIL-53.[27, 34] Therefore, with combination of the promising sorption capacity and excellent selectivity at membrane operation temperature (298 K), Cd-6F can provide great potential in gas separation.

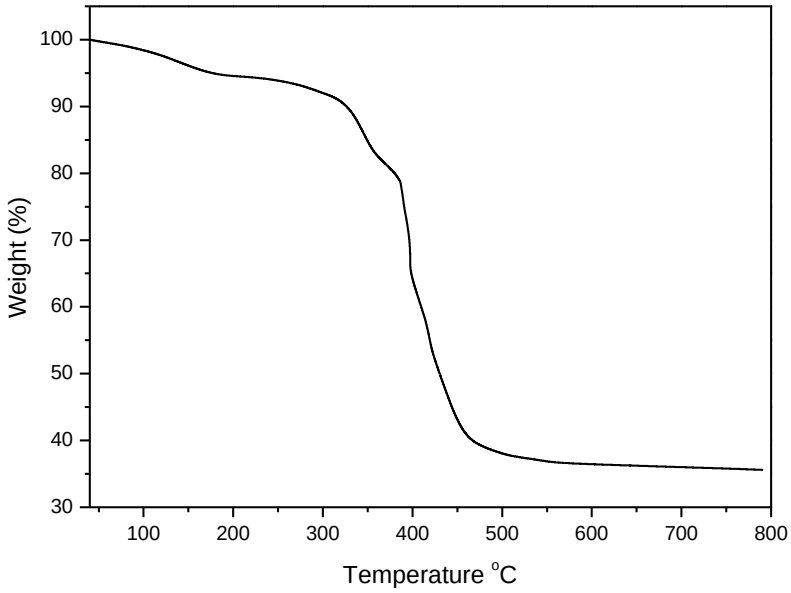

Figure 3-7 TGA curve of Cd-6F under air atmosphere

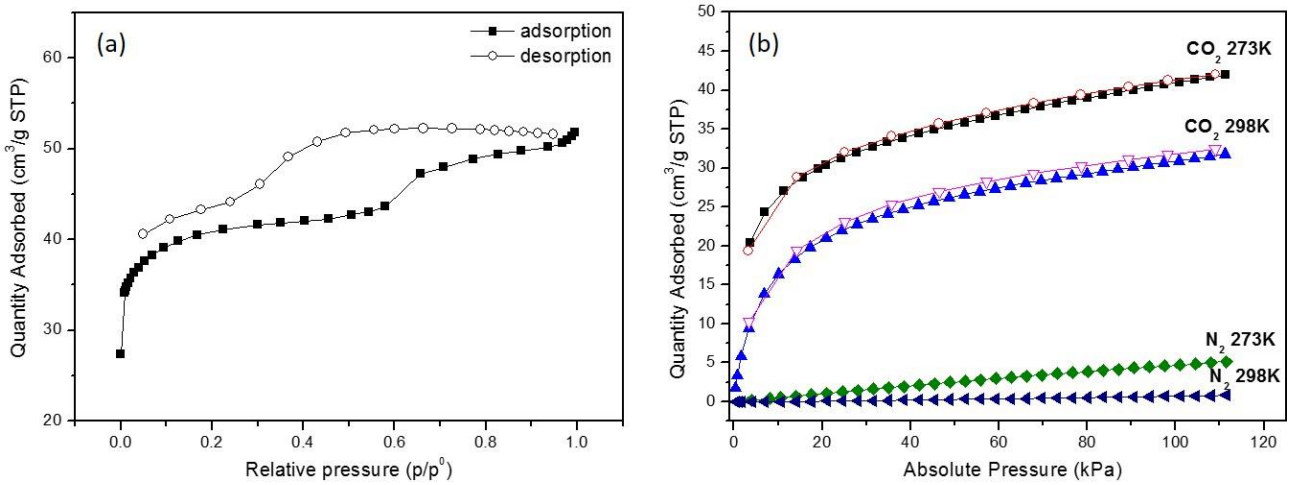

Figure 3-8 (a) Nitrogen sorption isotherm of Cd-6F at 77 K; (b) CO_2 and N_2 adsorption isotherms of Cd-6F at 273K and 298K (Solid: adsorption; hollow: desorption)

Table 3-1 Physical properties of Cd-6F

Cd-6FDA	
BET surface area (m^2 g^{-1})	157.0
Langmuir surface area (m^2 g^{-1})	163.1
Micropore volume (cm^3 g^{-1})	0.061

3.3.2 Characterization of Cd-6F mixed matrix membranes

In order to check the phase structure of MMMs and the stability of incorporated Cd-6F, the XRD patterns of MMMs synthesized in three routes with the same MOF loading were examined and are shown in Figure 3-9, along with the pure 6FDA-ODA polyimide. The XRD pattern of pure 6FDA-ODA shows a broad peak from 10° to 22°, which is consistent with the reported XRD pattern for 6FDA-ODA in the literature.[35] The patterns of MMM-A, MMM-B and MMM-C all display main reflection peaks of Cd-6F matching well with the Cd-6F XRD pattern in Figure 3-4, indicating that the membrane preparation procedures different routes does not change the crystallinity of Cd-6F.

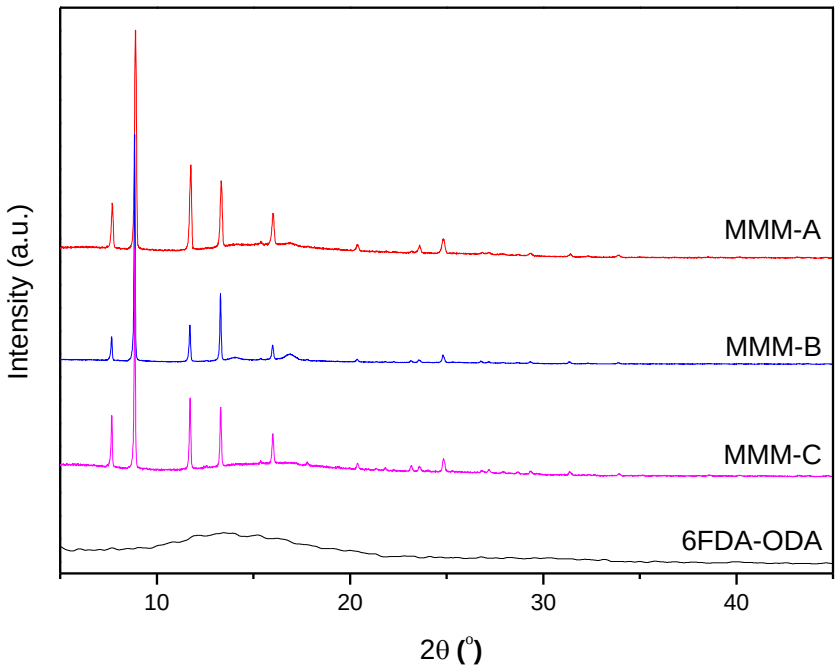

Figure 3-9 XRD pattern of Cd-6F, pure 6FDA-ODA and MMMs (10 wt.% MOF loading) synthesized from different routes

The FTIR-ATR spectra of the MMMs are shown in Figure 3-10. As to Cd-6F, bands at 1547 cm^{-1} and 1529 cm^{-1} represent the asymmetric stretching vibrations of the carboxylate groups in 4,4'-(hexafluoroisopropylidene) diphthalate, while that at 1409 cm^{-1} is for the symmetric stretching vibrations. As to the pure 6FDA-ODA polyimide, bands at 1725 cm^{-1} is attributed to asymmetric

stretch of the carbonyl group (imide I band), peaks at 1785 cm^{-1} is assigned to symmetric stretch of the carbonyl group (imide II band) and bands at 1374 cm^{-1} correspond to C−N stretch (imide rings). These characteristic peaks suggest that 6FDA-ODA membranes have imides functional groups.[33, 35] For the Cd-6F/6FDA-ODA MMMs with a Cd-6F loading of 10 wt.%, weak band around 1550 cm^{-1} to 1530 cm^{-1} appears, indicating the presence of Cd-6F in MMMs. On the other hand, there is no obvious difference between the FTIR-ATR spectra of MMM-A, MMM-B and MMM-C since all the MMMs have the similar chemical composition. Also signals of Cd-6F are overlapped by 6FDA-ODA peaks owing to the similar structure of 6FDA and relative low Cd-6F loading percentage in MMMs.

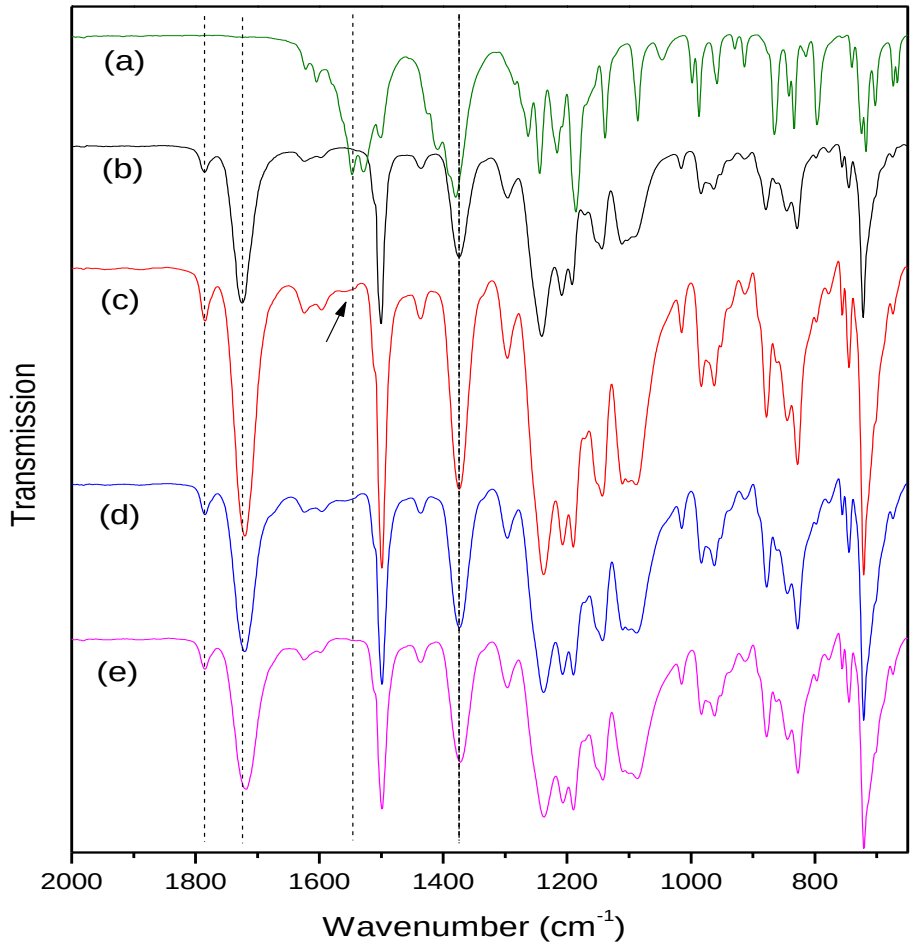

Figure 3-10 FTIR-ATR spectra of Cd-6F crystals (a), pure 6FDA-ODA (b) and Cd-6F/6FDA-ODA MMMs (c: 10% MMM-A, d: 10% MMM-B, e: 10% MMM-c)

As to the MMMs, the interfacial morphology of polymer matrix and filler can dramatically affect the membrane integrity and overall transport properties. Improving the polymer-particle adhesion and eliminating the interface voids are critical for enhancing the separation performance of MMMs. Therefore, Cd-6F/6FDA-ODA was intentionally chosen as the MOF/polymer pair for the MMM fabrication in this study. A specific interfacial interaction was designed as described in Figure 3-11.

The in-situ polymerization was carried out in the presence of Cd-6F. Cd-6F crystals were dispersed into solvent to form a MOF suspension before adding ODA and 6FDA monomers and initializing the polymerization reaction. During the reaction, ODA not only reacts with 6FDA, but also introduces a specific interaction between the $–COO^-$ on the surface of Cd-6F and the $–NH_2$ groups of ODA monomer at the terminal of poly (6FDA-ODA) chains. Such a MOF/polymer contact was targeted to achieve remarkable MOF adhesion to the polymer matrix.

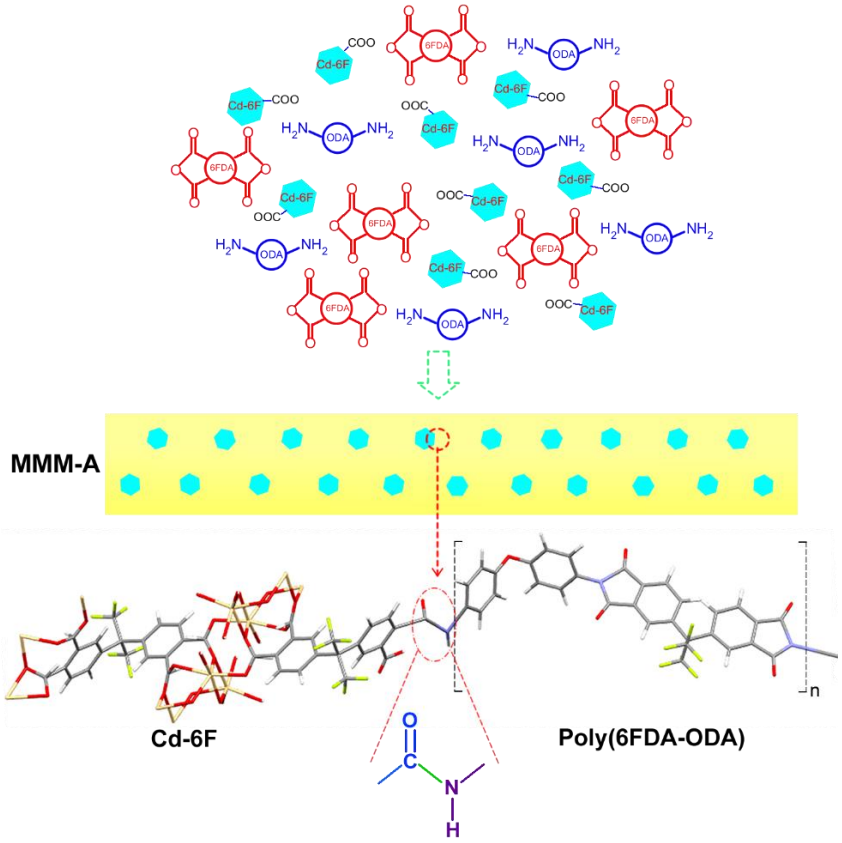

Figure 3-11 Diagram of designed interaction between Cd-6F and 6FDA-ODA in MMM-A

Figure 3-12 displays the SEM images of cross-section morphology of pure 6FDA-ODA and the corresponding MMMs synthesized from different procedures. As can be seen in Figure 3-12a, b, the cross-section of pure 6FDA-ODA polyimide is smooth and clean. In Figure 3-12c, d, the micrometer-sized Cd-6F crystals show excellent adhesion with the 6FDA-ODA polyimide in MMM-A, as indicated by arrows. No interfacial gaps are observed between Cd-6F and polymer. As to the MMM-B (Figure 3-12e, f) and MMM-C (Figure 3-12g, h), the interface between Cd-6F and polymer is clearly worse than that of the MMM-A. Some voids and poor adhesion at the MOF–polymer interface are observed, as indicated by circles. Therefore, different fabrication procedures play crucial roles on the morphology of Cd-6F/6FDA-ODA MMMs. The good compatibility with Cd-6F/6FDA-ODA in MMM-A can be explained by two main reasons: (1) Cd-6F was dispersed in the solvent before the

polymerization reaction and the reaction was carried out in the presence of Cd-6F; (2) There is specific interfacial interaction between Cd-6F and 6FDA-ODA polyimide under the condition of Route A.

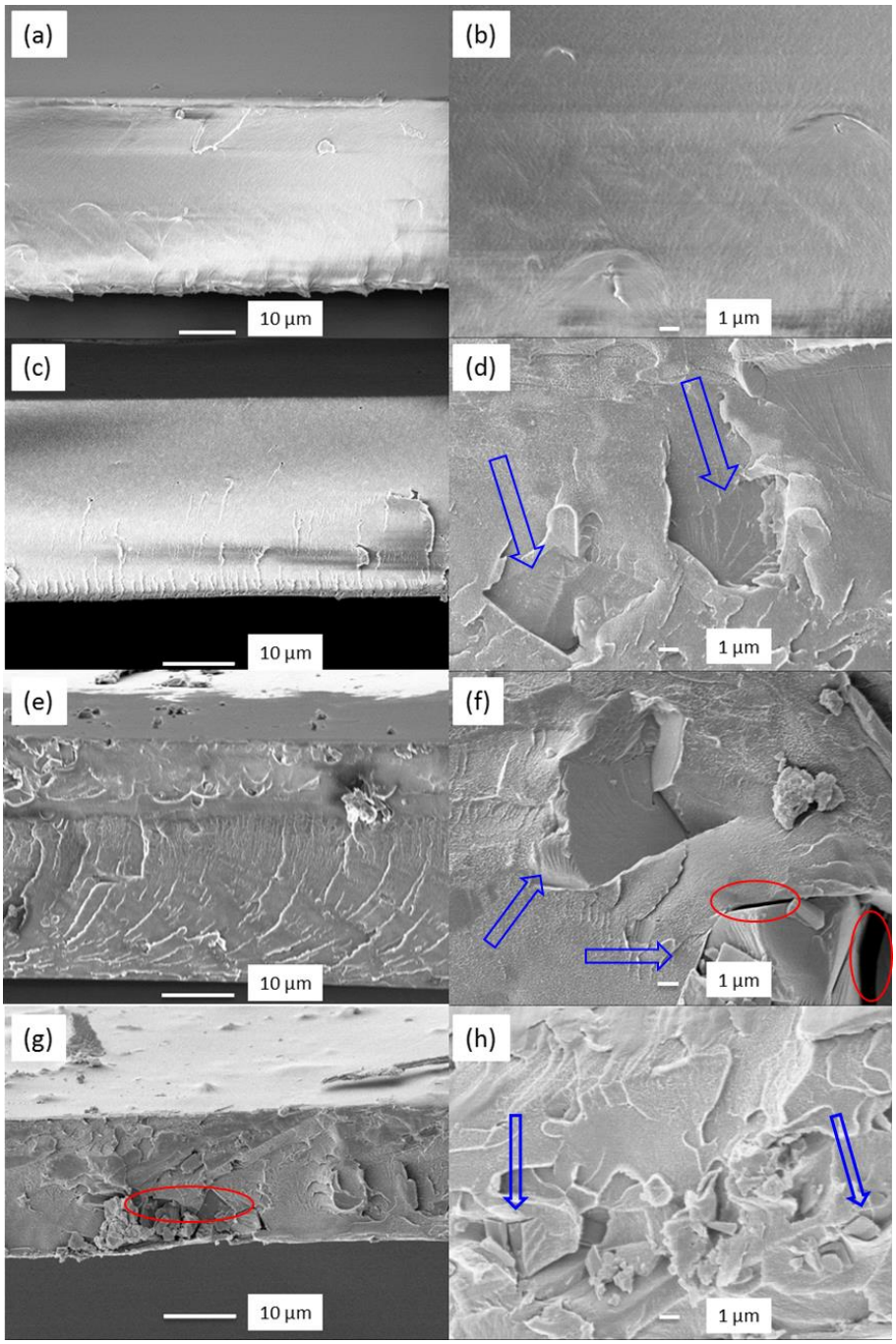

Figure 3-12 SEM images of pure 6FDA-ODA (a, b), and MMM-A (c, d), MMM-B (e, f), MMM-C (g, h). Arrows point to the MOF crystals embedded in polymer matrix. Circles indicate defects and voids between MOF and polymer matrix. The Cd-6F content of all the membranes is 10 wt.%.

In order to investigate the interaction between Cd-6F and 6FDA, an intended experiment was carried out by mixing Cd-6F with ODA in DMF solution for several hours without 6FDA. The ethanol

washed Cd-6F powders was characterized by FTIR, as shown in Figure 3-13. In the spectrum of ODA, the adsorptions at 815 cm^{-1}, 1620 cm^{-1} and around 3350 cm^{-1} are corresponding to N-H of primary amine groups. The 1495 cm^{-1} peak in the ODA spectrum can be assigned to C=C ring stretching. The peak at 1212 cm^{-1} indicates the Ar–O–Ar stretching. After reacting Cd-6F with ODA, a weak band at 1651 cm^{-1} appeared, which should be ascribed to C=O stretching vibration of amide. It is obvious that the peak intensity increased with the increase of reaction duration. On the other hand, peaks around 1620 cm^{-1} and 3350 cm^{-1} in the ODA spectrum weaken in the Cd-6F-ODA spectrum. This is because that the primary amine groups $–NH_2$ in ODA are transformed into secondary amine groups –NH– after reacting with Cd-6F. The –NH– adsorption are relative weak around 1620 cm^{-1} and 3350 cm^{-1}, these peaks in Cd-6F-ODA spectra will become not obvious after the interfacial reaction. These results indicate that Cd-6F could interact with ODA by generating–NH–CO– groups and more –NH–CO– groups can be formed on the surface of Cd-6F with prolonging reaction time.

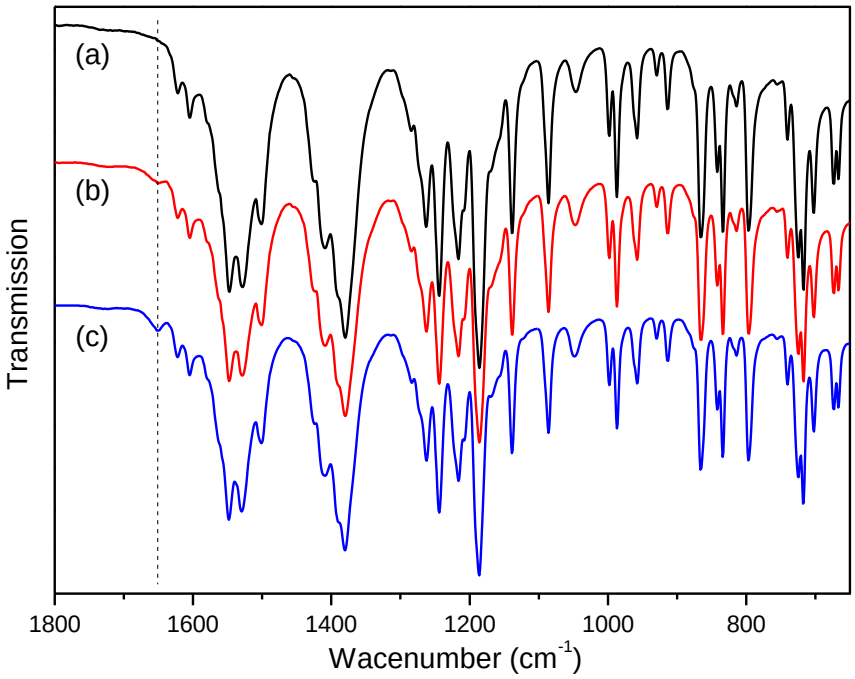

Figure 3-13 FTIR-ATR spectra of pure Cd-6F (a), Cd-6F mixed with ODA for 1 h (b), Cd-6F mixed with ODA for 6 h (c), and ODA (d)

^{13}C solid-state NMR was used to further confirm the interaction between Cd-6F and ODA monomer, as shown in Figure 3-14. Compared with the pattern of pure Cd-6F, a new peak at 165 ppm appeared (red square in Figure 3-14a), which can be assigned to C=O emphasized in red square in Figure 3-14b.[36, 37] This result agrees well with the FTIR test in Figure 3-13.

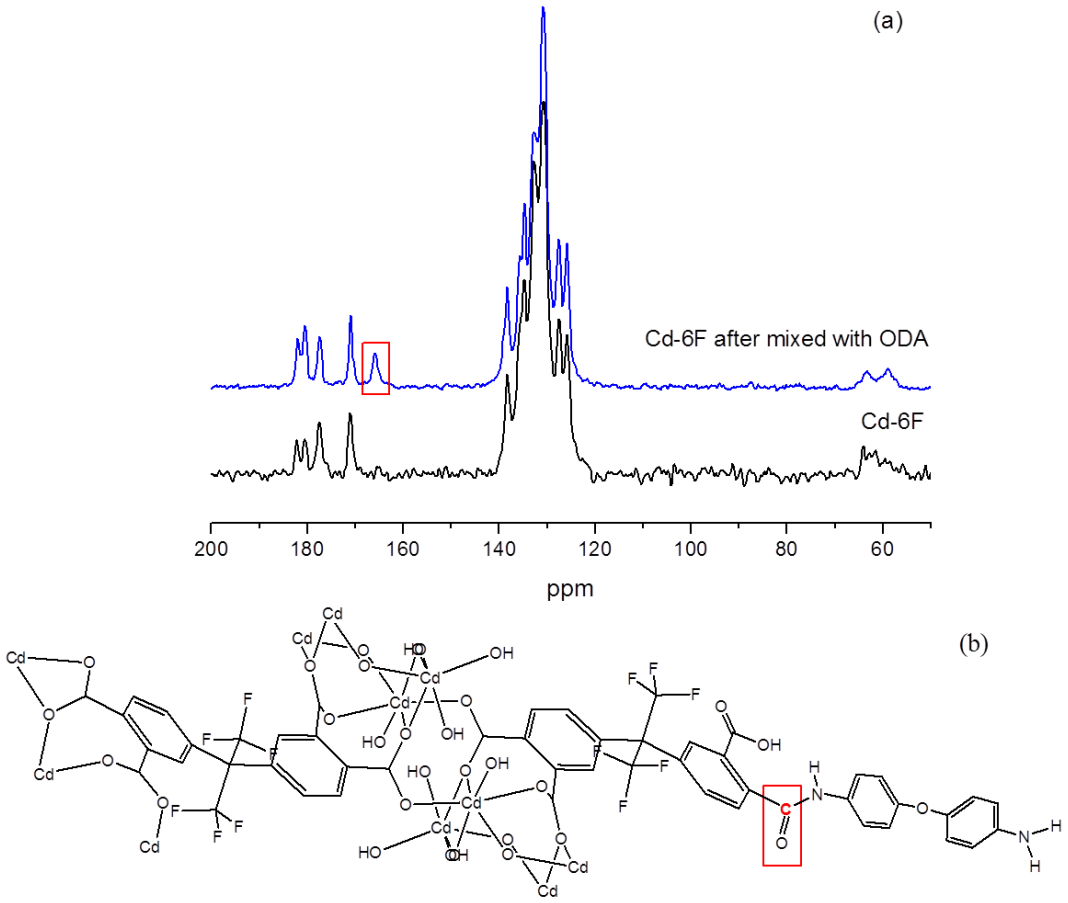

Figure 3-14 ^{13}C solid-state NMR spectra (a) of Cd-6F and Cd-6F mixed with ODA for 6 h and (b) structure of Cd-6F reacted with ODA

XPS was also applied to check the interaction between Cd-6F and ODA, the N1s high resolution scan is shown in Figure 3-15. In the pattern of Cd-6F reacted with ODA, the N 1s peak around 398-401 eV should be assigned to the nitrogen of ODA, which indicating that the existence of ODA reacted on the surface of Cd-6F. Chemical compositions of Cd-6F before and after reacting with ODA were further characterized by element analysis. As it can be seen in Table 3-2, after reacting with ODA for 1 h, only 0.52 wt.% of nitrogen on ODA treated Cd-6F was observed from element analysis. Since Cd-6F crystal does not contain N, the measured nitrogen signals can only be attributed to the amino group of ODA. By prolonging reaction time, an increment in nitrogen content of ODA treated Cd-6F was acquired (0.71 wt.%), indicating the enhancement of interfacial interaction between more ODA and Cd-6F.

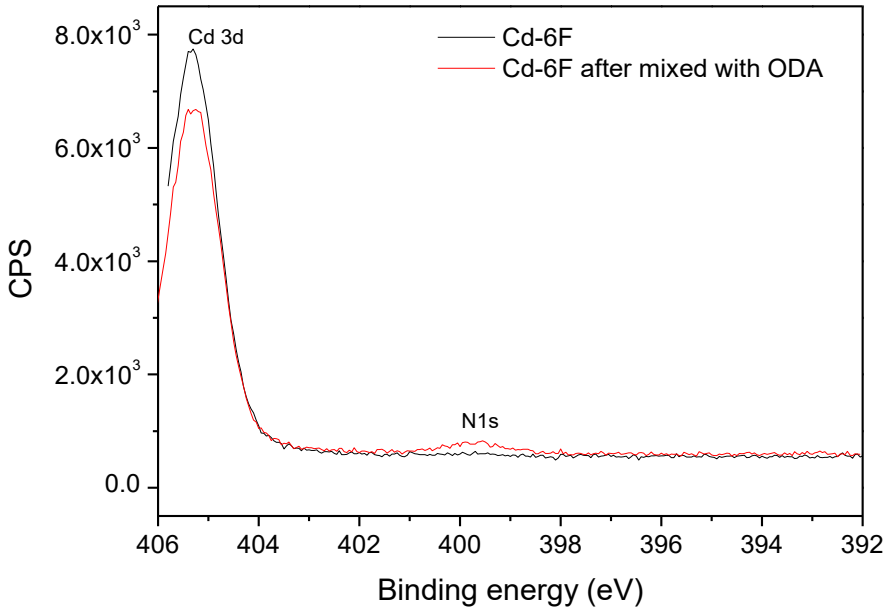

Figure 3-15 XPS N1s spectra of Cd-6F and Cd-6F mixed with ODA for 6 h

Table 3-2 Element analysis of pure Cd-6F, Cd-6F mixed with ODA for 1 h and Cd-6F mixed with ODA for 6 h

Samples	**Element content (wt.%)**		
	N	**C**	**H**
Pure Cd-6F	0.00	31.57	1.59
Cd-6F mixed with ODA for 1 h	0.52	32.60	1.65
Cd-6F mixed with ODA for 6 h	0.71	32.78	1.67

In IR and NMR results, new C=O bond can be observed after the interfacial reaction between Cd-6F and ODA. Also the 1620 cm^{-1} and 3350 cm^{-1} peaks in the IR spectrum of ODA become weaken in the IR spectrum of Cd-6F-ODA, which should be due to the change from primary amine groups –NH_2 to secondary amine groups –NH–. Both XPS and element analysis (Figure 3-15 and Table 3-2) reveal that the new bonds containing N are formed on the Cd-6F surface. Based on above results, the interfacial interaction between Cd-6F and ODA by generating –NH–CO– groups can be concluded. During the in-situ polymerization, the –NH_2 groups of ODA monomer at the terminal of poly (6FDA-ODA) chains could have interaction with Cd-6F crystals, leading to the improved adhesion of MOF/polymer in MMM-A. Meantime, the introduced interfacial interaction does not affect the structure of Cd-6F, most of Cd-6F crystals remain the same crystal structure as shown in the XRD spectra of MMM-A (Figure 3-9). This result demonstrates that the interaction between Cd-6F crystals

and polymer monomer may only occur on the surface of Cd-6F by reacting uncoordinated $–COO^-$ and $–NH_2$ groups. As a whole, the targeted MOF/polymer interface interaction can benefit the elimination of interfacial voids and enhance MOF/polymer adhesion without sacrificing MOFs structure stability.

3.3.3 Gas permeation of Cd-6F mixed matrix membranes

The ideal gas separation performance of pure 6FDA-ODA and MMMs with Cd-6F incorporation was measured. Figure 3-16 shows the gas permeability and selectivity at 25 ºC and 2 atm feed gas pressure. Averaged values were calculated from no less than three permeation tests over each membrane. As to the pure 6FDA-ODA, the gas permeation fluxes of CO_2, N_2 and CH_4 are 20.6, 0.78 and 0.62 Barrer, respectively. The CO_2/N_2 and CO_2/CH_4 selectivity are 26.4 and 33.1, respectively. These results are consistent with the published values of 6FDA-ODA membrane.[33] All the derived Cd-6F MMMs present higher gas permeability compared to the neat 6FDA-ODA polyimide membrane. It has been shown that inorganic particles could disrupt the polymer chain packing and create more free volume, resulting in the increase of the gas diffusivity as well as the permeability of the membrane.[38, 39] Therefore, the increment of gas permeability of Cd-6F MMMs in this study can be attributed to the larger free volume introduced by incorporation of Cd-6F particles. On the other hand, even with the same MOF loading percentage, the ideal selectivity of the MMMs varies with the membrane synthesis procedures. Compared to pure 6FDA-ODA polyimide membrane, MMM-A shows both higher permeability fluxes and selectivity values: CO_2 permeability of 37.8 Barrer with a CO_2/N_2 selectivity of 35.1, and CO_2/CH_4 selectivity of 44.8, as expected from the good MOFs/polymer compatibility resulted from the targeted interfacial interaction. Specifically, the tight MOF/polymer interface in MMM-A can eliminate the unselective gas diffusion through interfacial voids. In contrast to MMM-A from in-situ polymerization, MMM-B and MMM-C exhibit much lower ideal selectivity values than that of the pure polymer, owing to the poor contact between MOF and polymer matrix as shown in Figure 3-12. Especially for MMM-C, though this membrane fabrication process is quite common for most MMMs, obtaining good MOF/polymer interface is very challenging by incorporating micro-sized filler if the MOF/polymer interaction cannot be built. In this case, the gas separation performance will be deteriorated with the existence of interfacial voids. Therefore, in order to achieve a satisfactory separation performance in the MMMs with micro-sized MOFs, the polymer/MOF pair should be carefully chosen and the specific MOF/polymer interaction must be introduced through controlling the synthesis procedures and conditions.

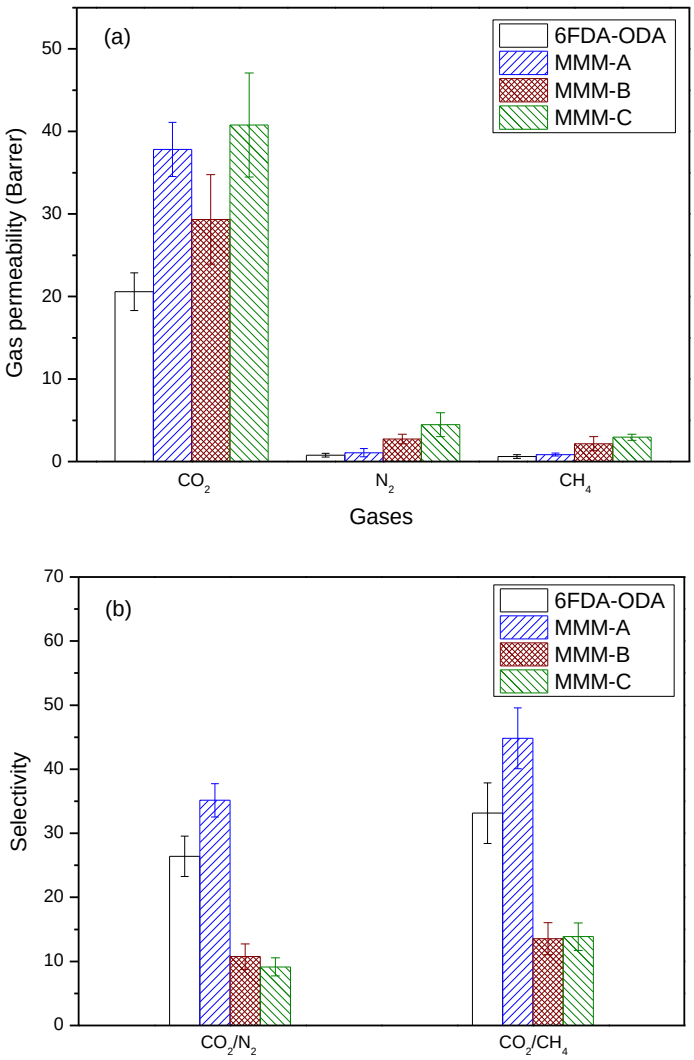

Figure 3-16 Gas permeability (a) and selectivity (b) of the pure 6FDA-ODA membrane and Cd-6F based MMMs

In order to investigate the gas solubility difference between the pure 6FDA-ODA membrane and MMM-A, the membrane gas sorption was measured at pressure up to 30 bar. Based on the solution-diffusion model, the penetrants need to dissolve in the membrane materials before diffusing through the membrane under the pressure gradient.[40] Figure 3-17 displays the CO_2 and N_2 adsorption results of 6FDA-ODA and MMM-A. The adsorption amount of CO_2 is much higher than that of N_2 in both membranes, which indicates these membranes have higher solubility of CO_2. As shown in Figure 3-17, after the introduction of Cd-6F, the sorption capacity of CO_2 rises slightly, while N_2 sorption drops. The reduction of N_2 sorption amount can be attributed to the low N_2 sorption capacity of Cd-6F. On the other hand, the gas sorption isotherms exhibit nonlinear pressure dependence, which is characteristic of the dual-mode sorption consisting of Henry's law sorption in the equilibrium region and Langmuir-type sorption in the non-equilibrium region.[41] The former is related to the dissolution

of gases into the dense equilibrium structure of rubbery polymers, while the latter corresponds to the sorption on the holes or "microvoids" from the non-equilibrium nature of glassy polymers. The dual-mode sorption model is expressed by:[42]

$$C = C_D + C_H = k_D p + \frac{C_H' b_p}{1 + b_p} \quad (3\text{-}5)$$

where C is the total gas concentration in a glassy polymer, C_D is the gas concentration based on Henry's law sorption, C_H is the gas concentration based on Langmuir sorption, k_D is the Henry's law coefficient, b and C'_H are the hole affinity parameter and the capacity parameter, respectively, in the Langmuir model.

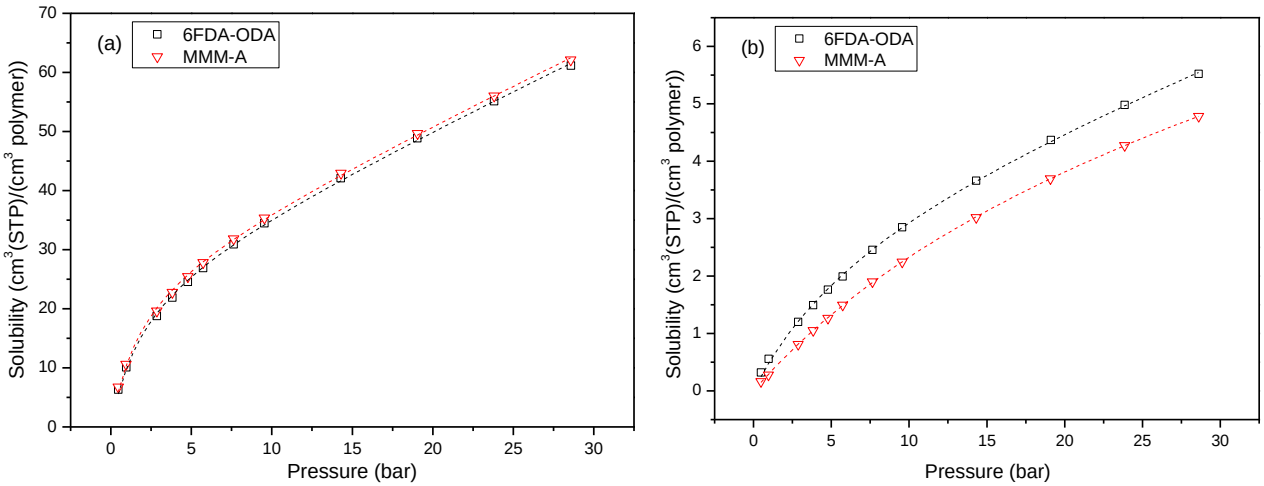

Figure 3-17 Sorption isotherms of (a) CO_2 and (b) N_2 in the 6FDA-ODA and MMM-A at 298K. The dotted lines are fitted lines according to the dual mode sorption model.

Table 3-3 Dual mode sorption parameters for CO_2 and N_2 in 6FDA-ODA and 10 wt.% MMM-A at 298K

Sample/gases	k_D (cm^3 (STP)/cm^3 bar)	C'_H (cm^3 (STP)/cm^3)	b (bar^{-1})
6FDA-ODA			
CO_2	1.282±0.0345	26.687±0.9680	0.489±0.0435
N_2	0.099±0.0087	3.459±0.3897	0.127±0.0179
Cd-6F/6FDA-ODA MMM-A			
CO_2	1.291±0.0314	27.269±0.8600	0.530±0.0427
N_2	0.050±0.0061	6.063±0.4813	0.043±0.0028

The measured CO_2 and N_2 sorption data can be well fitted by the dual-mode sorption model (Figure 3-17). The derived parameters are shown in Table 3-3. k_D represents the penetrant dissolved in the polymer matrix at equilibrium, C'_H shows the amount of the non-equilibrium excess free volume in the glassy state, b characterizes the sorption affinity for a particular gas–polymer system.[43] The magnitude of these values all follows the order of CO_2>N_2, the same as the gas condensability order. For CO_2 sorption, all parameters of the MMM-A have slight increments compared to those of the pure 6FDA-ODA membrane, which can be observed in Table 3-3. Cd-6F can disrupt the polymer chain packing to increase the free volume, resulting in the increment of C'_H. With introducing Cd-6F into 6FDA-ODA, the solubility and the sorption affinity of the membrane for CO_2 can be increased, reflecting on the increments of k_D and b. However, the reduction of k_D and b was observed for N_2. This can be due to the low adsorption abilities of Cd-6F for N_2. Cd-6F exhibits very low uptake of N_2 (0.72 cm^3 g^{-1}) at 298 K and ambient pressure (Figure 3-8b), leading to weaken the solubility and sorption affinity of N_2 (decrease of k_D and b). The increased k_D and b value of CO_2 and the decreased k_D and b value of N_2 indicate that more CO_2 and less N_2 can dissolve in MMMs by introducing Cd-6F into 6FDA-ODA. Combining these sorption results with the gas permeation test of MMM-A, the increase of permeability can be attributed to the increment of C'_H value owing to the increasing free volume created by the Cd-6F introduction. The enhanced solubility difference and selectivity for CO_2 over N_2 can be assigned to the opposite changing direction of k_D and b values for CO_2 and N_2 after the introduction of Cd-6F. As a whole, the improvement of membrane performance can be attributed to the increase of both diffusivity and solubility of CO_2.

3.4 Conclusions

In order to optimize the MOFs/polymer interface in the 6FDA-ODA polyimide matrix, Cd-6F synthesized from 6FDA ligand was chosen as the MMM filler and in-situ polymerization process was used to tailor the interfacial interaction in this novel Cd-6F/6FDA-ODA MMMs. By controlling the in-situ 6FDA-ODA polymerization procedure with the existence of Cd-6F, a specific interaction between the uncoordinated $–COO^-$ on the surface of Cd-6F and the $–NH_2$ groups of ODA monomer at the terminal of poly (6FDA-ODA) chains has been introduced. As a result, Cd-6F in MMM-A derived from in-situ polymerization of 6FDA-ODA with the existence of Cd-6F shows the best adhesion with the 6FDA-ODA matrix while MMM-B and MMM-C synthesized from mixing Cd-6F and polymerized polymer display poor MOF/polymer interface. Both gas permeance and CO_2 selectivity of MMM-A are significantly improved compared to pure 6FDA-ODA polymer membrane, while MMM-B and MMM-C show higher gas permeation flux but lower CO_2 selectivity (over N_2

and CH_4) compared to MMM-A. The synthesis route and the MOF/polymer pair can be tailored for maximizing the membrane performance through optimizing the interaction between MOF fillers and polymer matrix. The membrane fabrication strategy we have shown here exploits a new guidance for the MOF/polymer pair selection and the interface manipulation in the fabrication of high performance MMMs by taking the advantage of organic linker on the surface of MOFs.

Reference

(1) Koros, B., Three Hundred Volumes. Journal of Membrane Science, 2007, 300, 1-1.

(2) Alexander Stern, S., Polymers for Gas Separations: the Next Decade. Journal of Membrane Science, 1994, 94, 1-65.

(3) Nasir, R., Mukhtar, H., Man, Z., Mohshim, D. F., Material Advancements in Fabrication of Mixed-Matrix Membranes. Chemical Engineering & Technology, 2013, 36, 717-727.

(4) Robeson, L. M., Correlation of Separation Factor versus Permeability for Polymeric Membranes. Journal of Membrane Science, 1991, 62, 165-185.

(5) Robeson, L. M., The Upper Bound Revisited. Journal of Membrane Science, 2008, 320, 390-400.

(6) Bastani, D., Esmaeili, N., Asadollahi, M., Polymeric Mixed Matrix Membranes Containing Zeolites as a Filler for Gas Separation Applications: A Review. Journal Of Industrial And Engineering Chemistry, 2013, 19, 375-393.

(7) Pechar, T. W., Kim, S., Vaughan, B., Marand, E., Tsapatsis, M., Jeong, H. K., Cornelius, C. J., Fabrication and Characterization of Polyimide–Zeolite L Mixed Matrix Membranes for Gas Separations. Journal of Membrane Science, 2006, 277, 195-202.

(8) Ge, L., Zhu, Z., Rudolph, V., Enhanced Gas Permeability by Fabricating Functionalized Multi-Walled Carbon Nanotubes and Polyethersulfone Nanocomposite Membrane. Separation and Purification Technology, 2011, 78, 76-82.

(9) Ge, L., Zhu, Z., Li, F., Liu, S., Wang, L., Tang, X., Rudolph, V., Investigation of Gas Permeability in Carbon Nanotube (CNT)−Polymer Matrix Membranes via Modifying CNTs with Functional Groups/Metals and Controlling Modification Location. The Journal of Physical Chemistry C, 2011, 115, 6661-6670.

(10) Vu, D. Q., Koros, W. J., Miller, S. J., Mixed Matrix Membranes Using Carbon Molecular Sieves: I. Preparation and Experimental Results. Journal of Membrane Science, 2003, 211, 311-334.

(11) Weng, T.-H., Tseng, H.-H., Wey, M.-Y., Fabrication and Characterization of Poly(phenylene oxide)/SBA-15/Carbon Molecule Sieve Multilayer Mixed Matrix Membrane for Gas Separation. International Journal Of Hydrogen Energy, 2010, 35, 6971-6983.

(12) Zornoza, B., Irusta, S., Téllez, C., Coronas, J. n., Mesoporous Silica Sphere−Polysulfone Mixed Matrix Membranes for Gas Separation. Langmuir, 2009, 25, 5903-5909.

(13) Yang, T., Xiao, Y., Chung, T.-S., Poly-/Metal-Benzimidazole Nano-Composite Membranes for Hydrogen Purification. Energy & Environmental Science, 2011, 4, 4171-4180.

(14) Adams, R., Carson, C., Ward, J., Tannenbaum, R., Koros, W., Metal Organic Framework Mixed Matrix Membranes for Gas Separations. Microporous and Mesoporous Materials, 2010, 131, 13-20.

(15) Sumida, K., Rogow, D. L., Mason, J. A., McDonald, T. M., Bloch, E. D., Herm, Z. R., Bae, T. H., Long, J. R., Carbon Dioxide Capture in Metal-Organic Frameworks. Chemical Reviews, 2012, 112, 724-781.

(16) Jeazet, H. B. T., Staudt, C., Janiak, C., A Method for Increasing Permeability in O_2/N_2 Separation with Mixed-Matrix Membranes Made of Water-Stable MIL-101 and Polysulfone. Chemical Communications, 2011, 48, 2140-2142.

(17) Ferey, G., Hybrid Porous Solids: Past, Present, Future. Chemical Society Reviews, 2008, 37, 191-214.

(18) Li, J.-R., Sculley, J., Zhou, H.-C., Metal–Organic Frameworks for Separations. Chemical Reviews, 2012, 112, 869-932.

(19) Perez, E. V., Balkus Jr, K. J., Ferraris, J. P., Musselman, I. H., Mixed-Matrix Membranes Containing MOF-5 for Gas Separations. Journal of Membrane Science, 2009, 328, 165-173.

(20) Nik, O. G., Chen, X. Y., Kaliaguine, S., Functionalized Metal Organic Framework-Polyimide Mixed Matrix Membranes for CO_2/CH_4 Separation. Journal of Membrane Science, 2012, 413-414, 48-61.

(21) Ren, H., Jin, J., Hu, J., Liu, H., Affinity between Metal-organic Frameworks and Polyimides in Asymmetric Mixed Matrix Membranes for Gas Separations. Industrial & Engineering Chemistry Research, 2012, 51, 10156-10164.

(22) Rodenas, T., van Dalen, M., García-Pérez, E., Serra-Crespo, P., Zornoza, B., Kapteijn, F., Gascon, J., Visualizing MOF Mixed Matrix Membranes at the Nanoscale: Towards Structure-Performance Relationships in CO_2/CH_4 Separation Over NH_2-MIL-53(Al)@PI. Advanced Functional Materials, 2013, n/a-n/a.

(23) Song, Q. L., Nataraj, S. K., Roussenova, M. V., Tan, J. C., Hughes, D. J., Li, W., Bourgoin, P., Alam, M. A., Cheetham, A. K., Al-Muhtaseb, S. A., Sivaniah, E., Zeolitic Imidazolate Framework (ZIF-8) based Polymer Nanocomposite Membranes for Gas Separation. Energy & Environmental Science, 2012, 5, 8359-8369.

(24) Zhang, C., Dai, Y., Johnson, J. R., Karvan, O., Koros, W. J., High Performance ZIF-8/6FDA-DAM Mixed Matrix Membrane for Propylene/Propane Separations. Journal of Membrane Science,

2012, 389, 34-42.

(25) Wijenayake, S. N., Panapitiya, N. P., Versteeg, S. H., Nguyen, C. N., Goel, S., Balkus, K. J., Musselman, I. H., Ferraris, J. P., Surface Cross-Linking of ZIF-8/Polyimide Mixed Matrix Membranes (MMMs) for Gas Separation. Industrial & Engineering Chemistry Research, 2013, 52, 6991-7001.

(26) Askari, M., Chung, T.-S., Natural Gas Purification and Olefin/Paraffin Separation Using Thermal Cross-Linkable Co-Polyimide/ZIF-8 Mixed Matrix Membranes. Journal of Membrane Science, 2013, 444, 173-183.

(27) Ge, L., Zhou, W., Rudolph, V., Zhu, Z. H., Mixed Matrix Membranes Incorporated with Size-Reduced Cu-BTC for Improved Gas Separation. Journal of Materials Chemistry A, 2013, 1, 6350-6358.

(28) Bae, T.-H., Lee, J. S., Qiu, W., Koros, W. J., Jones, C. W., Nair, S., A High-Performance Gas-Separation Membrane Containing Submicrometer-Sized Metal–Organic Framework Crystals. Angewandte Chemie International Edition, 2010, 49, 9863-9866.

(29) Kim, T. H., Koros, W. J., Husk, G. R., O'Brien, K. C., Relationship between Gas Separation Properties and Chemical Structure in a Series of Aromatic Polyimides. Journal of Membrane Science, 1988, 37, 45-62.

(30) Coleman, M. R., Koros, W. J., Isomeric Polyimides based on Fluorinated Dianhydrides and Diamines for Gas Separation Applications. Journal of Membrane Science, 1990, 50, 285-297.

(31) Hou, L., Shi, W. J., Wang, Y. Y., Guo, Y., Jin, C., Shi, Q. Z., A Rod Packing Microporous Metal-Organic Framework: Unprecedented ukv Topology, High Sorption Selectivity and Affinity for CO_2. Chemical Communications, 2011, 47, 5464-5466.

(32) Jiang, H.-L., Lin, Q.-P., Akita, T., Liu, B., Ohashi, H., Oji, H., Honma, T., Takei, T., Haruta, M., Xu, Q., Ultrafine Gold Clusters Incorporated into a Metal–Organic Framework. Chemistry A European Journal, 2011, 17, 78-81.

(33) Ding, Y., Bikson, B., Nelson, J. K., Polyimide Membranes Derived from Poly(amic acid) Salt Precursor Polymers. 1. Synthesis and Characterization. Macromolecules, 2001, 35, 905-911.

(34) Rallapalli, P., Prasanth, K. P., Patil, D., Somani, R. S., Jasra, R. V., Bajaj, H. C., Sorption Studies of CO_2, CH_4, N_2, CO, O_2 and Ar on Nanoporous Aluminum Terephthalate [MIL-53(Al)]. Journal Of Porous Materials, 2010, 18, 205-210.

(35) Rubal, M., Wilkins, C. W., Cassidy, P. E., Lansford, C., Yamada, Y., Fluorinated Polyimide Nanocomposites for CO_2/CH_4 Separation. Polymers For Advanced Technologies, 2008, 19, 1033-1039.

(36) Fang, X., Xie, X. Q., Simone, C. D., Stevens, M. P., Scola, D. A., A Solid-State ^{13}C NMR Study

of the Cure of ^{13}C-Labeled Phenylethynyl End-Capped Polyimides. Macromolecules, 2000, 33, 1671-1681.

(37) Grobelny, J., Rice, D. M., Karasz, F. E., MacKnight, W. J., High-Resolution Solid-State Carbon-13 Nuclear Magnetic Resonance Study of Polybenzimidazole/Polyimide Blends. Macromolecules, 1990, 23, 2139-2144.

(38) Ahn, J., Chung, W.-J., Pinnau, I., Guiver, M. D., Polysulfone/Silica Nanoparticle Mixed-Matrix Membranes for Gas Separation. Journal of Membrane Science, 2008, 314, 123-133.

(39) Aroon, M. A., Ismail, A. F., Matsuura, T., Montazer-Rahmati, M. M., Performance Studies of Mixed Matrix Membranes for Gas Separation: A review. Separation and Purification Technology, 2010, 75, 229-242.

(40) Wijmans, J. G., Baker, R. W., The Solution-Diffusion Model: a Review. Journal of Membrane Science, 1995, 107, 1-21.

(41) Kanehashi, S., Nagai, K., Analysis of Dual-Mode Model Parameters for Gas Sorption in Glassy Polymers. Journal of Membrane Science, 2005, 253, 117-138.

(42) Merkel, T. C., Freeman, B. D., Spontak, R. J., He, Z., Pinnau, I., Meakin, P., Hill, A. J., Sorption, Transport, and Structural Evidence for Enhanced Free Volume in Poly(4-methyl-2-pentyne)/Fumed Silica Nanocomposite Membranes. Chemistry of Materials, 2002, 15, 109-123.

(43) Paul, D. R., Gas Sorption and Transport in Glassy Polymers. Berichte der Bunsengesellschaft für physikalische Chemie, 1979, 83, 294-302.

Chapter 4 Mixed matrix membranes with metal-organic framework-decorated CNT fillers for efficient CO_2 separation

Introduction

As mentioned in section 2.4.2, the dispersion of filler particles in polymer matrix is one of the important factors that affect the performance of MMMs. While the filler particle loading is increasing, especially for nano-size particle, the aggregation of filler is a crucial issue that needs to be considered. Non-selective interfacial voids generate and because filler aggregates cannot contact with polymer, which can cause the decrease of gas selectivity of the membrane. The dispersion problem of filler restricts further improvement of the membrane performance. In this chapter, a novel approach to improve MOF dispersion in polymer continuous phase and achieve high performance MMMs is proposed by introducing composite fillers CNT-MIL synthesized by in situ growth of NH_2-MIL-101(Al) on the external surface of the carbon nanotubes. The CNT-MIL composite is embedded into 6FDA-durene polymer to fabricate MMMs for CO_2/CH_4 separation. The CO_2/CH_4 separation performance of the MMMs are studied and compared to the pure polymer membrane and the MMM with only CNT or NH_2-MIL-101(Al) filler.

Contributions

In this chapter, a novel MMM filler is prepared by in-situ growth of metal–organic frameworks (MOFs) on CNTs and is used to fabricate high-performance MMMs for efficient separation of CO_2/CH_4. We found that the confined growth of NH_2-MIL-101(Al) on external surfaces of CNT can improve the dispersion of NH_2-MIL-101(Al), and good adhesion between the CNT-MIL fillers and polymer matrix was observed. Compared to pure polymeric membrane, mixed matrix membranes containing synthesized MOF/CNT composite displayed significantly improved CO_2 permeance (up to 150%) and selectivity (up to 37.5%). The separation performance of derived MMMs clearly transcends the 1991 upper bound and being on the 2008 upper bound for polymeric membrane performance. The strategy of growing MOFs on CNTs shown in this chapter can offer a valid method to enhance the MMMs separation performance by modification of fillers with existing MOFs which have high selectivity to specific gas. This chapter has been published in the ACS Applied Materials & Interfaces 2015, 67, 14750–14757.

Mixed matrix membranes with metal–organic frameworks decorated CNTs fillers for efficient CO_2 separation

Rijia Lin[1], Lei Ge*[1], Shaomin Liu[2], Victor Rudolph[1], Zhonghua Zhu*[1]

[1]School of Chemical Engineering, The University of Queensland, Brisbane 4072 Australia

[2]Curtin University of Technology, School of Chemical Engineering, Perth Australia

Abstract

Carbon nanotubes (CNTs) mixed matrix membranes (MMMs) show great potential to achieve superior gas permeance due to the unique structure of CNTs. However, the challenges of CNT dispersion in polymer matrix and elimination of interfacial defects are still hindering the MMMs to be prepared for high gas selectivity. A novel carbon nanotube/metal–organic frameworks (MOFs) composite derived from the growth of NH_2-MIL-101(Al) on the external surface of carbon nanotube have been synthesized and applied to fabricate polyimide based mixed matrix membranes. Extra amino groups and active sites were introduced to external surface of CNTs after MOF decoration. The good adhesion between the synthesized CNT-MIL fillers and polymer phase was observed, even at a high filler loading up to 15 %. Consequently, mixed matrix membranes containing the synthesized MOF/CNT composite exhibit not only a large CO_2 permeability but also a high CO_2/CH_4 selectivity, the combined performance of permeability and selectivity is even above the Robeson upper bound. The strategy of growing MOF on CNTs can be further utilized to develop a more effective approach to further improve MMMs performance through the decoration of MOFs on existing fillers that have high selectivity to specific gas.

4.1 Introduction

Gas separation utilizing polymeric membranes has emerged as an efficient process with significant technical and commercial impact.[1, 2] Nonetheless, most of the current polymeric membranes are limited by a trade-off between permeability and selectivity, referred as Robeson upper bound; the more permeable polymeric membranes are, the less selective and vice versa.[3, 4] In recent years, a breakthrough has been made by embedding filler materials such as inorganic particles into the polymeric matrix. The resultant mixed matrix membranes (MMMs) combine the advantages of both

inorganic particles and polymer membranes, providing the high separation capabilities of the filler particles with good processability and mechanical properties of the polymer.[5, 6]

Among the fillers, carbon nanotubes (CNTs) have been widely applied because of their unique structure.[7, 8] In particular, gas transport through the CNT tunnels is dramatically accelerated due to the smooth internal walls, conferring on CNT modified membranes the potential for superior gas permeance.[9, 10] However, as with many other nanomaterials, the CNTs are hydrophobic and preferentially aggregate and entangle together. This difficulty in dispersion remains an obstacle impeding their use for highly selective MMM gas separation.

In order to improve the CNT dispersion quality in the polymer matrix and eliminate interfacial defects, various surface modification strategies have been explored.[11, 12] One feasible approach is to graft functional groups on the CNTs exterior surface, which is frequently performed by strong acid treatment.[13, 14] Surface functionalization or doping is effective not only to improve the dispersion quality but also to increase the penetrates' solubility in the composite membranes; in particular, these functional groups carrying partial charges that can act as the anchor sites to absorb strongly polar gases such as CO_2.[7, 15] However, these methods sometimes damage the integrity of the CNTs making them inappropriate for use as the filler for MMM preparation.

Apart from grafting organic functional groups or metal doping, an alternative is to decorate metal–organic frameworks (MOFs) on CNTs, which acts to improve the adsorption selectivity of CNTs.[16] In the previous studies, MOF based composites such as MOF-zeolite, MOF-silica have also been used to fabricate MMMs.[17-19] The incorporation of MOF made zeolite or silica more compatible with polymer. The MMMs exhibited good interaction between polymers and these composite fillers. As a novel group of porous hybrid materials, MOFs can be grown from the precursors of metal and organic linkers, which possess well-define pore structure, high surface area and high adsorption affinity/selectivity.[20] Additionally, desired functionalities of MOFs can be easily achieved during synthesis process with different organic linkers, such as -NH_2, and -COO. By controlling the atomic ratios of metal/organic linkers, a variety of structures with different adsorpability and selectivity for specific gases can be flexibly synthesized.

In this work, we report the use of a novel MMM filler derived from in-situ growth of MOFs on the external surface of the carbon nanotubes to improve the separation performance. NH_2-MIL-101(Al), a MOF based on the MIL-101 topology which presents high sorption selectivity of CO_2 was chosen.[21] CNTs well covered with MOFs were successfully prepared. NH_2-MIL-101(Al) introduced amino groups and active sites to the external surface of CNTs. The MMMs were fabricated by dispersing the synthesized MOF/CNT composite into 6FDA-durene polyimide (Figure 4-1).

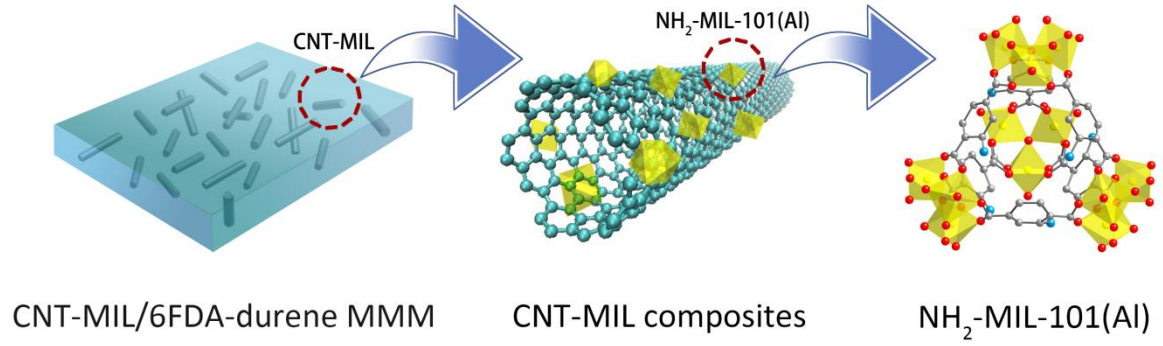

Figure 4-1 Schematic diagram of a 6FDA-durene MMM containing NH_2-MIL-101 (Al) decorated CNTs (symbol: Al, yellow; C, grey; O, red; N, blue)

4.2 Experimental section

4.2.1 Materials synthesis

4.2.1.1 Materials

Aluminium chloride hexahydrate ($AlCl_3 \cdot 6H_2O$), 2-amino terephthalic acid (NH_2-H_2BDC), 4, 4'-(Hexafluoroisopropylidene) diphthalic anhydride (6FDA), 2,3,5,6-Tetramethyl-1,3-phenyldiamine (durene), triethylamine, acetic anhydride, N,N-dimethylformamide (DMF), N,N-Dimethylacetamide (DMAc) and acetone were supplied by Sigma–Aldrich. The multi-walled carbon nanotubes (MWCNTs) produced from methane decomposition over a Fe catalyst in a fluidized-bed reactor were supplied by Tsinghua University, China. The purity in pristine samples exceeded 95 wt.%. The orientation of the carbon layers in a typical CNT is parallel to its axis. The external diameter of CNTs is around 30 nm.

4.2.1.2 Synthesis of NH_2-MIL-101(Al)

The NH_2-MIL-101 was synthesized based on a manner reported elsewhere.[21] 0.119 g $AlCl_3 \cdot 6H_2O$ and 0.131 g H_2BDC were dissolved into 70 mL of DMF. After 30 min stirring the mixture was transferred into a Teflon-line stainless steel autoclave and heated at 130 ºC for 6 h. After the hydrothermal reaction, the NH_2-MIL-101(Al) were separated by centrifugation and washed in acetone three times, with the product finally dried at 180 ºC under vacuum for 18 h.

4.2.1.3 Synthesis of carbon nanotubes and NH_2-MIL-101(Al) composites

Before synthesis of NH_2-MIL-101(Al)/CNTs composites, the carboxyl modified CNTs were prepared according to a method reported elsewhere.[22] A quantity of CNTs (0.5 g) was sonicated in a 300 ml mixture of concentrated H_2SO_4 (98 vol.%)/HNO_3 (70 vol.%) (3:1) for 3 h at 60 ºC. Subsequently, the

sample was washed with deionized water in several centrifugation/re-dispersion cycles and filtered, followed by drying under vacuum. This procedure provides CNTs with oxidized carboxylic groups on the outer walls (referred as CNT-COOH).

All of the NH_2-MIL-101(Al)/CNTs composite were also prepared under the same solvothermal procedures of NH_2-MIL-101(Al), except adding 40 mg of CNT-COOH to DMF by repeated sonication and stirring prior to adding H_2BDC. The synthesized NH_2-MIL-101(Al)/CNTs composite was referred as CNT-MIL. The mass ratio of CNT in composite is calculated based on the weight loss from element analysis.

4.2.1.4 Synthesis of 6FDA-durene polyimide

The preparation of 6FDA-durene polyimide (Figure 4-2) was carried out by chemical imidization the same as the work reported elsewhere.[23, 24] 1.426 g of durene was dissolved into 10 mL of DMAc. Once the durene was fully dissolved, 3.861 g of 6FDA powder was added, followed by 5 mL of DMAc. The mixture was stirred under nitrogen at room temperature for 24 h to form polyamic acid. Next, a mixture of triethylamine (3.2 mL) and acetic anhydride (1.2 mL) was added. The combined mixture was stirred under nitrogen at room temperature for another 24 h. The final polymer was precipitated in methanol, washed several times with methanol, and dried at 180 °C under vacuum for 18 h. The polyimide product is referred as 6FDA-durene.

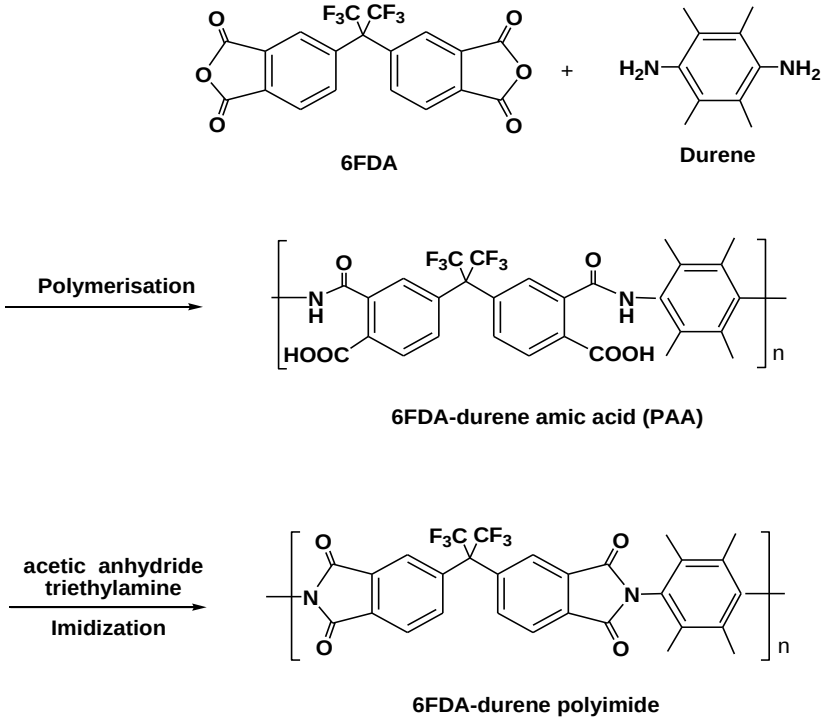

Figure 4-2 Multi-staged of 6FDA-durene polyimide synthesis

4.2.1.5 Membrane preparation

For pure 6FDA-durene membrane fabrication, 0.45 g 6FDA-durene membrane was dissolved in 3 mL DMF at room temperature and stirred until a clear solution was obtained. The resulting solution was cast onto a clean glass substrate, followed by drying at 180 ºC for 24 h in a vacuum oven. For the MMMs, certain amount of as-synthesised CNT-MIL, CNT-COOH or NH_2-MIL-101(Al) was suspended in DMF under sonication. 0.45 g 6FDA-durene was added to this suspension and the suspension was further stirred for 6 h. The resulting mixture was cast and dried at 180 ºC for 24 h under vacuum to form MMM. The selected thickness for casting procedure was 40 µm. The thickness of pure 6FDA-durene and MMMs were measured using a micrometer within the range of 30–40 µm. Before gas permeation tests and characterisation, the membranes were stored with desiccant.

The loadings of CNT-MIL and CNT-COOH in MMMs were adjusted to 5, 10, 15 wt% for the purposes of this study based on equation (4-1).

$$\phi = \frac{m_{Filler}}{m_{Filler} + m_{6FDA\text{-}durene}} \quad (4\text{-}1)$$

where m_{Filler} and $m_{6FDA\text{-}durene}$ are the mass of CNT-MIL/CNT-COOH filler and 6FDA-durene in the MMMs, respectively.

4.2.2 Characterization

The X-ray diffraction (XRD) data were obtained from a Brucker Advanced X-ray Diffractometer (40 kV, 30 mA) with Cu Kα (λ= 0.15406 nm) radiation at a scanning rate of 1^o min^{-1} from 2^o to 40^o. The morphologies of the samples were obtained with a JEOL JSM7100 scanning electron microscope (SEM) at 8 kV. High resolution transmission electron microscopy (HRTEM) was performed on a JEOL JEM-2100 microscope, with accelerating voltages of 200 kV. The samples were dispersed by sonication in ethanol, deposited on a holey carbon TEM grid and dried prior to examination.

Flash EA 1112 CHNS-O analyzer (Thermo Electron) was applied to quantify the content of hydrogen, carbon and nitrogen in CNT-COOH and CNT-MIL composite. the content of NH_2-MIL-101 in the composites can be calculated from the weight percentage of nitrogen by solving equation 4-2 and equation 4-3:

$$NH_2\text{-MIL-101}\,\% + \text{CNT-COOH}\,\% = 1 \quad (4\text{-}2)$$

$$\text{CNT-COOH}\% \times N_{CNT\text{-}COOH}\% + NH_2\text{-MIL-101}\% \times \frac{Mw_{NH_2\text{-}MIL\text{-}101}}{Mw_N \times 4} = N_{CNT\text{-}MIL}\% \quad (4\text{-}3)$$

where $N_{CNT\text{-}MIL}$% and $N_{CNT\text{-}COOH}$% are the weight percentages of nitrogen in CNT-MIL and CNT-COOH samples, respectively. $Mw_{NH_2\text{-}MIL\text{-}101}$ is the molecular weight of NH_2-MIL-101, Mw_N is the atomic weight of nitrogen. The $Mw_{NH_2\text{-}MIL\text{-}101}$ is calculated according to the formula of NH_2-MIL-101 referred in the literature.[21]

The N_2 adsorption isotherms were obtained from a Micromeritics TriStar II 3020 at 77 K, after degassing the sample at 200 ºC for 18 h. BET surface area is calculated over the range of relative pressures between 0.05 and 0.15. After N_2 adsorption, the samples were regenerated at 200 ºC under a pressure of 10 mTorr until no further pressure drop was observed. Then, the adsorption isotherms of CO_2 and CH_4 at 298 K were measured using the same instrument. The desorption isotherms of CO_2 and CH_4 were obtained by gradually decreasing the system pressure. The adsorption selectivity of CO_2 to CH_4 (S) is calculated according equation 4-4:

$$S = \frac{q_{CO_2} / q_{CH_4}}{p_{CO_2} / p_{CH_4}} \quad (4\text{-}4)$$

where S is the relative selectivity value, q is the amount of adsorbed gas ($cm^3\ g^{-1}$), p is the absolute gas pressure (kPa).

The high pressure sorption of CO_2 and CH_4 was measured in BEL-BG using a magnetic suspension balance (Rubotherm). About 0.7 g of pure 6FDA-durene or MMMs was degassed at 80 ºC under vacuum for 2 to 4 h before adsorption.

4.2.3 Permeation test

A variable feed pressure and the constant volume permeation system was used to measure the gas permeation of pure 6FDA-durene and MMMs, as described elsewhere.[25] The membranes were held under vacuum for approximately 5 min to achieve a steady state before the exposing to the selected gas. Before switching to the feed gas, the membrane has to be degassed for some time to ensure the complete desorbtion of initial permeate gas. The test was held at 25 ºC, 2atm feed pressure. Gas permeability values and deviation were calculated from permeation tests from three membranes of each loading.

The permeation coefficient is calculated using the following equation:

$$P = \frac{273.15 \times 10^{10}}{760\mathrm{AT}} \frac{VL}{\frac{P_0 \times 76}{14.7}} \frac{\mathrm{d}p}{\mathrm{d}t} \quad (4\text{-}5)$$

where P is the permeation coefficient in barrer (1 barrer $=1\times10^{-10}$ cm^3 (STP) cm cm^{-2} s^{-1} cm Hg^{-1}), A

is the effective area of the membrane (cm^2), T is the absolute temperature (K), V is the dead-volume of the downstream chamber (cm^3), L is the membrane thickness (cm), P_0 is the feed pressure (psi), and dp/dt is the steady rate of pressure increase in the downstream side (mm Hg s^{-1}).

The ideal selectivity for two gases is determined as:

$$\alpha = \frac{P_A}{P_B} \quad (4\text{-}6)$$

where P_A and P_B are the permeation coefficients of pure gas A and B, respectively.

For mixed-gas permeation, 50/50% CO_2/CH_4 gas mixture was fed at 3 atm to the retentate side of the membrane, while the permeate side of the membrane was swept with Ar at 1 atm. Gas composition in the permeate side was analyzed by a gas chromatograph (Shimadzu GC-8A) and the mixture gas selectivity was calculated accordingly. The separation factor α_{ab} shows the ability of a membrane to separate binary gas mixture, and it is defined as:

$$\alpha_{a,b} = \frac{y_{a,permeate} / y_{b,permeate}}{y_{a,retentate} / y_{b,retentate}} \quad (4\text{-}7)$$

where $y_{a,permeate}$ and $y_{b,permeate}$ are the molar ratios of the components A and B in permeate, $y_{a,retentate}$ and $y_{b,retentate}$ are the molar ratio of components A and B in retentate.[26]

4.3 Results and discussions

The X-ray diffraction (XRD) patterns of pure NH_2-MIL-101(Al) and CNT-MIL composite samples indicate the existence of the well-defined NH_2-MIL-101(Al) in the as-synthesized CNT-MIL (Figure 4-3).[27] Compared to pure NH_2-MIL-101(Al), the nucleation sites on CNT surface produced smaller NH_2-MIL-101(Al) crystals (Figure 4-4). The "grape-bunch" morphology is observed. The NH_2-MIL-101(Al) crystals cover the external surface of the CNTs, as illustrated by scanning electron microscopy (SEM) in Figure 4-4b. HRTEM was also applied to reveal the morphology of CNT-MIL (Figure 4-5). It can be observed that MOF particles are grown on the outer surfaces of CNTs with the particle size at around 50 nm, which is in line with the SEM results (Figure 4-4). The CNT internal channels are hollow and there is no evidence for the confined growth of MOFs inside CNTs. Similar morphology has also been observed in our previous studies on MOFs/CNTs composites.[16, 28] The content of NH_2-MIL-101(Al) in the CNT-MIL composite is 48.3 wt.% calculated from elemental analysis (Table 4-1).

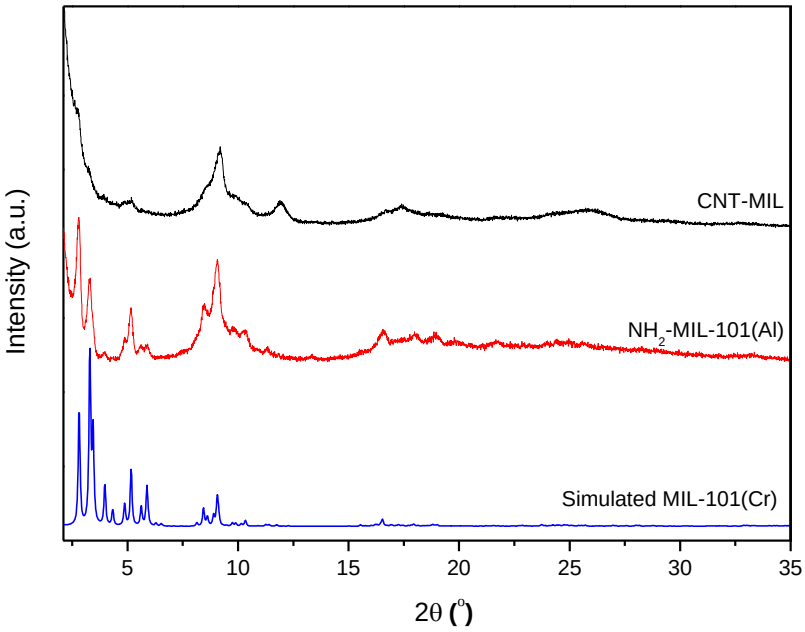

Figure 4-3 XRD pattern of NH_2-MIL-101 (Al), CNT-MIL composite and simulated MIL-101(Cr)

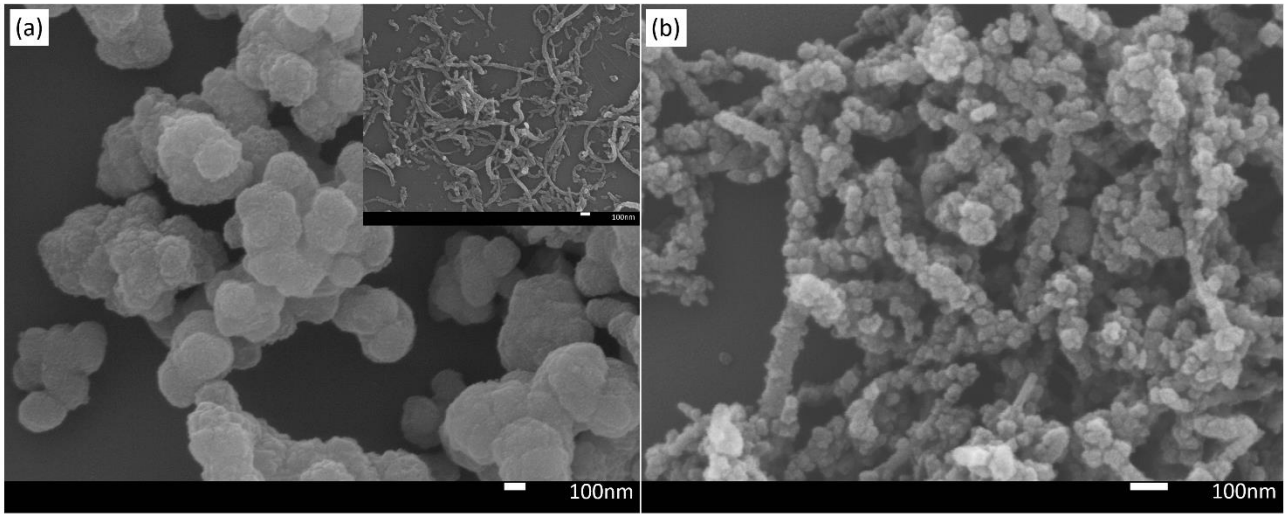

Figure 4-4 SEM images of (a) NH_2-MIL-101(Al) with CNT-COOH inset and (b) CNT-MIL composite

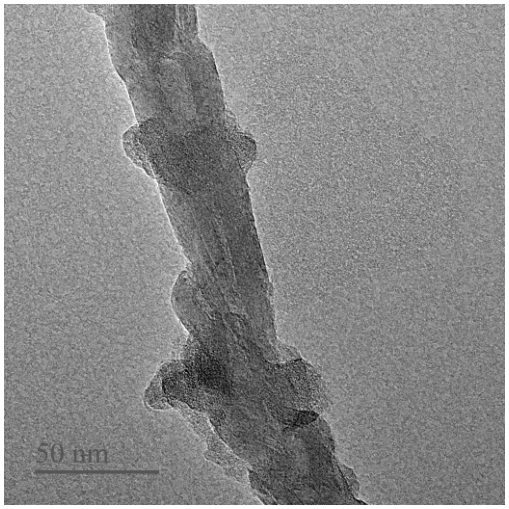

Figure 4-5 HRTEM image of CNT-MIL

Table 4-1 Element analysis of pure CNT-COOH and CNT-MIL

Samples	**Element content (wt.%)**		
	N	**C**	**H**
CNT-COOH	0.11	75.18	0.46
CNT-MIL	3.88	63.87	2.47

The BET surface area of pure NH_2-MIL-101(Al) and CNT-MIL measured from the N_2 adsorption/desorption isotherms are 1309 $m^2 g^{-1}$ and 651 $m^2 g^{-1}$, respectively. CO_2 and CH_4 adsorption isotherms of CNT-COOH, NH_2-MIL-101(Al) and CNT-MIL measured at 298 K are shown in Figure 4-6. CNT-MIL displays both higher CO_2 capacity and CO_2/CH_4 ideal selectivity (ratio of the single component adsorption capacities) than CNT-COOH. At 101 kPa and 298 K, CNT-MIL exhibited an ideal selectivity of 4.75 for CO_2 over CH_4, compared to 3.13 and 4.18 for CNT-COOH and NH_2-MIL-101, respectively. The MOF nano-crystals or functional groups on the external surface of CNTs are expected to induce charge transfer between modification sites and CNTs, thus decreasing the electrostatic potential on the CNT surface, leading to different adsorption selectivity and contributing to selectivity enhancement by varying solubility.[25]

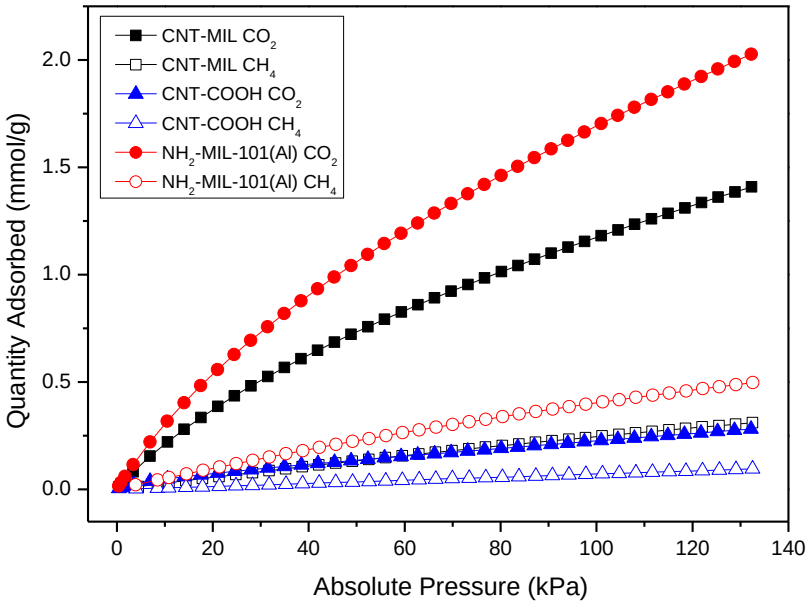

Figure 4-6 CO_2 and CH_4 adsorption isotherms of CNT-COOH, NH_2-MIL-101(Al) and CNT-MIL at 298K

The SEM images of CNT-MIL/6FDA-durene MMMs cross-sections (Figure 4-7) show good interfacial contact between the CNT-MIL particles and polymer matrix, with no observable interfacial gap. In contrast to the denser cross-section of pure 6FDA-durene membrane (Figure 4-7a), the presence of the concentric cavities in the MMMs indicates that there is strong interfacial interaction between CNT-MIL particles and 6FDA-durene.[29, 30] The cross-sections of CNT-COOH/6FDA-durene MMMs have similar morphology as that of CNT-MIL/6FDA-durene MMMs. Compared to CNT-MIL/6FDA-durene MMMs, more severe agglomerations of nanotubes (Figure 4-8) occurred in CNT-COOH/6FDA-durene MMMs at high loading (10 wt. %). Similar CNT aggregation in MMMs can also be observed in previous literature.[13, 15]

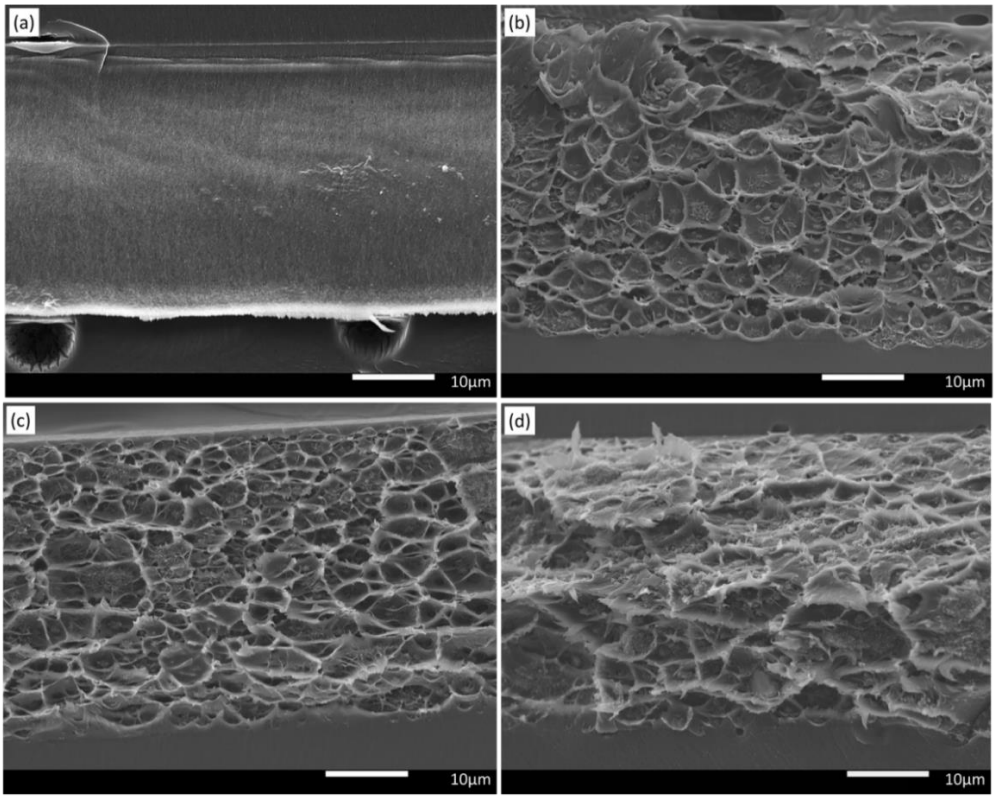

Figure 4-7 SEM images of pure 6FDA-durene (a) and CNT-MIL/6FDA-durene MMMs cross-sections with different amount of CNT-MIL (b: 5%; c: 10%; d: 15%)

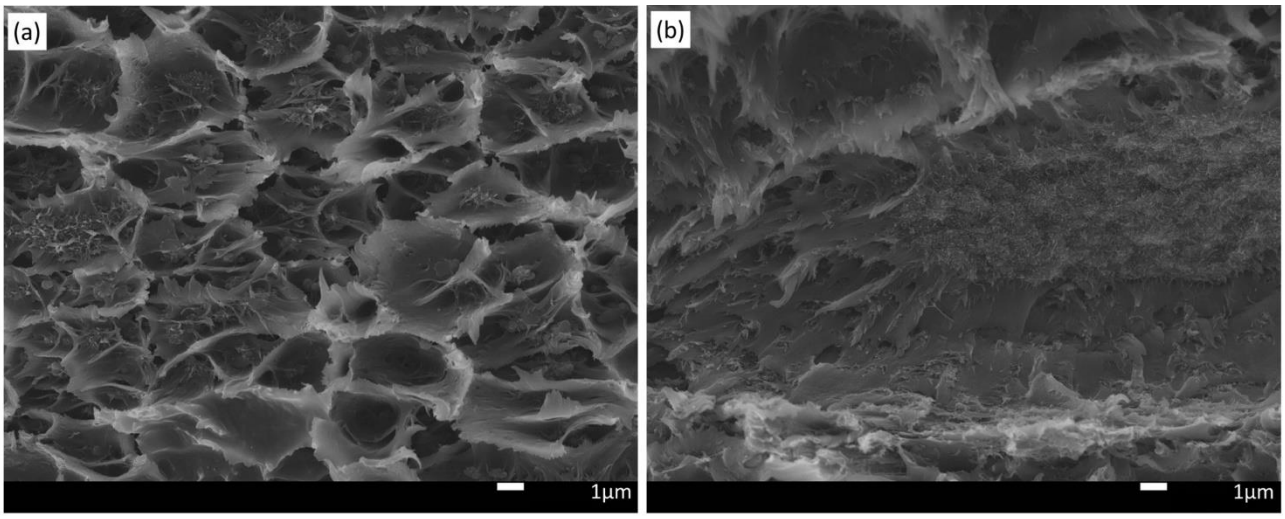

Figure 4-8 High magnification SEM images of MMMs cross-sections (a) 10% CNT-MIL/6FDA-durene MMM and (b) 10% CNT-COOH/6FDA-durene MMMs

Single gas permeation was measured to evaluate the performance of the as-synthesized membranes.

Figure 4-9 shows the gas permeability and selectivity of the pure polymeric membrane. The gas permeance of CO_2 from the pure 6FDA-durene is 618 barrer with CO_2/CH_4 selectivity of 21.6. These results are consistent with the published values of 6FDA-durene membrane.[31] For both CNT-MIL and CNT-COOH MMMs, the permeability of all the gases increased with the filler loading. For instance, a loading at 15 wt.% increased the CO_2 permeability of both CNT-MIL and CNT-COOH MMMs by a factor up to 2.5 compared to the pure polymeric membrane. Inorganic fillers can disrupt the polymer chain packing thus creating more free volume, which provides more channels for gas diffusion and achieves higher permeability of the resultant membranes.[32] The permeability enhancement of MMMs can be attributed to the larger free volume introduced by the incorporation of CNTs, the interfacial space between polymer and fillers, and the tunnels provided by the CNTs which can serve as fast channels for gas permeation.

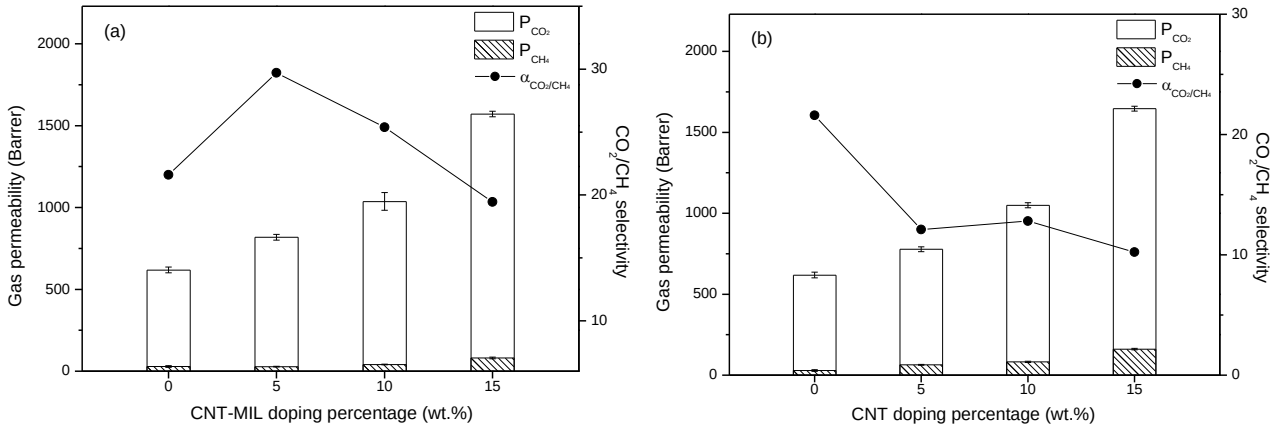

Figure 4-9 Gas permeability and selectivity of the pure 6FDA-durene membrane, CNT-MIL/6FDA-durene MMMs (a) and CNT/6FDA-durene MMMs (b)

On the other hand, the ideal selectivity of the MMMs varies with different fillers and loadings. CNT-COOH/6FDA-durene MMMs exhibit much lower ideal selectivity values than the pure polymer due to the lack of sufficient CO_2 selective groups on the surface of CNT-COOH in the polymer matrix. Under such circumstances, nonselective voids are produced on the interface between filler particles and the polymer, resulting in increased extra free volume but cutting down the gas selectivity. Similar observations of reduced selectivity by incorporating functionalized CNT into polymer matrix has also been found previously.[7, 15] The reduction of CO_2/CH_4 selectivity was also observed in NH_2-MIL-101(Al) MMMs, attributed to the interfacial voids formed between filler and polymer (Table 4-2 and Figure 4-10). The "sieve in a cage" morphology of NH_2-MIL-101(Al) MMMs is in line with other reported MMMs containing MOF fillers with larger particle size, serving to reduce the separation performance.[32, 33] The confined growth of MOFs on CNT external surfaces reduces crystal size, improving the MOFs/polymer interface in the subsequent MMMs fabrication.[16, 34] By decorating

MOFs on CNTs, 6FDA-durene MMMs containing 5 and 10 wt.% CNT-MIL provide higher CO_2/CH_4 selectivity compared to pure 6FDA-durene polyimide membrane with increased CO_2 permeability fluxes. At 10 wt.% loading of CNT-MIL, the MMM exhibited a high CO_2 permeability of 1037 Barrer with a CO_2/CH_4 selectivity of 25.4. The 50/50% CO_2/CH_4 mixed gas selectivity of 6FDA-durene and CNT-MIL/6FDA-durene MMMs are shown in the Table 4-3. The binary gas mixture separation on CNT-MIL/6FDA-durene MMMs showed similar CO_2/CH_4 selectivity as the ideal selectivity.

Table 4-2 Gas permeability and selectivity of NH_2-MIL-101/6FDA-durene membrane (25 ^oC, 2 atm feed gas pressure)

Sample	**Permeability (barrer)**		**Selectivity**
	CO_2	**CH_4**	**CO_2/CH_4**
10 wt.% NH_2-MIL-101/6FDA-durene	1365 ± 30.6	97 ± 0.6	14.1

Table 4-3 Ideal CO_2/CH_4 selectivity and mixed gas selectivity of 6FDA-durene and CNT-MIL/6FDA-durene MMMs

	Single gas ideal CO_2/CH_4 selectivity	50/50% CO_2/CH_4 mixed gas selectivity
6FDA-durene	21.6	21.9
5% CNT-MIL/6FDA-durene	29.7	26.6
10% CNT-MIL/6FDA-durene	25.4	22.9
15% CNT-MIL/6FDA-durene	19.4	19.5

We believe that the significant improvement in separation performance by the decoration of NH_2-MIL-101(Al) on CNTs can be explained as follows. Firstly, MOF decoration on CNTs enlarges adsorption capacity of CO_2 and CH_4 relative to CNT-COOH alone (Figure 4-6). The $–NH_2$ groups in NH_2-MIL-101(Al) facilitates CO_2 adsorption selectivity. In addition, the interaction between NH_2-MIL-101(Al) and CNT may further enhance the CO_2 adsorption selectivity by electrostatic

interactions, as observed previously from MOFs/CNTs composites.[16, 34] Secondly, the adsorption preference by the fillers is expected to enlarge the membrane solubility difference of CO_2 over CH_4.[32]

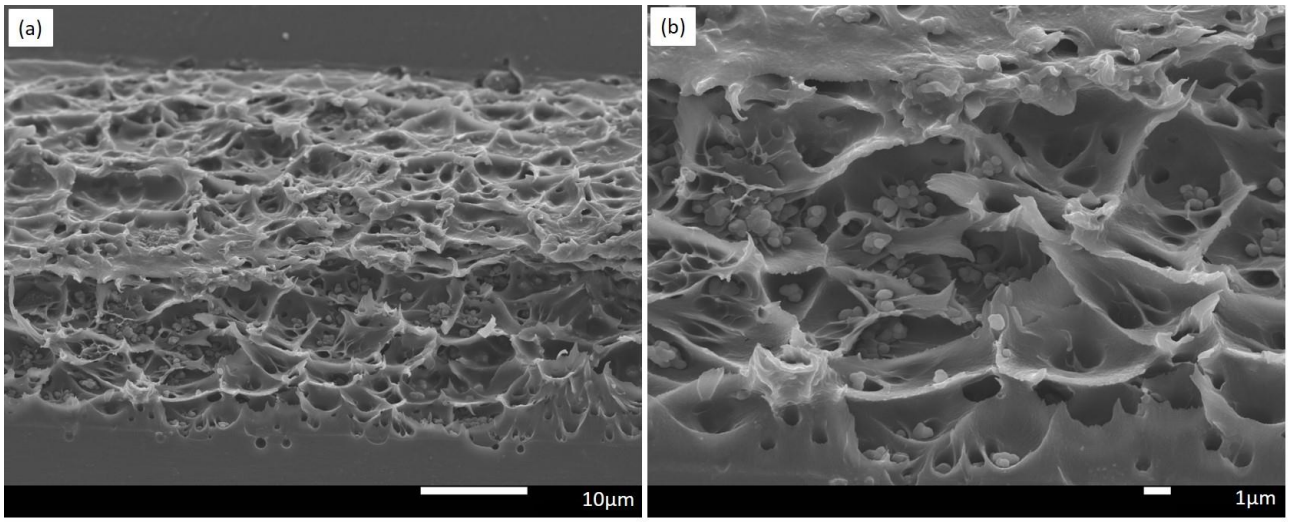

Figure 4-10 Cross-section SEM images of 10 wt.% NH_2-MIL-101/6FDA-durene MMM (a: low magnification; b: high magnification)

The gas solubility difference between the pure 6FDA-durene membrane and CNT-MIL/6FDA-durene MMMs was investigated through measuring pressure dependent membrane gas sorption isotherms up to 30 bar (Figure 4-11). Based on the solution-diffusion model, the penetrants need to dissolve in the membrane materials before diffusing through the membrane under the pressure gradient.[35] Figure 4-11 shows the CO_2 and CH_4 adsorption results of 6FDA-durene and 10% CNT-MIL/6FDA-durene MMM. The adsorption amount of CO_2 is much higher than that of CH_4 in both membranes, which indicates these membranes have higher solubility of CO_2. The gas sorption isotherms exhibit nonlinear pressure dependence, which is characteristic of the dual-mode sorption consisting of Henry's law sorption in the equilibrium region and Langmuir-type sorption in the non-equilibrium region.[36] The former is related to the dissolution of gases into the dense equilibrium structure of rubbery polymers, while the latter corresponds to the sorption on the holes or "microvoids" from the non-equilibrium nature of glassy polymers. The dual-mode sorption model is expressed by:[37]

$$C = C_D + C_H = k_D p + \frac{C_H' b_p}{1 + b_p} \quad (4\text{-}8)$$

where C is the total gas concentration in a glassy polymer, C_D is the gas concentration based on Henry's law sorption, C_H is the gas concentration based on Langmuir sorption, k_D is the Henry's law

coefficient, b and C'_H are the hole affinity parameter and the capacity parameter, respectively, in the Langmuir model. k_D represents the penetrant dissolved in the polymer matrix at equilibrium, C'_H shows the amount of the non-equilibrium excess free volume in the glassy state, b characterizes the sorption affinity for a particular gas–polymer system.[38] The measured CO_2 and CH_4 sorption data can be well fitted by the dual-mode sorption model (Figure 4-11). The derived parameters are shown in Table 4-4.

Table 4-4 Dual mode sorption parameters for CO_2 and CH_4 in 6FDA-durene and 10% CNT-MIL/6FDA-durene at 298K

Sample/gases	**k_D (cm^3 (STP)/cm^3 bar)**	**C'_H (cm^3 (STP)/cm^3)**	**b (bar^{-1})**
6FDA-durene			
CO_2	2.814 ± 0.1224	72.830 ± 3.1327	0.660 ± 0.0808
CH_4	0.480 ± 0.0728	42.547 ± 3.0655	0.149 ± 0.0146
CNT-MIL/6FDA-durene			
CO_2	3.163 ± 0.1230	81.273 ± 3.1255	0.677 ± 0.0748
CH_4	0.467 ± 0.0212	45.096 ± 0.8585	0.166 ± 0.0045

For CO_2 sorption, all parameters of the 10 wt. % CNT-MIL/6FDA-durene MMM increase compared to those of the pure 6FDA-durene membrane (Table 4-4). The increment of C'_H can be assigned to the disruption of polymer chain packing causing by the CNT-MIL. More free volume is created, resulting to the increase of membrane permeability. The increments of k_D and b reflect the improved CO_2 solubility and sorption affinity of membrane after the introduction of CNT-MIL. On the other hand, the k_D for CH_4 decreased. The increment of k_D for CO_2 and the reduction of k_D for CH_4 indicate that more CO_2 and less CH_4 can be dissolved in MMMs with the incorporation of CNT-MIL (Table 4-4). Similar trends were also observed in other reported MOF MMMs with increased CO_2 solubility selectivity, contributing to membrane separation performance.[39] In the CNT-MIL/6FDA-durene MMMs, the abundant CO_2 selective groups in decorated NH_2-MIL-101(Al) facilitate the augmentation of CO_2 solubility and selectivity in MMMs. To conclude, the improvement of

membrane performance by MOFs decoration on CNTs can be attributed to the increase of both diffusivity and solubility of CO_2. Compared with the some surface modification methods (surface functionalization or metal doping),[25] MOF decoration on CNT is a more effective way to improve the membrane performance.

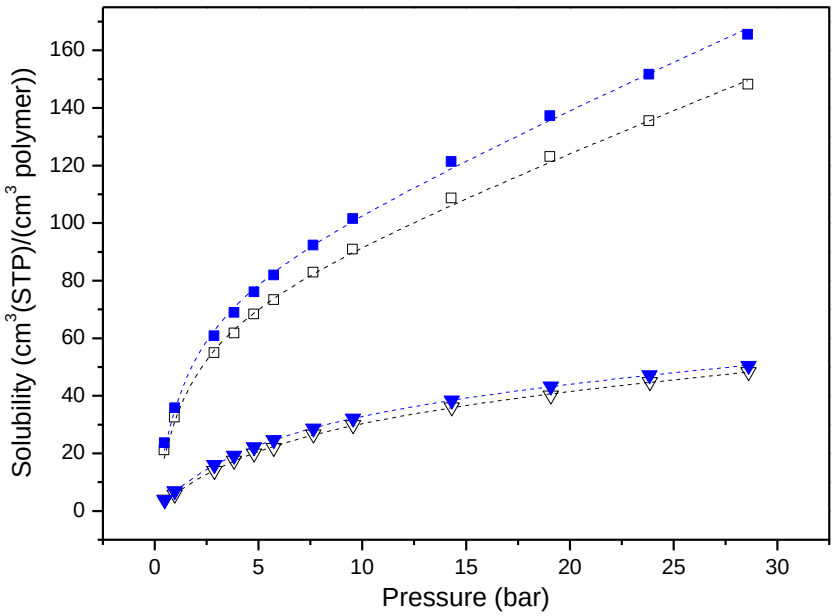

Figure 4-11 Sorption isotherms of CO_2 (square) and CH_4 (triangle) in the 6FDA-durene (hollow) and 10% CNT-MIL/6FDA-durene (solid) at 298 K. The dotted lines are fitted lines according to the dual mode sorption model.

The separation performance of our membranes for the CO_2/CH_4 gas pair is compared with other MMMs in the literature with respect to Robeson trade-off line[4] (Figure 4-12). The performance of CNT-MIL/6FDA-durene MMMs clearly transcends the 1991 upper bound for polymeric membrane performance. Specifically, CNT-MIL/6FDA-durene with CNT-MIL content of 5% and 10% exhibit excellent CO_2 permeability (818 and 1037 barrer) and good CO_2/CH_4 selectivity (29.7 and 25.4), lying on the 2008 upper bound. As shown in Figure 4-12, the as-synthesized CNT-MIL/6FDA-durene MMMs show a higher permeability and better selectivity than the reported MMMs containing MOFs or CNTs alone, indicating potential for CO_2 separation, eg. biogas or field natural gas. Here the NH_2-MIL-101(Al) decoration and the interaction in CNT-MIL play a critical role for improved CO_2 permeation in the MMMs. The introduction of many and specific functional groups as well as active sorption sites for the target gas has improved the separation performance of the MMMs. The strategy of CNT modification by MOF decoration can be a more effective way to improve the membrane performance of CNT based MMMs than some organic functionalization methods and to fabricate

high quality mixed matrix membranes.

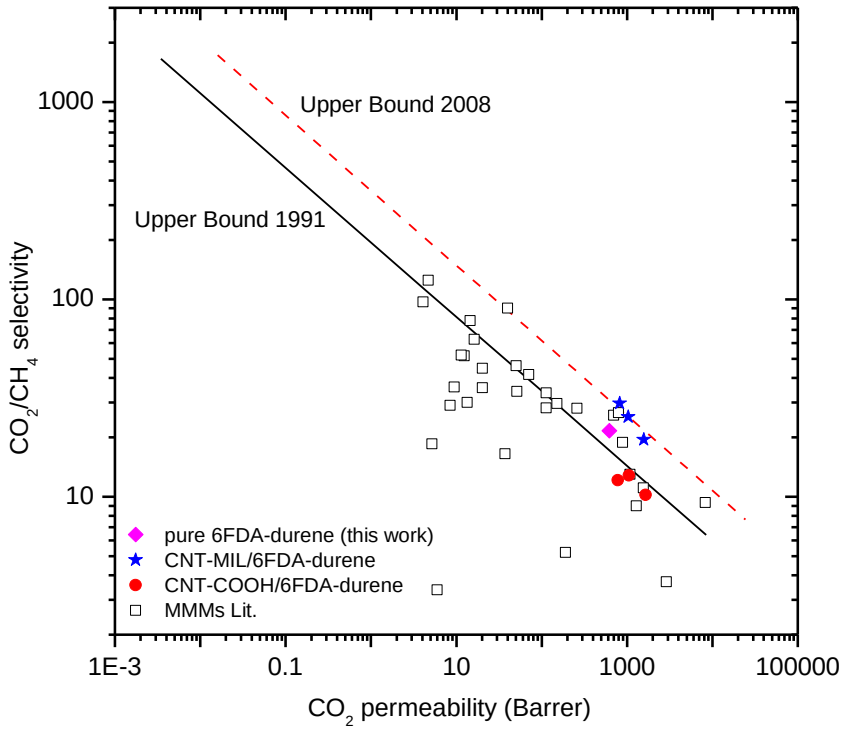

Figure 4-12 Gas separation performance of the CNT-MIL MMMs for the CO_2/CH_4 gas pair with respect to Robeson trade-off line, was compared with the compiled data on other MOFs or CNTs based MMMs in literatures. Detailed citations of MMMs are presented in the table in Appendix.

4.4 Conclusions

Here we report high performance MMMs for efficient separation of CO_2/CH_4 by taking advantages of a novel CNT-MOF composite filler. By in-situ growth of NH_2-MIL-101(Al) on the external surface of carbon nanotubes, amino groups and active sites were introduced. The synthesized CNT-MIL fillers showed good adhesion with the polymer matrix even at a high loading. Mixed matrix membranes containing CNT-MIL displayed significant improvement in both gas permeance and CO_2 selectivity compared to pure 6FDA-durene polyimide membrane. In contrast, 6FDA-durene MMMs with pure CNTs showed lower CO_2 selectivity over CH_4. The extra filler/polymer interface and polar groups provided by MOFs are key factors contributing the efficient CO_2 separation in CNT/polymer MMMs. The strategy we have shown here may lead to the development of a more effective way to further improve MMMs performance through the modification of MOFs on existing fillers that have larger adsorption differences to specific gases. The developed CNT-MOF composites can also be promising for application in adsorption, sensing and electrochemical reactions.

References

(1) Nasir, R., Mukhtar, H., Man, Z., Mohshim, D. F., Material Advancements in Fabrication of Mixed-Matrix Membranes. Chemical Engineering & Technology, 2013, 36, 717-727.

(2) Scholes, C. A., Stevens, G. W., Kentish, S. E., Membrane Gas Separation Applications in Natural Gas Processing. Fuel, 2012, 96, 15-28.

(3) Robeson, L. M., Correlation of Separation Factor versus Permeability for Polymeric Membranes. Journal of Membrane Science, 1991, 62, 165-185.

(4) Robeson, L. M., The Upper Bound Revisited. Journal of Membrane Science, 2008, 320, 390-400.

(5) Dong, G. X., Li, H. Y., Chen, V. K., Challenges and Opportunities for Mixed-Matrix Membranes for Gas Separation. Journal of Materials Chemistry A, 2013, 1, 4610-4630.

(6) Goh, P. S., Ismail, A. F., Sanip, S. M., Ng, B. C., Aziz, M., Recent Advances of Inorganic Fillers in Mixed Matrix Membrane for Gas Separation. Separation and Purification Technology, 2011, 81, 243-264.

(7) Kim, S., Chen, L., Johnson, J. K., Marand, E., Polysulfone and Functionalized Carbon Nanotube Mixed Matrix Membranes for Gas Separation: Theory and Experiment. Journal of Membrane Science, 2007, 294, 147-158.

(8) Ismail, A. F., Rahim, N. H., Mustafa, A., Matsuura, T., Ng, B. C., Abdullah, S., Hashemifard, S. A., Gas Separation Performance of Polyethersulfone/Multi-Walled Carbon Nanotubes Mixed Matrix Membranes. Separation and Purification Technology, 2011, 80, 20-31.

(9) Ackerman, D. M., Skoulidas, A. I., Sholl, D. S., Karl Johnson, J., Diffusivities of Ar and Ne in Carbon Nanotubes. Molecular Simulation, 2003, 29, 677-684.

(10) Skoulidas, A. I., Ackerman, D. M., Johnson, J. K., Sholl, D. S., Rapid Transport of Gases in Carbon Nanotubes. Physical Review Letters, 2002, 89, 185901-185904.

(11) Hirsch, A., Vostrowsky, O., Functionalization of Carbon Nanotubes, in: A.D. Schlüter (Ed.) Functional Molecular Nanostructures, Springer Berlin Heidelberg, 2005, pp. 193-237.

(12) Balasubramanian, K., Burghard, M., Chemically Functionalized Carbon Nanotubes. Small, 2005, 1, 180-192.

(13) Ge, L., Zhu, Z., Rudolph, V., Enhanced Gas Permeability by Fabricating Functionalized Multi-Walled Carbon Nanotubes and Polyethersulfone Nanocomposite Membrane. Separation and Purification Technology, 2011, 78, 76-82.

(14) Weng, T.-H., Tseng, H.-H., Wey, M.-Y., Preparation and Characterization of Multi-Walled Carbon Nanotube/PBNPI Nanocomposite Membrane for H_2/CH_4 Separation. International Journal

Of Hydrogen Energy, 2009, 34, 8707-8715.

(15) Kim, S., Pechar, T. W., Marand, E., Poly(imide siloxane) and Carbon Nanotube Mixed Matrix Membranes for Gas Separation. Desalination, 2006, 192, 330-339.

(16) Yang, Y., Ge, L., Rudolph, V., Zhu, Z., In Situ Synthesis of Zeolitic Imidazolate Frameworks/Carbon Nanotube Composites with Enhanced CO_2 Adsorption. Dalton Transactions, 2014, 43, 7028-7036.

(17) Zornoza, B., Seoane, B., Zamaro, J. M., Tellez, C., Coronas, J., Combination of MOFs and Zeolites for Mixed-Matrix Membranes. ChemPhysChem, 2011, 12, 2781-2785.

(18) Sorribas, S., Zornoza, B., Téllez, C., Coronas, J., Mixed Matrix Membranes Comprising Silica-(ZIF-8) Core–Shell Spheres with Ordered Meso–Microporosity for Natural- and Bio-Gas Upgrading. Journal of Membrane Science, 2014, 452, 184-192.

(19) Kudasheva, A., Sorribas, S., Zornoza, B., Téllez, C., Coronas, J., Pervaporation of Water/Ethanol Mixtures through Polyimide Based Mixed Matrix Membranes Containing ZIF-8, Ordered Mesoporous Silica and ZIF-8-Silica Core-Shell Spheres. Journal of Chemical Technology & Biotechnology, 2015, 90, 669-677.

(20) Li, J.-R., Sculley, J., Zhou, H.-C., Metal–Organic Frameworks for Separations. Chemical Reviews, 2012, 112, 869-932.

(21) Serra-Crespo, P., Ramos-Fernandez, E. V., Gascon, J., Kapteijn, F., Synthesis and Characterization of an Amino Functionalized MIL-101(Al): Separation and Catalytic Properties. Chemistry of Materials, 2011, 23, 2565-2572.

(22) Banerjee, S., Hemraj-Benny, T., Wong, S. S., Covalent Surface Chemistry of Single-Walled Carbon Nanotubes. Advanced Materials, 2005, 17, 17-29.

(23) Liu, Y., Wang, R., Chung, T.-S., Chemical Cross-Linking Modification of Polyimide Membranes for Gas Separation. Journal of Membrane Science, 2001, 189, 231-239.

(24) Wijenayake, S. N., Panapitiya, N. P., Versteeg, S. H., Nguyen, C. N., Goel, S., Balkus, K. J., Musselman, I. H., Ferraris, J. P., Surface Cross-Linking of ZIF-8/Polyimide Mixed Matrix Membranes (MMMs) for Gas Separation. Industrial & Engineering Chemistry Research, 2013, 52, 6991-7001.

(25) Ge, L., Zhu, Z., Li, F., Liu, S., Wang, L., Tang, X., Rudolph, V., Investigation of Gas Permeability in Carbon Nanotube (CNT)−Polymer Matrix Membranes via Modifying CNTs with Functional Groups/Metals and Controlling Modification Location. The Journal of Physical Chemistry C, 2011, 115, 6661-6670.

(26) Koros, W., Ma, Y., Shimidzu, T., Terminology for Membranes and Membrane Processes. Journal of Membrane Science, 1996, 120, 149-159.

(27) Srirambalaji, R., Hong, S., Natarajan, R., Yoon, M., Hota, R., Kim, Y., Ho Ko, Y., Kim, K., Tandem Catalysis with a Bifunctional Site-Isolated Lewis Acid-Bronsted Base Metal-Organic Framework, NH_2-MIL-101(Al). Chemical Communications, 2012, 48, 11650-11652.

(28) Ge, L., Yang, Y., Wang, L., Zhou, W., De Marco, R., Chen, Z., Zou, J., Zhu, Z., High Activity Electrocatalysts from Metal–Organic Framework-Carbon Nanotube Templates for the Oxygen Reduction Reaction. Carbon, 2015, 82, 417-424.

(29) Zhang, Y., Musselman, I. H., Ferraris, J. P., Balkus Jr, K. J., Gas Permeability Properties of Matrimid® Membranes Containing the Metal-Organic Framework Cu-BPY-HFS. Journal of Membrane Science, 2008, 313, 170-181.

(30) Ordonez, M. J. C., Balkus Jr, K. J., Ferraris, J. P., Musselman, I. H., Molecular Sieving Realized with ZIF-8/Matrimid Mixed-Matrix Membranes. Journal of Membrane Science, 2010, 361, 28-37.

(31) Lin, W.-H., Chung, T.-S., Gas Permeability, Diffusivity, Solubility, and Aging Characteristics of 6FDA-durene Polyimide Membranes. Journal of Membrane Science, 2001, 186, 183-193.

(32) Ge, L., Zhou, W., Rudolph, V., Zhu, Z. H., Mixed Matrix Membranes Incorporated with Size-Reduced Cu-BTC for Improved Gas Separation. Journal of Materials Chemistry A, 2013, 1, 6350-6358.

(33) Nik, O. G., Chen, X. Y., Kaliaguine, S., Functionalized Metal Organic Framework-Polyimide Mixed Matrix Membranes for CO_2/CH_4 Separation. Journal of Membrane Science, 2012, 413-414, 48-61.

(34) Ge, L., Wang, L., Rudolph, V., Zhu, Z., Hierarchically Structured Metal–Organic Framework/Vertically-Aligned Carbon Nanotubes Hybrids for CO_2 Capture. RSC Advances, 2013, 3, 25360-25366.

(35) Wijmans, J. G., Baker, R. W., The Solution-Diffusion Model: a Review. Journal of Membrane Science, 1995, 107, 1-21.

(36) Kanehashi, S., Nagai, K., Analysis of Dual-Mode Model Parameters for Gas Sorption in Glassy Polymers. Journal of Membrane Science, 2005, 253, 117-138.

(37) Merkel, T. C., Freeman, B. D., Spontak, R. J., He, Z., Pinnau, I., Meakin, P., Hill, A. J., Sorption, Transport, and Structural Evidence for Enhanced Free Volume in Poly(4-methyl-2-pentyne)/Fumed Silica Nanocomposite Membranes. Chemistry of Materials, 2002, 15, 109-123.

(38) Paul, D. R., Gas Sorption and Transport in Glassy Polymers. Berichte der Bunsengesellschaft für physikalische Chemie, 1979, 83, 294-302.

(39) Lin, R., Ge, L., Hou, L., Strounina, E., Rudolph, V., Zhu, Z., Mixed Matrix Membranes with Strengthened MOFs/Polymer Interfacial Interaction and Improved Membrane Performance. ACS Applied Materials & Interfaces, 2014, 6, 5609-5618.

Chapter 5 Propylene/propane selective mixed matrix membranes with grape-branched MOFs/CNTs filler

Introduction

Dispersion of the filler particles and the interfacial morphology between filler and polymer are two important factors that affect the overall separation performance of the membranes and the membrane integrity. Therefore, structural features of MMMs such as the spatial distribution of the filler and the volume of the interfacial voids are essential in evaluating the gas separation performance. Nonetheless, it is difficult to obtain these parameters through traditional experimental method. As mentioned in chapter 4, we provide a strategy to improve the dispersion of MOF through growing MOF on CNT for separation of specific gas pair. In this chapter, MOF/CNT composites derived from the growth of ZIF-8 on the surface of CNTs have been synthesized and applied to fabricate polyimide-based MMMs for propylene/propane separation. To evaluate the advantage of the composite filler, tomographic focused ion beam scanning electron microscopy (FIB-SEM) is used to quantitative analyse the spatial distribution of filler and the interfacial void space in the MMMs from the obtained 3D information. The C_3H_6/C_3H_8 separation performance of the MMMs are studied and compared to the pure polymer membrane and the MMM with only ZIF-8 filler.

Contributions

This chapter presents the fabrication of high permeable MMMs for C_3H_6/C_3H_8 separation by introducing designed ZIF-8/CNT composite filler. FIB-SEM was used as a powerful technique to quantitative analyse volume of filler and voids in the matrix also evaluate the distribution of the fillers. We found that the in-situ growth of ZIF-8 on CNT improves the dispersion of ZIF-8. The MMM achieves a good adhesion between filler and polymer, only 0.086% voids volume fraction is determined. Both C_3H_6 permeability and C_3H_6/C_3H_8 selectivity of ZIF-8/CNT MMMs are enhanced with comparison to pure polymer membrane. The strategy we show here can provide an efficient way to improve MOF dispersion for enhanced gas separation performance. Moreover, by using FIB-SEM, quantitative study of composite structure can offer more information for the design of novel composite materials. This chapter has been published in the Journal of Chemistry Materials A, DOI: 10.1039/C5TA10553F.

Propene/propane selective mixed matrix membranes with grape-branched MOFs/CNTs filler

Rijia Lin,[a] Lei Ge,*[a] Hui Diao,[b] Victor Rudolph,[a] Zhonghua Zhu,*[a]

[a]School of Chemical Engineering, The University of Queensland, Brisbane 4072 Australia

[b]Centre for Microscopy & Microanalysis, Faculty of Science, The University of Queensland, Brisbane 4072 Australia

Abstract

In this study, we fabricated mixed matrix membranes (MMMs) comprising a novel carbon nanotube/metal–organic framework (MOF) filler for efficient propylene/propane separation. Tomographic focused ion beam scanning electron microscopy was applied to quantitatively evaluate the filler dispersion and filler/polymer interfacial voids ratio. The dispersion of ZIF-8 in MMMs was improved by confined growth of ZIF-8 on the carbon nanotube (CNT) surfaces, yielding a simultaneous enhancement of C_3H_6 membrane permeability and C_3H_6/C_3H_8 selectivity. Excellent adhesion between the ZIF-8/CNT fillers and polymer matrix is observed, with only 0.086% void volume fraction, even at a high filler loading. The in-situ growth of MOF on CNT shown here can provide an effective way to design mixed matrix membranes with improved filler dispersion, structural features and separation performance

5.1 Introduction

Industrial propylene/propane separation is one of the most important but challenging processes in the petrochemical industry, traditionally performed by highly energy-intensive fractional distillation, which requires more than 200 stages as well as high reflux ratio from 12 to 20 due to close volatilities of propylene and propane.[1-3] To address this issue, gas separation utilizing membrane technology has emerged as an efficient process with significant technical and commercial impact. Compared with fractional distillation, membrane separation has superiorities such as more energy saving, easy operation, lower production and equipment cost.[4, 5]

Polymeric membranes display some advantages over inorganic membranes for benefit of material cost and ease of scale up. However, most pure polymeric membranes are still far from the commercial

demand of permeability/selectivity and fractional distillation substitution. In other words, the conventional pure polymeric membranes suffer from the limit of trade-off between C_3H_6 permeability and C_3H_6/C_3H_8 selectivity which is addressed as a Robeson upper bound for C_3H_6/C_3H_8 separation.[2] One effective approach to overcome the gas separation upper bound of pure polymeric membrane is mixed matrix membranes (MMMs), which is formed by embedding selective filler materials into polymer matrix. With proper selection of the filler/polymer pair, mixed matrix membranes benefit from both the ease of processing of the polymeric materials and superior separation property of the filler particles.[6, 7] The adsorption behavior and pore structure of inorganic fillers have been utilized for various separation system by considering the feature of penetrator.

Zeolitic imidazolate frameworks (ZIFs), as a subclass of metal organic frameworks (MOFs), which is consist of inorganic metal ions and organic imidazole/imidazolate linkers in zeolitic topologies, have been considered as appropriate materials for membranes fabrication, due to their excellent thermal and chemical stability.[8-10] Among them, ZIF-8 is regarded as a potential candidate to be used as material for the membrane separation of propylene/propane, which presents high kinetic selectivity for these two similar gas molecules,[11] and the corresponding supported ZIF-8 membranes showed impressive propylene/propane separation performance.[12-17]

A few recent studies sought to fabricate the ZIF-8 based mixed matrix membranes for C_3H_6/C_3H_8 separation. Zhang et al.[18] reported a ZIF-8/6FDA-DAM MMM with 48.0 wt% ZIF-8 loading, showing C_3H_6 permeability of 56.2 Barrer and ideal C_3H_6/C_3H_8 selectivity of 31.0. The C_3H_6/C_3H_8 selectivity was significantly enhanced after the incorporation of ZIF-8. Askari et al.[19] synthesized 40 wt% ZIF-8/6FDA-Durene-DABA (9/1) MMM with a C_3H_6 permeability of 47.3 Barrer after thermally annealing at 400 ºC. The ideal C_3H_6/C_3H_8 selectivity improved 134% from 11.68 to 27.38 compared to pure polymer. The above ZIF-8 based MMMs showed dramatically increase in C_3H_6/C_3H_8 selectivity with comparison of the pure polymer, however, their C_3H_6 permeabilities are still far from commercial requirements. Moreover, the dispersion of nano-ZIF-8 with high concentration in polymer matrix remains problem, which restricts further improvement of membrane performance.

In this study, a noval approach to achieve high performance MMMs was proposed by introducing composite fillers synthesized by in situ growth of ZIF-8 on the external surface of the carbon nanotubes (Figure 5-1). Focused ion beam scanning electron microscopy (FIB-SEM) was used to quantitative analyse the volume of filler and voids in the polymeric matrix as well as evaluate the distribution of the fillers and their contact with the polymeric matrix. Improved dispersion of ZIF-8 in polymeric matrix has been realized with the aid of CNT skeleton. Both enhanced C_3H_6 permeability

and C_3H_6/C_3H_8 separation performance of ZIF-8/CNT MMMs are observed.

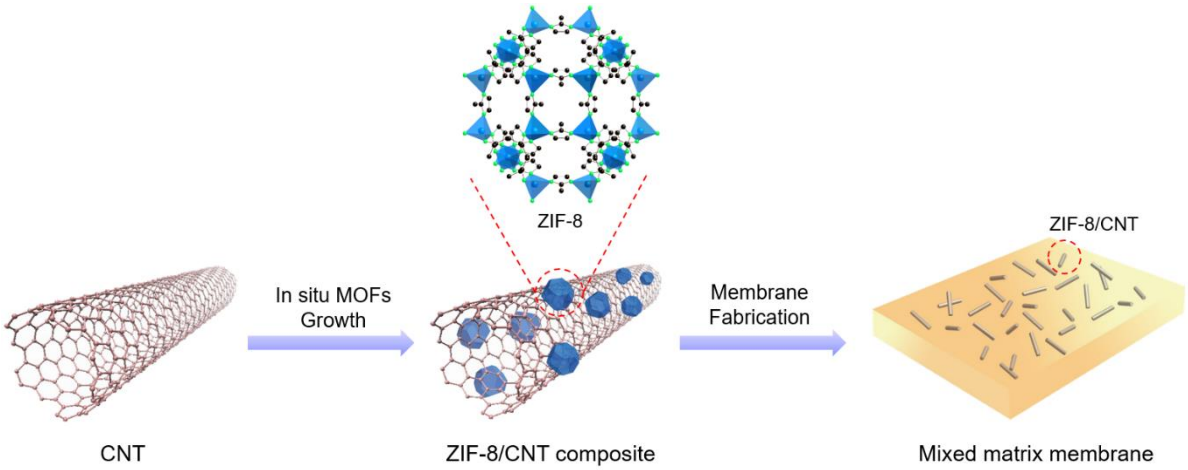

Figure 5-1 Schematic diagram of a 6FDA-durene MMM containing ZIF-8 decorated CNTs

5.2 Experimental section

5.2.1 Materials synthesis

5.2.1.1 Materials

Zinc nitrate hexahydrate ($Zn(NO_3)_2 \cdot 6H_2O$), 2-methylimidazole (Hmim), 4, 4'-(hexafluoroisopropylidene) diphthalic anhydride (6FDA), 2,3,5,6-tetramethyl-1,3-phenyldiamine (durene), triethylamine, acetic anhydride, N,N-dimethylformamide (DMF), N,N-dimethylacetamide (DMAc) and methanol were supplied by Sigma–Aldrich. The multi-walled carbon nanotubes (MWCNTs) produced from methane decomposition over a Fe catalyst in a fluidized-bed reactor were supplied by Tsinghua University, China. The purity in pristine samples exceeded 95 wt.%. The orientation of the carbon layers in a typical CNT is parallel to its axis.

5.2.1.2 Synthesis of ZIF-8

The ZIF-8 was synthesized based on a reported previously.[20] 0.5866 g $Zn(NO_3)_2 \cdot 6H_2O$ and 1.2978 g Hmim were dissolved into 60 mL of methanol. The mixture was transferred into a Teflon-line stainless steel autoclave after 15 min stirring, heated at 90 °C for 6 h. After the solvothermal reaction, the ZIF-8 crystals were separated by centrifugation and washed in methanol for three times, the product was finally dried at 100 °C under vacuum overnight.

5.2.1.3 Synthesis of ZIF-8/CNT composites

The preparation of ZIF-8/CNT composite was carried out the same as the work reported in our previous paper.[21] 0.5 g CNTs were treated with 300 ml mixture of concentrated H_2SO_4 (98

vol.%)/HNO_3 (70 vol.%) (3:1) at 60 °C for 3 h. Subsequently, the mixture was sonicated for 0.5 h. After that the samples was washed with deionized water for several times. The samples were finally filtered and dried under vacuum. CNTs with oxidized carboxylic groups were obtained and referred as CNT-COON. ZIF-8/CNT composites were prepared under the same solvothermal procedures of ZIF-8 as above, except 120 mg of CNT-COOH was dispersed in Hmim methanol solution by repeating sonication and stirring process prior to adding the $Zn(NO_3)_2 \cdot 6H_2O$. The total volume of solution is constant at 60 ml. The synthesized ZIF-8/CNT composite was referred as ZC.

5.2.1.4 Synthesis of 6FDA-durene polyimide

As shown in Figure 5-2, the 6FDA-durene polyimide was synthesized with a two-step reaction base on the work reported elsewhere.[22, 23] In the first step, polyamic acid was form by polymeric reaction between equimolar amounts of durene (1.426 g) and 6FDA (3.861 g) in DMAc. The polyamic acid solutions were made up to 20% solids. The mixture was stirred under nitrogen at room temperature for 24 h. In the second step, a mixture of triethylamine (3.2 mL) and acetic anhydride (1.2 mL) was added to the polyamic acid solution. The combined mixture was stirred under nitrogen at room temperature for another 24 h. Polyamic acid was imidized to form polyimides. The final polymer was precipitated in methanol, washed several times with methanol, and dried at 180 °C under vacuum for 18 h. The polyimide product is referred as 6FDA-durene.

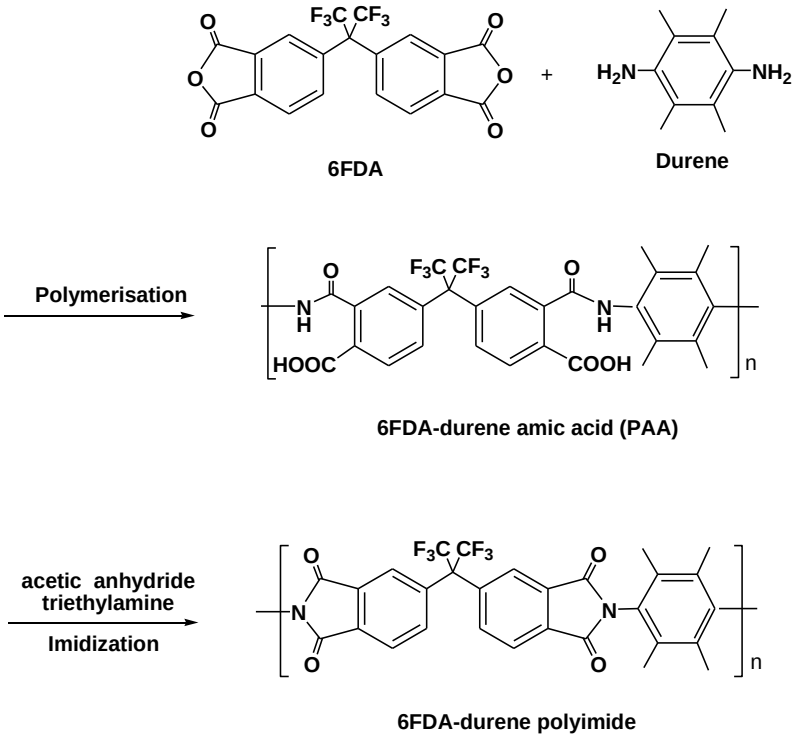

Figure 5-2 Multi-staged of 6FDA-durene polyimide synthesis

5.2.1.5 Membrane preparation

For pure 6FDA-durene membrane, 0.45 g 6FDA-durene was dissolved into 3 mL DMF at room temperature. The resulting solution was cast onto a clean glass plate, followed by drying at 180 ºC for 24 h in a vacuum oven. For the MMMs, certain amount of as-synthesized ZC or ZIF-8 was dispersed in DMF under sonication. 0.45 g 6FDA-durene was dissolved into this suspension and the suspension was further stirred for 6 h. The resulting mixture was cast and dried at 180 ºC for 24 h under vacuum. The selected thickness for casting procedure was 40 µm. The thickness of pure 6FDA-durene and MMMs were measured using a micrometer within the range of 30–40 µm. Before gas permeation tests and characterisation, the membranes were stored with desiccant.

The loadings of filler in MMMs were adjusted to 5, 10, 15 wt% for the purposes of this study based on equation (5-1).

$$\phi = \frac{m_{Filler}}{m_{Filler} + m_{6FDA\text{-}durene}} \quad (5\text{-}1)$$

where m_{Filler} and $m_{6FDA\text{-}durene}$ are the mass of filler and 6FDA-durene in the MMMs, respectively.

5.2.2 Characterization

The X-ray diffraction (XRD) data were obtained from a Brucker Advanced X-ray Diffractometer (40 kV, 30 mA) with Cu Kα (λ= 0.15406 nm) radiation at a scanning rate of 1º min^{-1} from 5º to 40º.

The thermal stability of ZC and content of ZIF-8 in the ZC composite were measured by a Perkin Elmer Instruments STA 6000 Thermo Gravimetric Analyzer (TGA). All samples were heated under an air atmosphere at 100 ºC for 120 min first to remove the moisture, then heated from 100 ºC to 800 ºC with a uniform heating rate of 5 ºC min^{-1}.

The content of ZIF-8 in the composite can be calculated by solving eqs 5-2 and 5-3.[24]

$$\mathrm{ZIF\%} + \mathrm{CNT\%} = 1 \quad (5\text{-}2)$$

$$35.46\% \times \mathrm{ZIF\%} + \mathrm{Residue_{CNT}\%} \times \mathrm{CNT\%} = \mathrm{Residue_{composite}\%} \quad (5\text{-}3)$$

Where ***ZIFs%*** and ***CNTs%*** are the weight percentages of ZIF-8 and CNTs in the composites, and $\boldsymbol{Residue_{CNTs}\%}$ and $\boldsymbol{Residue_{composite}\%}$ are the weight percentage of residue in CNTs and composites after the thermo gravimetric analysis (TGA), respectively.

The content of ZIF-8 in the ZC composite is 53.1 wt% as calculated from thermo TGA results. The density of ZC composite was calculated to be 1.49 g cm^{-3} based on the density and ratio of ZIF-8 and CNT in the composite. The density of the 6FDA-durene polyimide is 1.33 g cm^{-3}.[25]

The N_2 adsorption isotherms were obtained from a Micromeritics TriStar II 3020 at 77 K, after degassing the sample at 200 °C for 24 h. BET surface area was calculated over the range of relative pressures between 0.005 and 0.05. The morphologies of the samples were obtained with a JEOL JSM7100 scanning electron microscope (SEM) at 8 kV. High resolution transmission electron microscopy (HRTEM) was performed on a JEOL JEM-2100 microscope, with accelerating voltages of 200 kV. The samples were dispersed by sonication in ethanol, deposited on a holey carbon TEM grid and dried prior to examination.

Focused ion beam scanning electron microscopy (FIB-SEM) was performed in a FEI SCIOS FIB/SEM dual beam system to assess the distribution of the ZC and ZIF-8 filler in the polymer matrix and the contact of the two phase. The specimen was sputtered with a conducting layer of Pt for 100 s. A trench was milled on the surface of the membrane by using a Ga^+ focused ion beam (Figure 5-3). Serial milling of slices with a thickness of 30 nm were removed from the specimen up to a depth of 8 μm by the Ga^+ FIB at 30kV and 1nA. A series of exposed cross-section SEM images in back-scattered electron (BSE) imaging mode were collected sequentially during the automatic slice-and-view experiments using an in-lens backscattered electron detector at 2kV. In the BSE SEM image, the different constituents of membrane can be recognized through the different grayscale. Fillers are brightest whereas polymer appear a medium grayscale, and voids are darker than the polymer matrix. The segmentation of the individual phases (e.g. 6FDA-durene, ZC and voids) was conducted by image thresholding.[26, 27] The stack of these SEM images was aligned, and the analyzed volume can be reconstructed in three-dimensional (video). Avizo (FEI Visualization Sciences Group) was used to reconstruct the tomogrames, segment different phases and quantify the corresponding 3D volume.

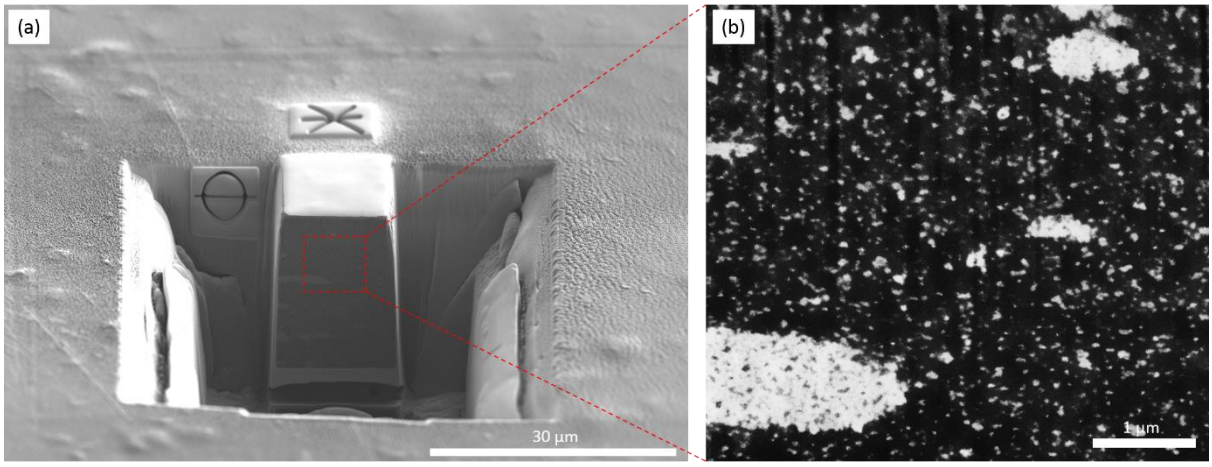

Figure 5-3 Typical FIB-SEM images of 15 wt% ZIF-8/6FDA-durene MMM (a) FIB milling hole (b) cross-sectional image in the BSE mode

5.2.3 Permeation test

A variable feed pressure and the constant volume permeation system was used to measure the gas permeation of membranes, as described elsewhere.[28] The membranes were held under vacuum for approximately 5 min to achieve a steady state before being exposed to the selected gas. Before switching to the feed gas, the membrane has to be degassed for some time to ensure the complete desorption of initial permeate gas. The test was held at 25 ºC, 2atm feed pressure. The permeation coefficient is calculated using the following equation:

$$P = \frac{273.15\times10^{10}}{760\mathrm{AT}} \frac{VL}{\frac{P_0\times76}{14.7}} \frac{\mathrm{d}p}{\mathrm{d}t} \quad (5\text{-}4)$$

where P is the permeation coefficient in barrer (1 barrer =1×10^{-10} cm^3 (STP) cm cm^{-2} s^{-1} cm Hg^{-1}), A is the effective area of the membrane (cm^2), T is the absolute temperature (K), V is the dead-volume of the downstream chamber (cm^3), L is the membrane thickness (cm), P_0 is the feed pressure (psi), and dp/dt is the steady rate of pressure increase in the downstream side (mm Hg s^{-1}).

The ideal selectivity for two gases is determined as:

$$\alpha = \frac{P_\mathrm{A}}{P_\mathrm{B}} \quad (5\text{-}5)$$

where P_A and P_B are the permeation coefficients of pure gas A and B, respectively.

5.3 Results and discussions

The X-ray diffraction (XRD) patterns of pure ZIF-8 and ZC composite samples are shown in Figure 5-4. The diffraction pattern of ZC matches well with that of pure ZIF-8, indicating the confine growth on CNT does not affect the synthesis of pure phase ZIF-8. Figure 5-5 presents the scanning electron microscopy (SEM) images of pure ZIF-8 and the ZC composite. A grape-branched morphology is observed for the as-synthesized composite with ZIF-8 crystals fully covering the external surface of the CNTs, which can be attributed to the strong interaction between ZIF-8 and CNTs.[21, 24] Further evidence of the formation of is shown by HRTEM in Figure 5-6, where ZIF-8 crystals with the size of around 50 nm grow on the CNTs external surface. The oxygen functional groups on CNT surface provide the nucleation sites and allow the formation of MOFs by heterogeneous nucleation. The BET surface area of pure ZIF-8 and ZC measured from the N_2 adsorption/desorption isotherms (Figure 5-7) are 1929 and 1307 m^2 g^{-1}, respectively. High surface area and adsorption capacity of ZC

nanocomposites are obtained due to the interaction between ZIF-8 and CNTs through in-situ growth of ZIF-8 on CNTs. [21, 24]

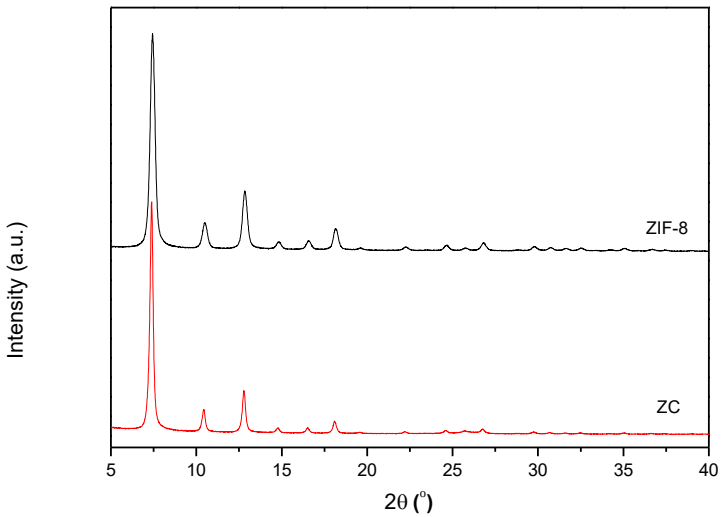

Figure 5-4 XRD pattern of ZIF-8 and ZC

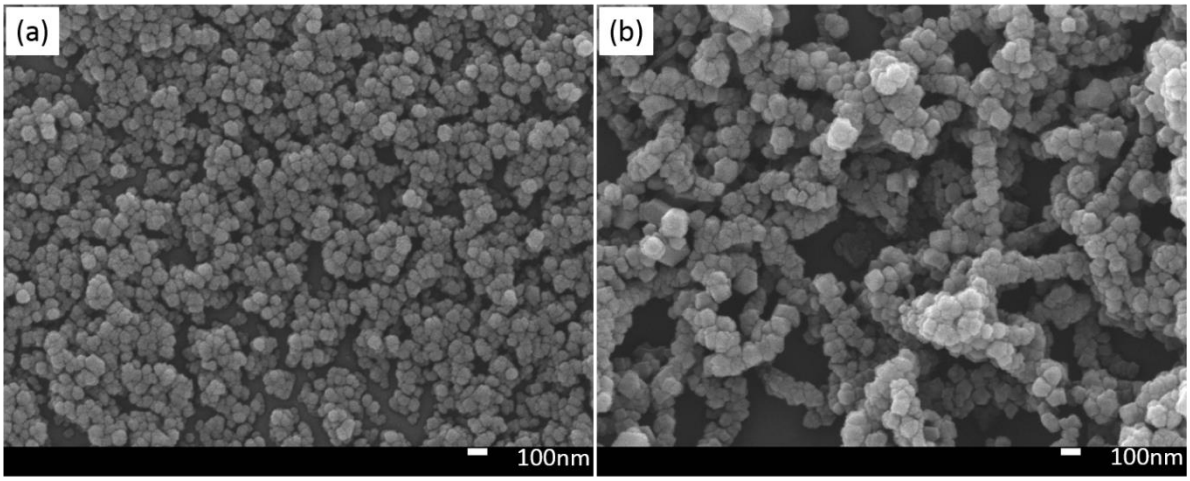

Figure 5-5 SEM images of (a) ZIF-8 and (b) ZC composite

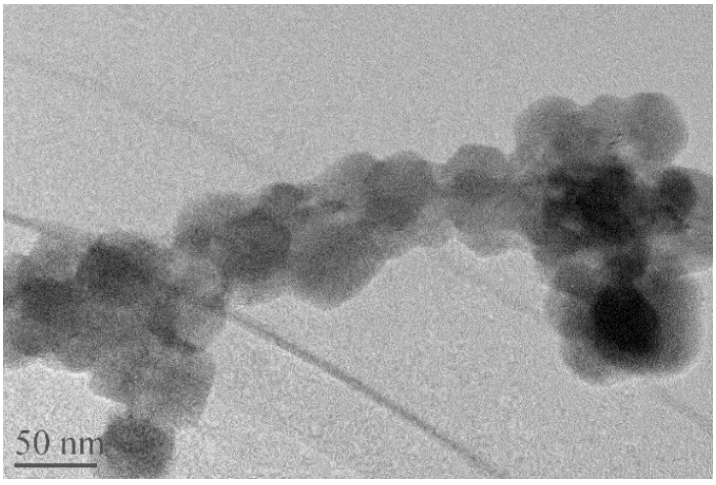

Figure 5-6 TEM image of ZC

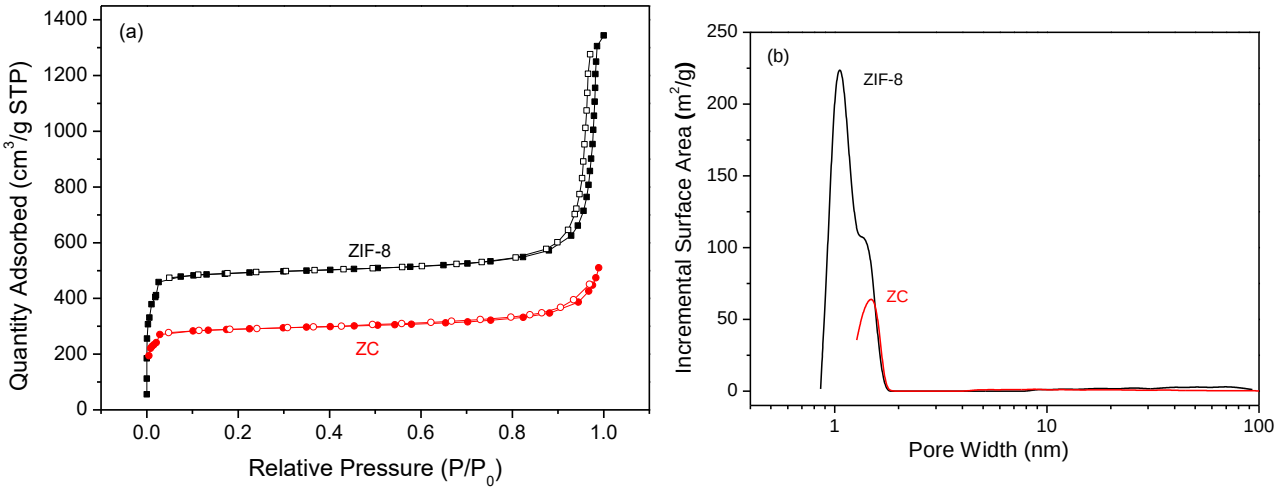

Figure 5-7 (a) N_2 adsorption/desorption isotherms of ZIF-8 and ZC at 77 K (solid symbols = adsorption; empty symbols = desorption); (b) pore size distribution of ZIF-8 and ZC

Figure 5-8 depicts the SEM images of pure 6FDA-durene membrane and ZC/6FDA-durene MMMs cross-section with filler loading ratio. As is shown in Figure 5-8, the ZC fillers have good interfacial contact with the polymer matrix, even at a high loading. A crater-like morphology is observed whose center corresponds to the ZC fillers. The formation of this morphology can be attributed to the strong interfacial interaction provided by linker functionality of ZIF-8. Similar observations in MMMs can also be found in previous literature.[29, 30]

The ideal propylene/propane separation performance of the as-synthesized membranes was measured to evaluate the performance of the as-synthesized membranes. Figure 5-9 shows the single gas permeability and C_3H_6/C_3H_8 selectivity of the pure 6FDA-durene membrane and ZC/6FDA-durene MMMs. The enhancement of both C_3H_6 and C_3H_8 permeability of the ZC/6FDA-durene MMMs with increasing filler loading ratio was observed. Compared with the pure polymer membrane, the C_3H_6 permeability of the MMM with 15 wt% ZC doubled. The distinct enhance of permeability can be explained by: the packing of the polymer chain is disrupted by the inorganic particles and as a consequence, more free volume is introduced in the MMM. The extra-introduced free volume provides more channels for gas diffusion, and therefore higher permeability can be achieved.[31]

By ZC incorporation into polymer matrix, the permeability of C_3H_6 increases more significant than C_3H_8, resulting in a superior C_3H_6/C_3H_8 selectivity compared to the pure 6FDA-durene membrane. The remarkable C_3H_6/C_3H_8 selectivity increment (16.1) is observed in the MMM with 15 wt% ZC, compared the pure 6FDA-durene membrane (8.2). This phenomenon can be attributed to the highly discrimination of ZIF-8 for the diffusion of this gas pair. The diffusivity of propylene is much higher than that of propane in the framework of ZIF-8.[11, 13] In contrast, without the present of CNT, the 15 wt% ZIF-8/6FDA-durene MMM displays a much lower C_3H_6/C_3H_8 selectivity though with higher

C_3H_8 permeability (Table 5-1). Compared to ZC/6FDA-durene MMMs, large content of filler agglomerations can be observed in ZIF-8/6FDA-durene MMM (Figure 5-10), leading to the deterioration of separation efficiency. We suggest that the confined growth of ZIF-8 on external surfaces of CNT can improve the dispersion of ZIF-8 and MOFs/polymer interface interaction in the subsequent MMMs, contributing to the increase of gas/filler interaction and the reduction of the unselective interfacial voids.

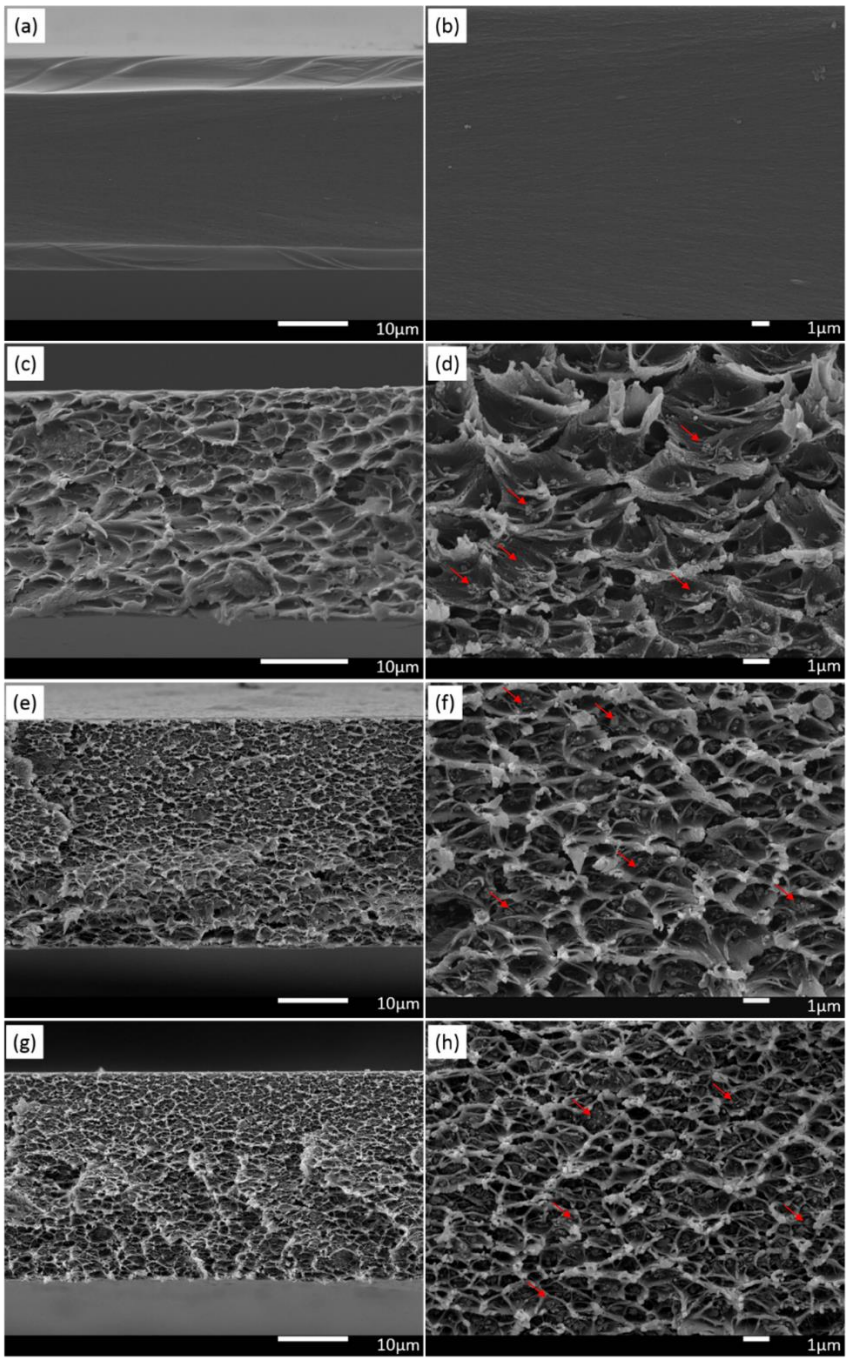

Figure 5-8 SEM images of pure 6FDA-durene (a, b) and ZC/6FDA-durene MMMs cross-sections with different amount of ZC (c, d: 5wt%; e, f: 10wt%; g, h: 15wt%). Arrows point to the ZC particles embedded in polymer matrix.

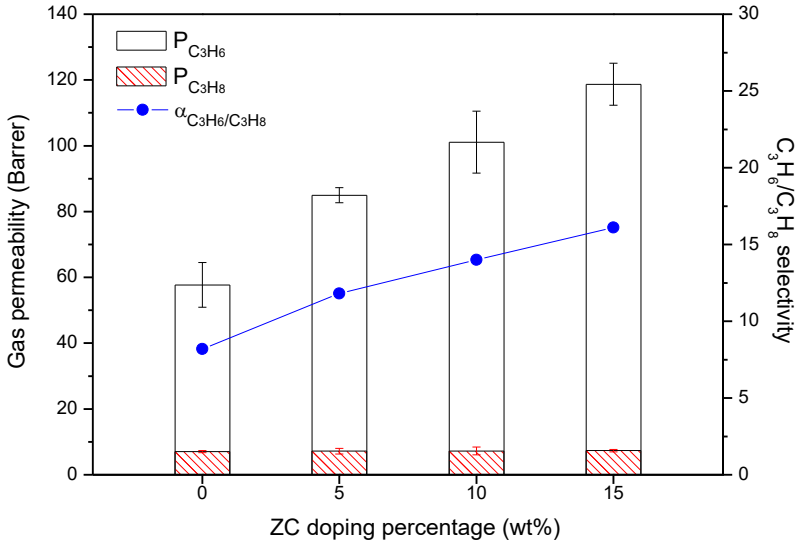

Figure 5-9 Gas permeability and selectivity of the pure 6FDA-durene membrane and ZC/6FDA-durene MMMs

Table 5-1 Gas permeability and selectivity of 15 wt% ZIF-8/6FDA-durene MMM (25 °C, 2 atm feed gas pressure)

Sample	**Permeability (Barrer)**		**Selectivity**
	C_3H_6	**C_3H_8**	**C_3H_6/C_3H_8**
15 wt% ZIF-8/6FDA-durene MMM	120.4±4.87	9.66±1.25	12.46

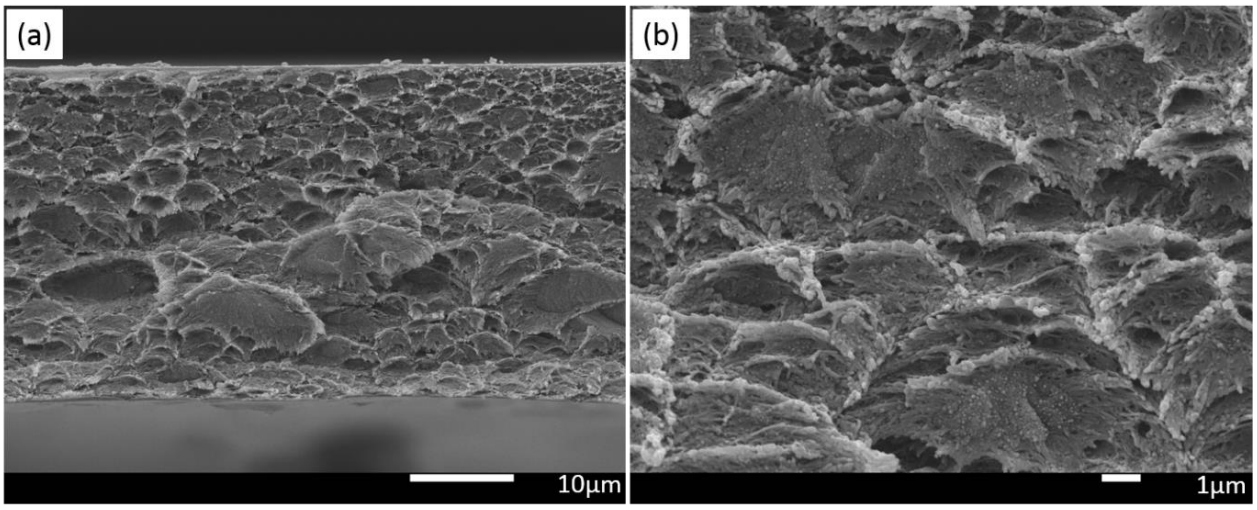

Figure 5-10 Cross-section SEM images of 15 wt% ZIF-8/6FDA-durene MMM (a: low magnification; b: high magnification)

The well dispersion of filler particles and the elimination of interfacial voids are vital to the overall transport performance of the membranes and membrane integrity. To investigate these structural features of MMMs, a tomography focused ion beam scanning electron microscopy was applied in this study. The 15 wt% ZC/6FDA-durene MMM sample with best C_3H_6/C_3H_8 separation performance was chosen. Figure 5-11 shows the 3D surface-rendered view of the fillers and void volume in ZC/6FDA-durene MMM. The volume fractions of voids, filler and polymer are summarized in the Table 5-2. The mass based MOF loading can be determined by quantification of the segmented volume. As shown in Table 5-2, the MOF weight loading determined from the image analysis and density calculation is in good agreement with the bulk MOF loading (15 wt%). As can be seen in Figure 5-11c, MMM still achieve a well distribution of the ZC filler within the polymer matrix even at such a high loading. The volume corresponding to the voids was shown in Figure 5-11d. Based on the 3D tomographic images, the volume fraction of voids determined by image analysis is only 0.086%. Such little volume fraction of voids confirms the excellent interface between ZC filler and the polymer matrix.

Table 5-2 Volume and mass fraction of different phase in 15 wt% ZC/6FDA-durene MMM derived from the image analysis of the reconstructed FIB-SEM tomogram

Material	Volume fraction (%v/v)	Mass fraction (wt%)
Filler	13.8	15.4
Polymer	86.2	84.6
Void	0.086	

Figure 5-11e and Figure 5-12 present the filler volume variation in different depth of ZC/6FDA-durene MMM and ZIF-8/6FDA-durene MMM, respectively. Greater fluctuation of ZIF-8 volume distribution can be observed in ZIF-8/6FDA-durene MMM (Figure 5-12) attributing to the poor dispersion and agglomerations of ZIF-8 in polymer matrix. On the other hand, less fluctuation of volume distribution over depth in ZC/6FDA-durene MMM suggests that the uniform dispersion of ZC filler (Figure 5-11e), which can be ascribed to the improvement of ZIF-8 dispersion by CNT skeleton. The filler particle volume distributions of 15 wt% ZC/6FDA-durene MMM and 15 wt% ZIF-8/6FDA-durene MMM derived from image analysis of the FIB-SEM tomogram are shown in

Figure 5-11f and Figure 5-12b, respectively. Considering the incorporation of nano-sized ZIF-8 into polymer matrix, sever agglomerations of ZIF-8 can be found in 15 wt% ZIF-8/6FDA-durene MMM. On the contrary, better dispersion of ZC can be found in ZC/6FDA-durene MMM. To conclude, the MOF decoration on CNT can be a potential modification method to solve the filler aggregation problem and improve filler/polymer interface, lead to the significant improvement of membrane performance.

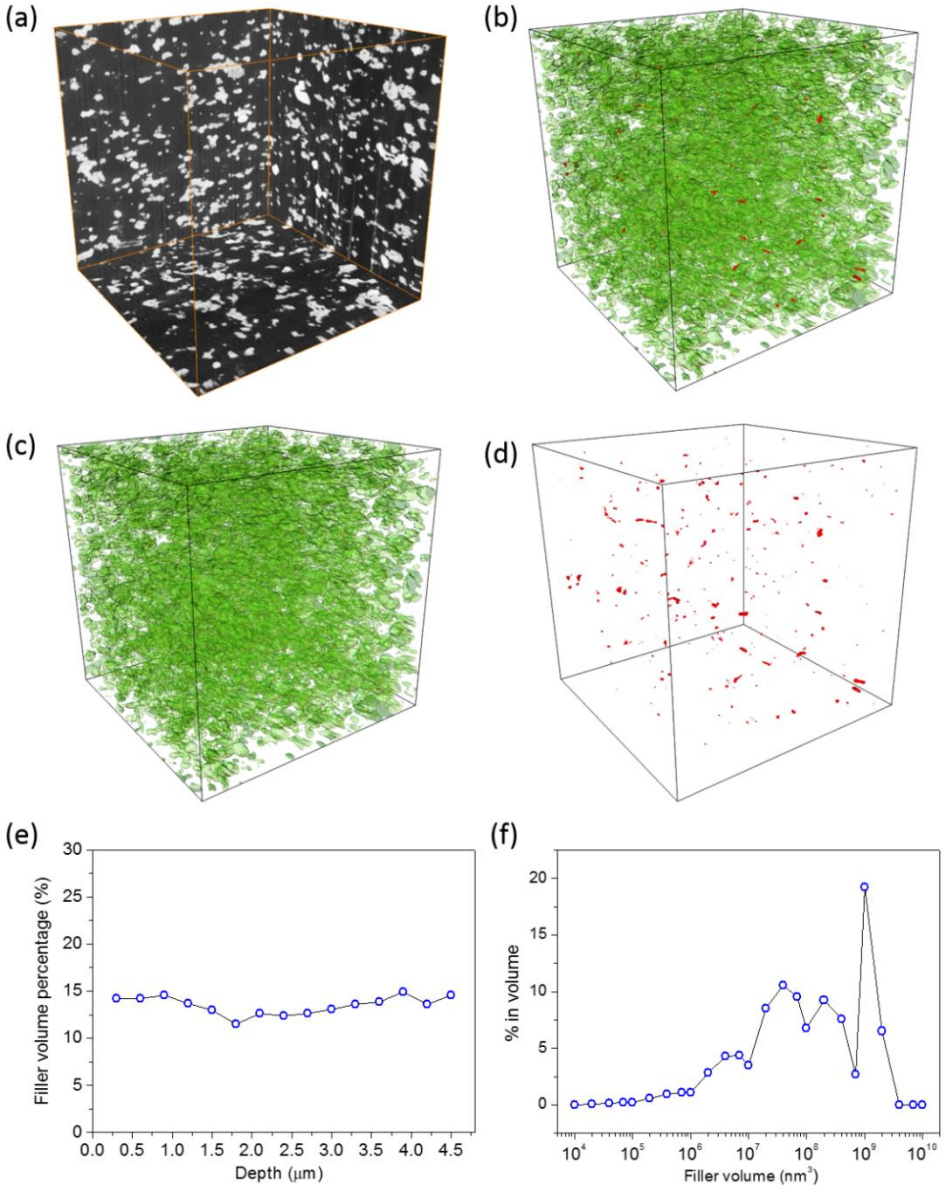

Figure 5-11 (a) Typical 3D restructured volume of the portion of 15 wt% ZC/6FDA-durene MMM. The corresponding surface-rendered view of the segmented FIB-SEM tomograms for MMM (b), ZC fillers (c) and voids (d). ZC appear in green and voids in red. Box size: 5.0 μm× 5.1 μm× 5.0 μm. (e) Filler volume variation in different depth of 15 wt% ZC/6FDA-durene MMM. (f) Filler particle size distribution in 15 wt% ZC/6FDA-durene MMM derived from image analysis of the FIB-SEM tomogram.

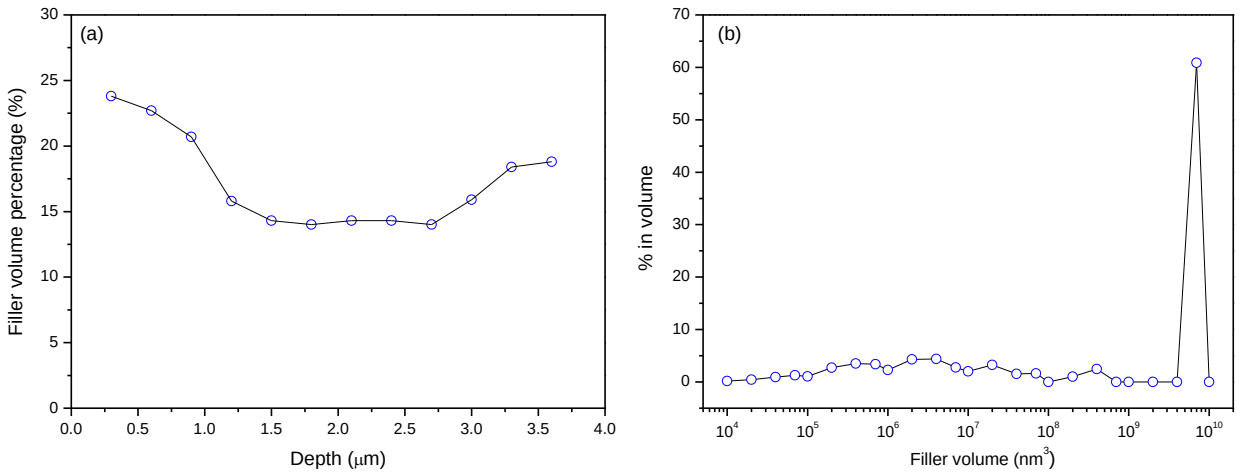

Figure 5-12 (a) Filler volume variation in different depth of 15 wt% ZIF-8/6FDA-durene MMM; (b) Filler particle size distribution in 15 wt% ZIF-8/6FDA-durene MMM derived from image analysis of the FIB-SEM tomogram

5.4 Conclusions

We report high permeable MMMs for efficient separation of C_3H_6/C_3H_8 by taking advantages of designed MOF/CNT composite filler. the derived mixed matrix membranes present significant improvements in both C_3H_6 gas permeance and C_3H_6/C_3H_8 selectivity compared to the pure 6FDA-durene polyimide membrane. To address the merit of the composite filler, tomographic FIB-SEM was used as a powerful technique to evaluate the spatial distribution of filler and the interfacial void space in the MMMs via providing 3D information. By quantitative analysis of FIB-SEM results, we found that in-situ growing ZIF-8 on the external surface of carbon nanotubes can significantly improve the dispersion of ZIF-8 in the polymer matrix, and this ZIF-8/CNT particle also showed good adhesion with the polymer in mixed matrix membranes even at a high loading. The improved ZIF-8 dispersion and filler/polymer interface lead to the efficient C_3H_6 separation in MMMs. The strategy we employed here exploits an efficient way to improve MOF dispersion and gas/filler interaction for efficient gas separation. Furthermore, by utilizing the quantitative study of composite structure, the findings can provide some insights in the design of high quality composite materials for various applications, such as gas separation, catalysis, sensing and electrochemical reactions.

References

(1) Baker, R. W., Future Directions of Membrane Gas Separation Technology. Industrial & Engineering Chemistry Research, 2002, 41, 1393-1411.

(2) Burns, R. L., Koros, W. J., Defining the Challenges for C_3H_6/C_3H_8 Separation Using Polymeric Membranes. Journal of Membrane Science, 2003, 211, 299-309.

(3) Das, M., Koros, W. J., Performance of 6FDA–6FpDA Polyimide for Propylene/Propane Separations. Journal of Membrane Science, 2010, 365, 399-408.

(4) Koros, B., Three Hundred Volumes. Journal of Membrane Science, 2007, 300, 1-1.

(5) Nasir, R., Mukhtar, H., Man, Z., Mohshim, D. F., Material Advancements in Fabrication of Mixed-Matrix Membranes. Chemical Engineering & Technology, 2013, 36, 717-727.

(6) Zornoza, B., Tellez, C., Coronas, J., Gascon, J., Kapteijn, F., Metal Organic Framework based Mixed Matrix Membranes: An Increasingly Important Field of Research with a Large Application Potential. Microporous and Mesoporous Materials, 2013, 166, 67-78.

(7) Dong, G. X., Li, H. Y., Chen, V. K., Challenges and Opportunities for Mixed-Matrix Membranes for Gas Separation. Journal of Materials Chemistry A, 2013, 1, 4610-4630.

(8) Hayashi, H., Cote, A. P., Furukawa, H., O'Keeffe, M., Yaghi, O. M., Zeolite A Imidazolate Frameworks. Nature Materials, 2007, 6, 501-506.

(9) Banerjee, R., Phan, A., Wang, B., Knobler, C., Furukawa, H., O'Keeffe, M., Yaghi, O. M., High-throughput synthesis of zeolitic imidazolate frameworks and application to CO2 capture. Science, 2008, 319, 939-943.

(10) Phan, A., Doonan, C. J., Uribe-Romo, F. J., Knobler, C. B., O'Keeffe, M., Yaghi, O. M., Synthesis, Structure, and Carbon Dioxide Capture Properties of Zeolitic Imidazolate Frameworks. Accounts Of Chemical Research, 2010, 43, 58-67.

(11) Li, K., Olson, D. H., Seidel, J., Emge, T. J., Gong, H., Zeng, H., Li, J., Zeolitic Imidazolate Frameworks for Kinetic Separation of Propane and Propene. Journal Of The American Chemical Society, 2009, 131, 10368-10369.

(12) Pan, Y. C., Li, T., Lestari, G., Lai, Z. P., Effective Separation of Propylene/Propane Binary Mixtures by ZIF-8 Membranes. Journal of Membrane Science, 2012, 390, 93-98.

(13) Liu, D., Ma, X., Xi, H., Lin, Y. S., Gas transport Properties and Propylene/Propane Separation Characteristics of ZIF-8 Membranes. Journal of Membrane Science, 2014, 451, 85-93.

(14) Kwon, H. T., Jeong, H. K., Highly Propylene-Selective Supported Zeolite-Imidazolate Framework (ZIF-8) Membranes Synthesized by Rapid Microwave-Assisted Seeding and Secondary Growth. Chemical Communications, 2013, 49, 3854-3856.

(15) Shah, M. N., Gonzalez, M. A., McCarthy, M. C., Jeong, H. K., An Unconventional Rapid Synthesis of High Performance Metal-Organic Framework Membranes. Langmuir, 2013, 29, 7896-7902.

(16) Kwon, H. T., Jeong, H. K., In Situ Synthesis of Thin Zeolitic-Imidazolate Framework ZIF-8

Membranes Exhibiting Exceptionally High Propylene/Propane Separation. Journal Of The American Chemical Society, 2013, 135, 10763-10768.

(17) Hara, N., Yoshimune, M., Negishi, H., Haraya, K., Hara, S., Yamaguchi, T., Diffusive Separation of Propylene/Propane with ZIF-8 Membranes. Journal of Membrane Science, 2014, 450, 215-223.

(18) Zhang, C., Dai, Y., Johnson, J. R., Karvan, O., Koros, W. J., High Performance ZIF-8/6FDA-DAM Mixed Matrix Membrane for Propylene/Propane Separations. Journal of Membrane Science, 2012, 389, 34-42.

(19) Askari, M., Chung, T.-S., Natural Gas Purification and Olefin/Paraffin Separation Using Thermal Cross-Linkable Co-Polyimide/ZIF-8 Mixed Matrix Membranes. Journal of Membrane Science, 2013, 444, 173-183.

(20) Cravillon, J., Münzer, S., Lohmeier, S.-J., Feldhoff, A., Huber, K., Wiebcke, M., Rapid Room-Temperature Synthesis and Characterization of Nanocrystals of a Prototypical Zeolitic Imidazolate Framework. Chemistry of Materials, 2009, 21, 1410-1412.

(21) Ge, L., Yang, Y., Wang, L., Zhou, W., De Marco, R., Chen, Z., Zou, J., Zhu, Z., High Activity Electrocatalysts from Metal–Organic Framework-Carbon Nanotube Templates for the Oxygen Reduction Reaction. Carbon, 2015, 82, 417-424.

(22) Liu, Y., Wang, R., Chung, T.-S., Chemical Cross-Linking Modification of Polyimide Membranes for Gas Separation. Journal of Membrane Science, 2001, 189, 231-239.

(23) Wijenayake, S. N., Panapitiya, N. P., Versteeg, S. H., Nguyen, C. N., Goel, S., Balkus, K. J., Musselman, I. H., Ferraris, J. P., Surface Cross-Linking of ZIF-8/Polyimide Mixed Matrix Membranes (MMMs) for Gas Separation. Industrial & Engineering Chemistry Research, 2013, 52, 6991-7001.

(24) Yang, Y., Ge, L., Rudolph, V., Zhu, Z., In Situ Synthesis of Zeolitic Imidazolate Frameworks/Carbon Nanotube Composites with Enhanced CO_2 Adsorption. Dalton Transactions, 2014, 43, 7028-7036.

(25) Lin, W.-H., Chung, T.-S., Gas Permeability, Diffusivity, Solubility, and Aging Characteristics of 6FDA-durene Polyimide Membranes. Journal of Membrane Science, 2001, 186, 183-193.

(26) Rodenas, T., van Dalen, M., García-Pérez, E., Serra-Crespo, P., Zornoza, B., Kapteijn, F., Gascon, J., Visualizing MOF Mixed Matrix Membranes at the Nanoscale: Towards Structure-Performance Relationships in CO_2/CH_4 Separation Over NH_2-MIL-53(Al)@PI. Advanced Functional Materials, 2014, 24, 249-256.

(27) Rodenas, T., Luz, I., Prieto, G., Seoane, B., Miro, H., Corma, A., Kapteijn, F., Llabrés i Xamena, F. X., Gascon, J., Metal–Organic Framework Nanosheets in Polymer Composite Materials for Gas Separation. Nature Materials, 2015, 14, 48-55.

(28) Ge, L., Zhu, Z., Li, F., Liu, S., Wang, L., Tang, X., Rudolph, V., Investigation of Gas Permeability in Carbon Nanotube (CNT)−Polymer Matrix Membranes via Modifying CNTs with Functional Groups/Metals and Controlling Modification Location. The Journal of Physical Chemistry C, 2011, 115, 6661-6670.

(29) Zhang, Y., Musselman, I. H., Ferraris, J. P., Balkus Jr, K. J., Gas Permeability Properties of Matrimid® Membranes Containing the Metal-Organic Framework Cu-BPY-HFS. Journal of Membrane Science, 2008, 313, 170-181.

(30) Ordonez, M. J. C., Balkus Jr, K. J., Ferraris, J. P., Musselman, I. H., Molecular Sieving Realized with ZIF-8/Matrimid Mixed-Matrix Membranes. Journal of Membrane Science, 2010, 361, 28-37.

(31) Ge, L., Zhou, W., Rudolph, V., Zhu, Z. H., Mixed Matrix Membranes Incorporated with Size-Reduced Cu-BTC for Improved Gas Separation. Journal of Materials Chemistry A, 2013, 1, 6350-6358.

Chapter 6 Ionic liquids as the MOFs/polymer interfacial binder for efficient membrane separation

Introduction

As mentioned in section 2.5.1, it is challenging for micron-sized MOFs to reach excellent compatibility and affinity with the polymer matrix. Compared to nano-sized MOF particles, micron-sized MOFs are more common and easier to be synthesized. However, studies on interfacial control of conventional micron-sized MOFs based MMMs are still limited. Micron-sized MOFs normally show poor adhesion with the polymer chains, so the application of micron-sized MOFs as MMM fillets requires stronger interfacial interaction. In this chapter, a novel and effective method to eliminate interfacial non-selective voids in micron-sized MOF MMMs and enhance CO_2 separation performance is presented by introducing ionic liquid (IL) as the MOF/polymer interfacial binder. Thin layer of ionic liquid is decorated on the external surface of CuBTC and this CuBTC-IL composite was embedded into 6FDA-durene polymer to fabricate MMMs for CO_2 separation. The filler/IL/polymer interfacial morphology of MMMs and the CO_2 separation performance over N_2 and CH_4 are studied.

Contributions

In this chapter, CuBTC covered by thin layer of IL has been prepared and used to fabricate high performance MMMs for CO_2 separation. The IL layer behaves like the wetting agent and binding material between filler and polymer to enhance the MOF/polymer adhesion and eliminate the MOFs/polymer interface voids due to the favourable MOF/IL and IL/polymer interaction. With the decoration of IL, the interfacial non-selective voids in MMM was significantly reduced compare to that of MMM with untreated CuBTC. MMMs containing synthesized CuBTC-IL showed higher CO_2 selectivity compare to pure polymer membrane and MMMs with untreated CuBTC. 10% CuBTC-IL/6FDA-durene MMM presented excellent CO_2 permeability (1101.6 Barrer) and good CO_2/CH_4 selectivity (29.3), surpassed the 2008 Robeson's upper bound for polymer membrane. The MOF modification by IL decoration shown in this chapter can provide an effective method to enhance the filler/polymer affinity, and can be applicable to the large sized fillers. This chapter is in preparation for submitting to ACS Applied Materials & Interfaces.

Ionic liquids as the MOFs/polymer interfacial binder for efficient membrane separation

Rijia Lin, Lei Ge,* Victor Rudolph, Zhonghua Zhu*

School of Chemical Engineering, The University of Queensland, Brisbane 4072 Australia

Abstract

Obtaining strong interfacial affinity between filler and polymer is important for the fabrication of mixed matrix membranes (MMMs) with improved permeability and selectivity simultaneously. However, it is still a challenge for micron-sized metal organic frameworks (MOFs) to achieve excellent compatibility and defect-free interface with the polymer matrix. Thin layer of ionic liquid (IL) was immobilized on micron-sized CuBTC in order to eliminate the interfacial non-selective voids in MMMs with micron-sized MOFs and minimize free ionic liquid (IL) in polymer matrix, and then the obtained CuBTC-IL composite was incorporated into 6FDA-durene to fabricate MMMs. As a MOF/polymer interfacial binder, IL can enhance the MOF/polymer affinity due to the favourable MOF/IL and IL/polymer interaction. Compared to MMM with solo CuBTC incorporation, the MMM with IL wrapped CuBTC succeed in restricting the formation of interfacial voids. The enhanced adhesion between MOF particles and polymer phase reduced non-selective void and leaded to the significant increment in CO_2 selectivity. The IL decoration method can be an effective approach to eliminate the interfacial voids in MMMs, extending the filler selection to wide-range of large size fillers.

6.1 Introduction

Gas separation utilizing polymer membrane has drawn attention for its high energy efficiency, low production cost, and low environmental impact. However, achieving high performance of pure polymer membrane is challenging because of the trade-off between permeability and selectivity. With combination of the processing versatility of polymers with the good gas separation capability of inorganic particles, mixed matrix membranes (MMMs) derived from incorporation of inorganic filler into polymer matrix have been regarded as an alternative approach to overcome the trade-off problem of polymer membranes.

Among the porous inorganic materials, metal-organic frameworks (MOFs) are novel inorganic-

organic hybrid materials, consisting of inorganic metal centre or cluster connected by organic linkers to create one-, two-, and three-dimensional porous structures.[1] MOFs have been proposed as promising candidates for developing novel MMMs with high gas separation performance due to their remarkable properties, such as high surface area and porosity, controllable pore size, tunable pore surface properties, and high adsorption affinity.[2, 3] Moreover, organic parts of MOFs can provide stronger contact with the polymer chains and favourable compatibility with the polymer matrix.

To enhance the membrane permeability and selectivity at the same time, the interfacial morphology between the filler and polymer is the most important challenge that need to be considered during the design and fabrication of MMMs. The poor affinity between MOFs and polymer leads to the formation of defects and non-selective interfacial voids, deteriorating membrane separation efficiency and integrity of membrane structure.

To minimize/eliminate interfacial voids and surpass the membrane performance trade-off limit, various approaches have been applied to enhance the MOF/polymer compatibility and interaction: (1) Altering the surface properties of MOFs by surface treatments.[4-7] Venna et al.[7] modified the surface of UiO-66-NH_2 with phenyl acetyl group to improve its interaction with Matrimid® polymer. The MMMs showed enhanced CO_2 permeability by 200% and increased CO_2/N_2 ideal selectivity by 25%. Interactions between MOF and polymer are expected to be improved through the π–π stacking of the aromatic rings and hydrogen bonding between the amide groups from the modified MOF and the imide groups from the polymer. (2) Applying smaller MOFs or reducing the size of the filler.[8] In most cases, nano and submicron-sized MOFs show stronger interaction with the polymeric matrix as well as good dispersion because smaller particles can provide more polymer/particle interfacial area.[9-12] Bae *et al.*[12] decreased the size of ZIF-90 by a nonsolvent-induced crystallization method and fabricated a MMM with the as-synthesized submicron-sized ZIF-90 and 6FDA-DAM polyimide. An interfacial void-free MMM with high gas separation performance was achieved. In our previous work, Lei *et al.*[13] reduced the size of CuBTC by using a facial sonication post-treatment and improve the poorly attached interface between MOF/polymer. (3) Inducing MOF/polymer interaction into membrane fabrication. In our previous work,[14] we chose Cd-6F MOF with 6FDA linker, which is also one of the monomers of the polymer matrix 6FDA-ODA. Through in-situ polymerization, Cd-6F can react with ODA of the polymer chains. The incorporation of interfacial interaction between MOF and polymer eliminate the formation of interfacial voids, thus improving the membrane separation performance.

Although a number of studies have been conducted on improving interfacial morphology between the MOFs and polymer, most of them study nano and submicron-sized MOFs or specific

MOF/polymer pairs, the studies on interfacial control of conventional micron-sized MOFs based MMMs are still limited. Compared to nano-sized MOF particles, micrometer-sized MOFs are more common and easier to be synthesized. Micron-sized MOFs normally show poor compatibility with the polymer matrix, so the implement of micrometer-sized MOFs as fillets requires stronger interfacial adhesion.[13] Incorporating a third "binding" material with gas separation properties that seal the interfacial voids can be promising. Ionic liquids (IL) are salts in the liquid state which are formed by a combination of organic cations and organic or inorganic anions. IL has attractive physicochemical properties such as excellent thermal and electrochemical stability, extremely low volatility, high CO_2 solubility and selectivity.[15] In this study, CuBTC, a typical micron-sized MOF, was chose and decorated with ionic liquid, the derived CuBTC-IL particles was applied into 6FDA-durene polyimide to fabricate MMMs. IL 1-ethyl-3-methylimidazolium bis(trifluoromethylsulfonyl)imide (Emim[Tf_2N]) was chose for its abilities to be fast CO_2 absorbent. With the aid of ionic liquid, the interfacial voids of the membrane were significantly reduced due to the favourable MOF/IL and IL/polymer adhesion, thus improving both membrane permeability and CO_2 selectivity compared to pure polymer membrane and MMMs with untreated CuBTC.

6.2 Experimental Section

6.2.1 Materials synthesis

6.2.1.1 Materials

All chemicals including copper(II) nitrate trihydrate ($Cu(NO_3)_2{\cdot}3H_2O$), 1,3,5-benzene tricarboxylic acid (BTC), 1-ethyl-3-methylimidazolium bis(trifluoromethylsulfonyl)imide (Emim[Tf_2N]), 4,4'-(hexafluoroisopropylidene) diphthalic anhydride (6FDA), 2,3,5,6-tetramethyl-1,3-phenyldiamine (durene), triethylamine, acetic anhydride, N,N-dimethylformamide (DMF), N,N-dimethylacetamide (DMAc), chloroform, methanol and ethanol were supplied by Sigma–Aldrich.

6.2.1.2 Synthesis of CuBTC and CuBTC-IL

The CuBTC was synthesized similar to previous work.[16] 0.667 g BTC was dissolved in 20 ml of a 50%/50% mixture of ethanol–DMF. In another beaker, 1.384 g $Cu(NO_3)_2{\cdot}3H_2O$ were dissolved in 10 ml H_2O. Two solutions were then mixed and stirred for 10 min before transferring into a Teflon-lined stainless steel autoclave and heated at 100 °C for 10 h. The resulting CuBTC crystals were separated by centrifugation and washed in DMF for twice, and washed in ethanol for three times. The product was finally dried at 100 °C under vacuum overnight.

1.0 g of CuBTC crystals were added into 10 mL of Emim[Tf_2N] and stirred for 0.5 hr, after that the crystals were filtered. The resulting IL-impregnated CuBTC crystals were washed in chloroform for five times and centrifuged. The final product was dried at 80 ºC under vacuum until constant weight. The weight of the product was 1.16g and was designated as CuBTC-IL.

6.2.1.3 Synthesis of 6FDA-durene polyimide

As shown in Figure 6-1, the 6FDA-durene polyimide was synthesized with a two-step reaction base on the work reported elsewhere.[17, 18] In the first step, polyamic acid was form by polymeric reaction between equimolar amounts of durene (1.426 g) and 6FDA (3.861 g) in DMAc. The polyamic acid solutions were made up to 20% solids. The mixture was stirred under nitrogen at room temperature for 24 h. In the second step, a mixture of triethylamine (3.2 mL) and acetic anhydride (1.2 mL) was added to the polyamic acid solution. The combined mixture was stirred under nitrogen at room temperature for another 24 h. Polyamic acid was imidized to form polyimides. The final polymer was precipitated in methanol, washed several times with methanol, and dried at 180 °C under vacuum for 18 h. The polyimide product is referred as 6FDA-durene.

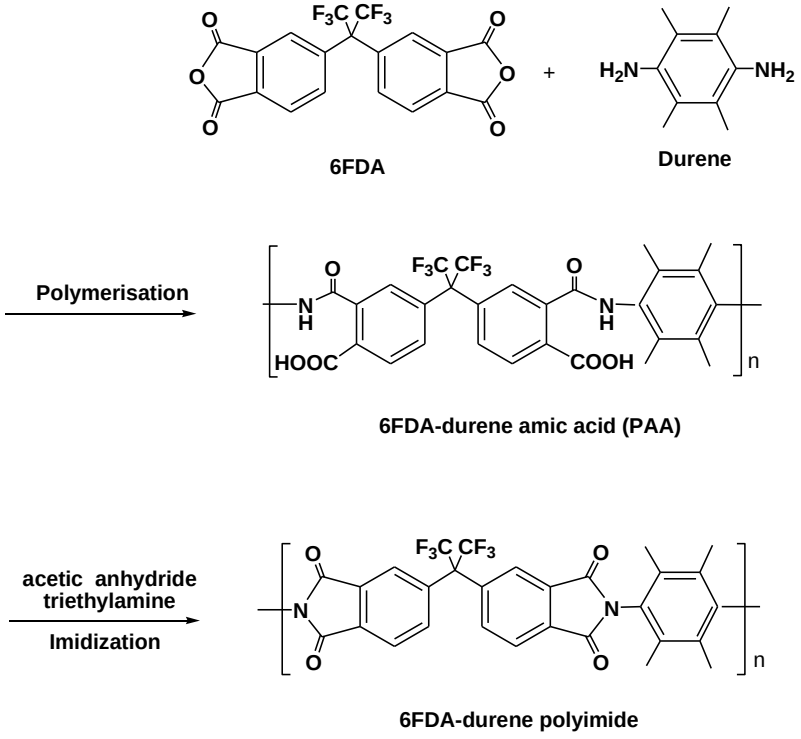

Figure 6-1 Multi-staged of 6FDA-durene polyimide synthesis

6.2.1.4 Membrane preparation

For pure 6FDA-durene membrane, 0.45 g 6FDA-durene was dissolved into 3 mL chloroform. The resulting solution was cast onto a clean glass plate and covered to slowly dry at room temperature for

24 h. After that, membrane was dried at 150 ºC for 24 hunder vacuum. For the MMMs, certain amount of as-synthesised CuBTC or CuBTC-IL was dispersed in chloroform under sonication. 0.45 g 6FDA-durene was dissolved into this suspension and the suspension was further stirred for 6 h. The resulting mixture was cast and dried at room temperature for 24 h, followed by dried at 150 ºC for another 24 h under vacuum. The selected thickness for casting procedure was 50 μm. The loadings of CuBTC in MMMs were adjusted to 5, 10, 15 wt% for the purposes of this study based on equation (6-1).

$$\phi = \frac{m_{CuBTC}}{m_{CuBTC} + m_{IL} + m_{6FDA\text{-}durene}} \quad (6\text{-}1)$$

where m_{Filler}, $m_{CuBTC\ in\ filler}$ and $m_{6FDA\text{-}durene}$ are the mass of filler, the mass of CuBTC in the CuBTC-IL composite and 6FDA-durene in the MMMs, respectively.

To compare the directly mixing IL into the polymer and filler precursor,[19] a reference MMM was prepared by mixing 0.065g CuBTC and 0.13g IL in 3 mL chloroform followed by adding 0.45 g 6FDA-durene, the resulting mixture was also cast and dried the same as the preparation of CuBTC-IL MMMs. Then the MMMs with 10 wt% CuBTC and 20 wt% IL was obtained. The thickness of pure 6FDA-durene and MMMs were measured using a micrometer within the range of 50-70 μm. Before gas permeation tests and characterisation, the membranes were stored with desiccant.

6.2.2 Characterization

The X-ray diffraction (XRD) data were obtained from a Brucker Advanced X-ray Diffractometer (40 kV, 30 mA) with Cu Kα (λ= 0.15406 nm) radiation at a scanning rate of $1^{o}\ min^{-1}$ from 5^{o} to 50^{o}.

The Fourier transform infrared spectroscopy (FTIR) spectra were obtained with a PerkinElmer Spectrum 100 spectrometer by using KBr pellets in transmission mode. All spectra were collected from 650 to 4000 cm^{-1} wavenumbers.

The N_2 adsorption isotherms were obtained from a Micromeritics TriStar II 3020 at 77 K, after degassing the sample at 150 ºC for 16 h. BET surface area was calculated over the range of relative pressures between 0.005 and 0.05.

The morphologies of the samples were obtained with a JEOL JSM7100 scanning electron microscope (SEM) at 8 kV.

Focused ion beam scanning electron microscopy (FIB-SEM) was performed in a FEI SCIOS FIB/SEM dual beam system to assess the contact of the inorganic phase and the continuous phase. The specimen was sputtered with a conducting layer of Pt for 100 s. A trench was milled on the surface of the membrane by using a Ga^{+} focused ion beam (Figure 6-2). Serial milling of slices with

a thickness of 80 nm were removed from the specimen up to a depth of 30 μm by the Ga^+ FIB at 30kV and 3nA. A series of exposed cross-section SEM images in back-scattered electron (BSE) imaging mode were collected sequentially during the automatic slice-and-view experiments using an in-lens backscattered electron detector at 2kV. In the BSE SEM image, the different constituents of the membrane can be recognized through the different grayscale. Fillers are brightest whereas polymer appear a medium grayscale, and voids are darker than the polymer matrix. The segmentation of the individual phases (e.g. 6FDA-durene, filler and void) was conducted by image thresholding.[9, 20] The stack of these SEM images was aligned, and the analysed volume can be reconstructed in three-dimensional. Avizo (FEI Visualization Sciences Group) was used to reconstruct the tomograms, segment different phases and quantify the corresponding 3D volume.

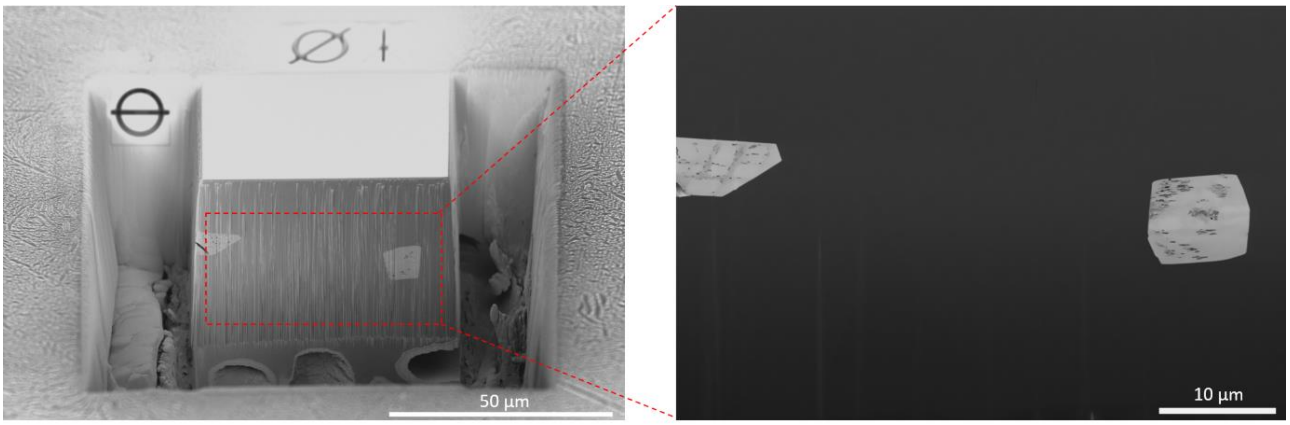

Figure 6-2 Typical FIB-SEM images of 10% CuBTC-IL/6FDA-durene MMM (a) FIB milling hole (b) cross-sectional image in the BSE mode

6.2.3 Permeation test

A variable feed pressure and the constant volume permeation system was used to measure the gas permeation of membranes, as described elsewhere.[21] The membranes were held under vacuum for approximately 5 min to achieve a steady state before being exposed to the selected gas. Before switching to the feed gas, the membrane has to be degassed for some time to ensure the complete desorbtion of initial permeate gas. The test was held at 25 °C, 2 atm feed pressure. The permeation coefficient is calculated using the following equation:

$$P = \frac{273.15\times10^{10}}{760\mathrm{AT}} \frac{VL}{\frac{P_0\times76}{14.7}} \frac{\mathrm{d}p}{\mathrm{d}t} \quad (6\text{-}2)$$

where P is the permeation coefficient in barrer (1 barrer =1×10^{-10} cm^3 (STP) cm cm^{-2} s^{-1} cm Hg^{-1}), A is the effective area of the membrane (cm^2), T is the absolute temperature (K), V is the dead-volume of the downstream chamber (cm^3), L is the membrane thickness (cm), P_0 is the feed pressure (psi), and dp/dt is the steady rate of pressure increase in the downstream side (mm Hg s^{-1}).

The ideal selectivity for two gases is determined as:

$$\alpha = \frac{P_A}{P_B} \quad (6\text{-}3)$$

where P_A and P_B are the permeation coefficients of pure gas A and B, respectively.

6.3 Results and Discussions

The X-ray diffraction (XRD) patterns of pure CuBTC and CuBTC-IL samples are shown in Figure 6-3. The diffraction pattern of IL treated CuBTC matches well with that of the pristine CuBTC, indicating the IL impregnation does not change the crystallinity of CuBTC. Figure 6-4 presents the scanning electron microscopy (SEM) images of pure CuBTC and IL-treated CuBTC samples. The crystal morphology of CuBTC displays an octahedral shape with sharp edges, with the particle size of around 10-30 μm (Figure 6-4a, 6-4b). After the IL impregnation, the edge of crystals disappeared and the gaps between crystals were filled, indicating an IL layer coated on the external surface of the CuBTC (Figure 6-4c, 6-4d). After washed by chloroform, it can be found that there still a thin IL layer remained on the surface of the CuBTC (Figure 6-4e, 6-4f), which can be attributed to the interaction between IL and CuBTC. The BET surface area of pure CuBTC and CuBTC-IL calculated from the N_2 adsorption/desorption isotherms (Figure 6-5) are 1416 and 35.7 m^2g^{-1}, respectively. The significant decrease in surface area of CuBTC-IL is attributed to the blockage of pores with IL and the well-covered IL layer on the CuBTC crystals.

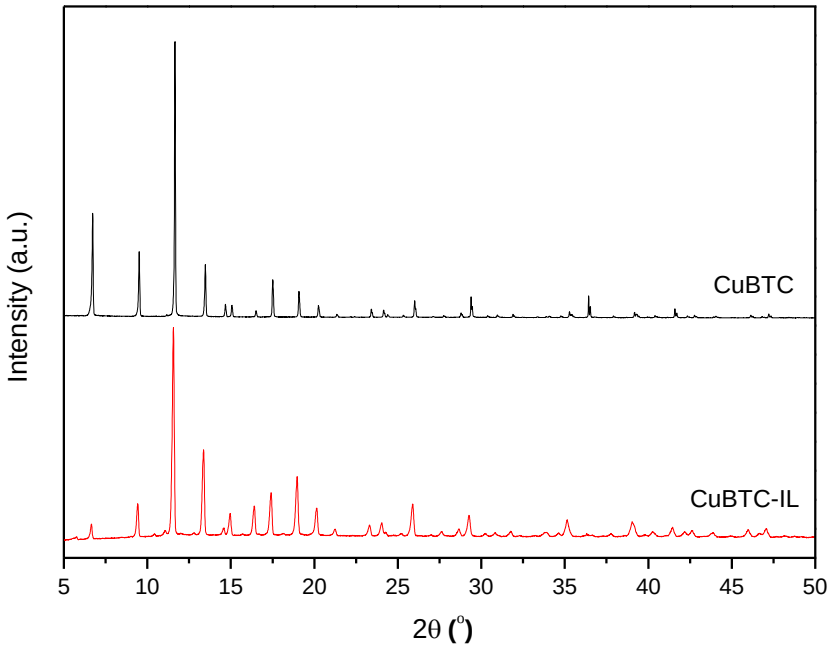

Figure 6-3 XRD pattern of CuBTC and CuBTC-IL

The FTIR spectra of as-synthesized CuBTC, CuBTC-IL crystals and pure IL are shown in Figure 6-6. The characteristic infrared bands below 1300 cm^{-1} correspond to the vibrations of the BTC linker. The peaks from 1300 to 1700 cm^{-1} belong to the carboxylate linker which indicate the coordination of BTC to the copper sites. The peak 1646 cm^{-1} is assigned to the asymmetric stretching vibrations of the carboxylate in BTC and the peaks at 1448 cm^{-1} and 1371 cm^{-1} are related to the symmetric stretching vibrations of the carboxylate groups.[22] In the spectrum of CuBTC-IL, after the functionalization of IL, new bands appeared at 792 cm^{-1} (S-N), 836 cm^{-1} (ring C-H), 1054 cm^{-1} (S-N-S), 1134 cm^{-1} (S=O) and 1189 cm^{-1} (C-F), indicating the existence of IL in CuBTC-IL particles.[23, 24] It is noteworthy that bands at 836 cm^{-1} (ring C-H) and 1189 cm^{-1} (C-F) in CuBTC-IL spectrum shifted compared to the characteristic bands of pure IL. These can be attributed to the specific interaction between CuBTC and IL.[25, 26]

The gas permeance and selectivity of MMMs are strongly dependent on the morphology of the membranes. Figure 6-7 displays the cross-sectional SEM images of CuBTC MMM and CuBTC-IL MMM. In Figure 6-7a and 6-7b, some voids and poor adhesion between CuBTC and polymer are observed in CuBTC MMM. This “sieve in a cage” morphology of CuBTC MMMs is consistent with other reported MMMs containing MOF fillers with large particle size, leading to the reduction of separation performance.[13, 27] As to the CuBTC-IL MMM (Figure 6-7c, 6-7d), the CuBTC-IL crystals show excellent adhesion with the polymer, no interfacial gaps was observed. Here the introduction of IL is the key factor in the elimination of interfacial voids.

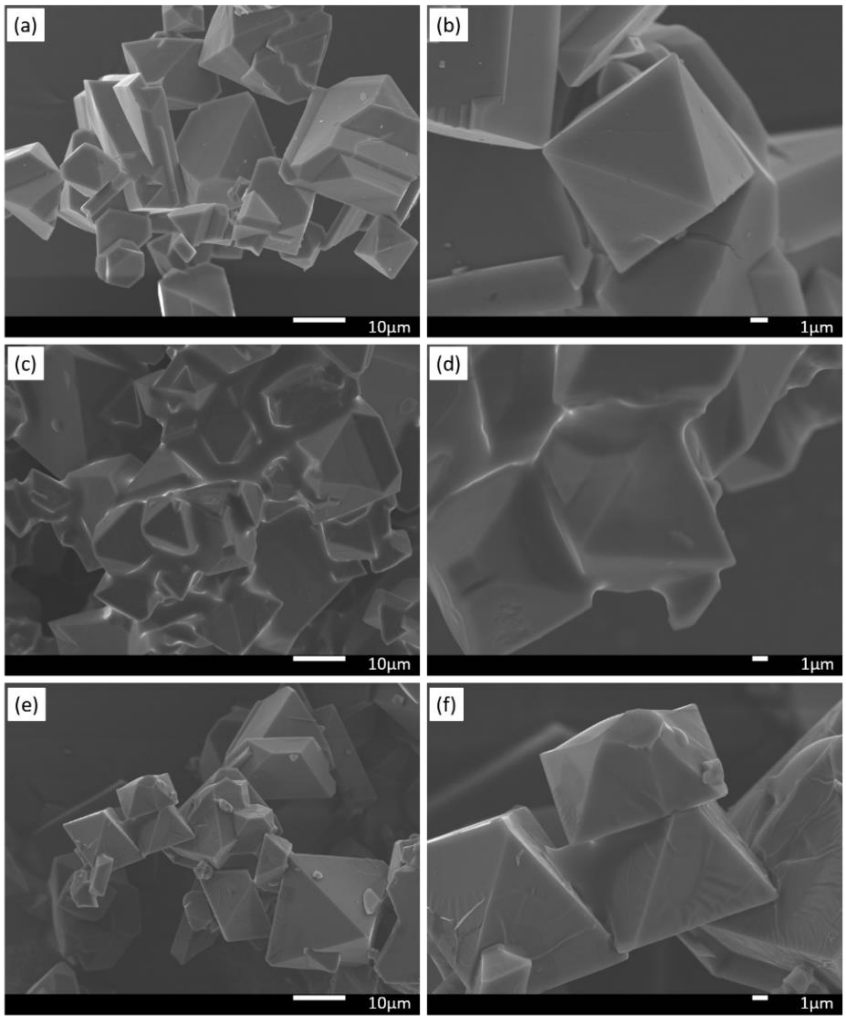

Figure 6-4 SEM images of (a, b) CuBTC, (c, d) unwashed CuBTC-IL and (e, f) washed CuBTC-IL

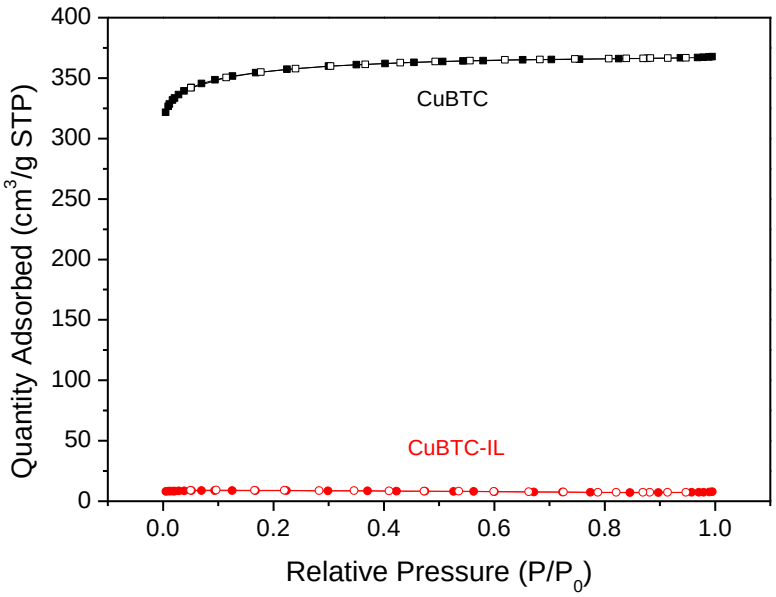

Figure 6-5 N_2 adsorption/desorption isotherms of CuBTC and CuBTC-IL at 77 K

(solid symbols = adsorption; empty symbols = desorption)

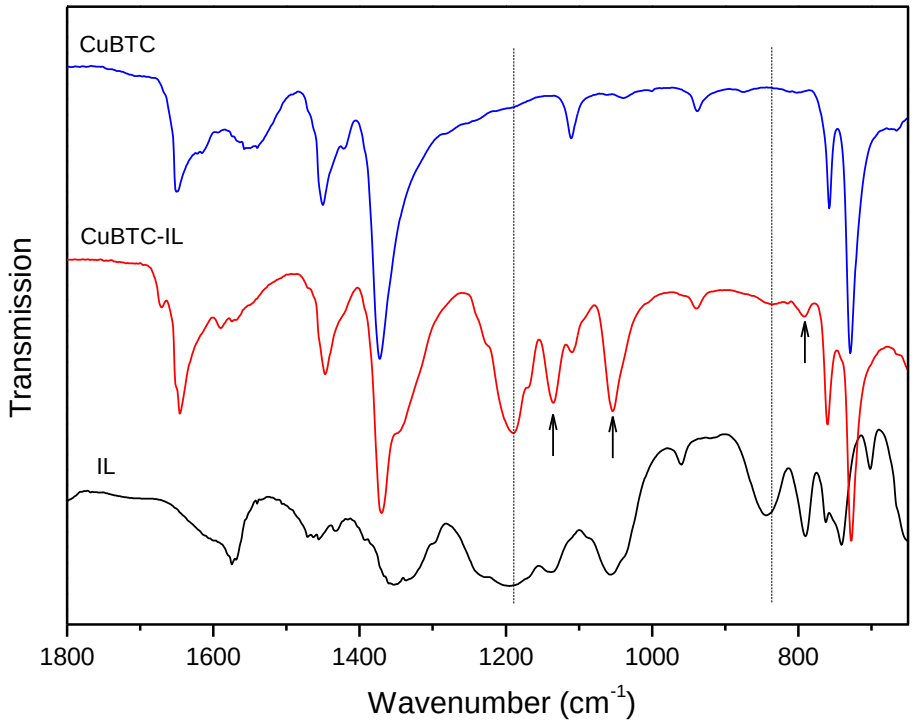

Figure 6-6 FTIR spectra of CuBTC (a) and CuBTC-IL (b)

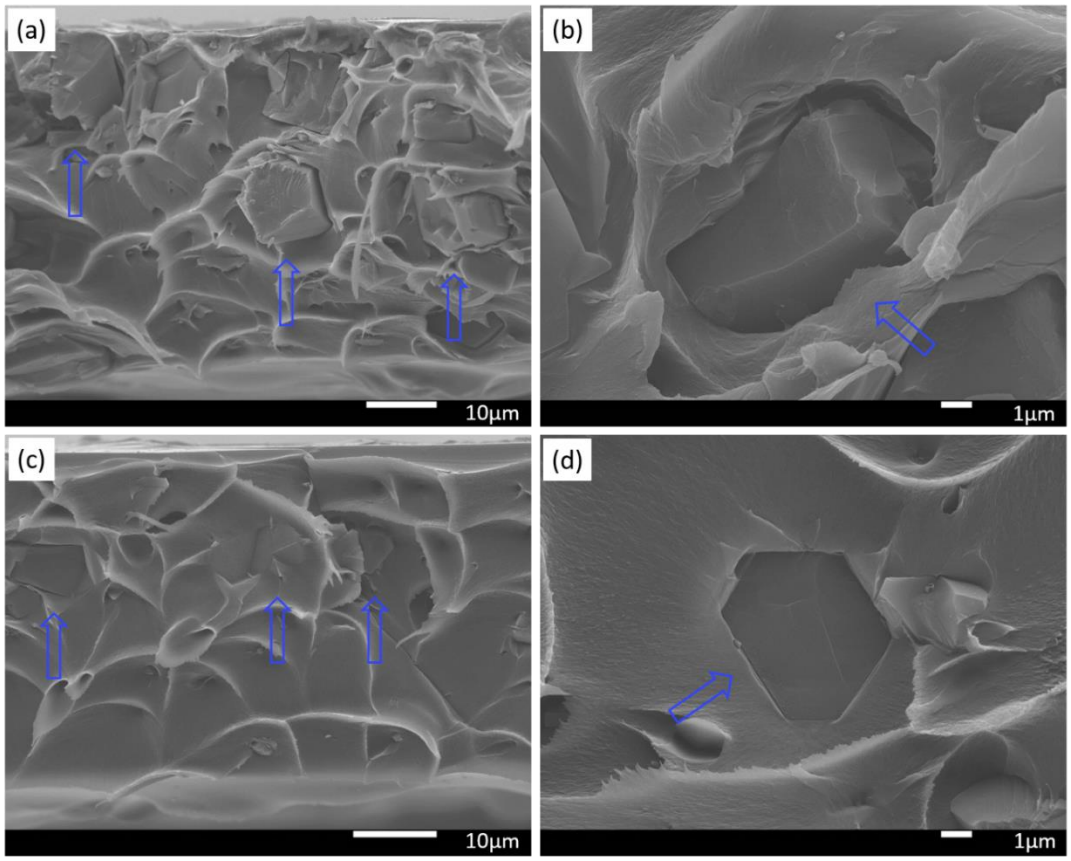

Figure 6-7 Cross-section SEM images of (a, b) 10 wt% CuBTC/6FDA-durene MMM and (c, d) 10% CuBTC-IL/6FDA-durene MMM (Arrows point to the MOF crystals embedded in polymer matrix)

The ideal gas separation performance of the as-synthesized membranes was measured. Figure 6-8a shows the single gas permeability and CO_2/N_2, CO_2/CH_4 selectivity of the pure 6FDA-durene membrane, CuBTC/6FDA-durene MMM and CuBTC-IL/6FDA-durene MMMs. As to the pure 6FDA-durene, the gas permeabilities of CO_2, N_2 and CH_4 are 774.3, 36.1 and 35.2 Barrer, respectively. The CO_2/N_2 and CO_2/CH_4 selectivity are 21.5 and 22.0, respectively. These results are consistent with the published values of 6FDA-durene membrane.[28] All the derived CuBTC-IL MMMs present higher CO_2 permeability compared to the neat 6FDA-durene membrane. The CO_2 permeability of 5, 10, 15% CuBTC-IL/6FDA-durene MMMs are 1236.6, 1101.6, and 827.5 Barrer, respectively. It has been shown that inorganic fillers can disrupt the polymer chain packing thus creating more free volume, which provides more channel for gas diffusion and results in the increase of the permeability of the membrane.[29, 30] Therefore, the CO_2 permeability enhancement of the MMMs in this study can be attributed to the additional free volume introduced by incorporation of the CuBTC-IL particles. On the other hand, a decrease of CO_2 permeability of the CuBTC-IL/6FDA-durene MMMs with increasing filler loading ratio was observed. This behaviour can be attributed to the introduction of IL to the polymer matrix that occupies the free volume in the polymer and reduce CO_2 diffusivity. With the increasing CuBTC-IL loading, the amount of free IL in the MMMs increases, thus diminishing the CO_2 permeability of the membranes. Similar observation can also be found in previous literature.[15, 31] The CO_2 permeability of MMM prepared by directly mixing 10 wt% CuBTC and 20 wt% IL into 6FDA-durene was also tested for comparison. As shown in Table 6-1, with incorporation of 20 wt% of IL, the CO_2 permeability of CuBTC MMM significantly reduced to only 145.0 Barrer, indicating the free volume occupied by free IL. It is worth noting that most of the reported studies simply mixed IL with inorganic filler into the polymer matrix to fabricate three-component MMMs. The weight percentage of IL in MMMs can be more than 20 wt%.[19, 32] The extra IL usage will lead to the blockage of free volume and the decrease of CO_2 diffusion. Moreover, without considering IL-filler interaction, the coverage of IL on filler may not be sufficient to eliminate interfacial voids. In such case, simply mixing IL and filler cannot be an efficient process for improving the filler/polymer interface and membrane performance. Therefore, homogenously modifying MOFs surface with small amount of IL can be more promising in this study, as the rigidity of polymer chains influenced by extra IL can be minimized with preserving sufficient surface modification on MOFs.

With regards to the CO_2 selectivity, the CuBTC-IL/6FDA-durene MMMs are also superior to the pure 6FDA-durene membrane which is shown in Figure 6-8b. 5, 10 and 15% CuBTC-IL/6FDA-durene MMMs all provide both higher CO_2/N_2 and CO_2/CH_4 selectivity compared to pure 6FDA-durene membrane with increased CO_2 permeability fluxes. The 10% CuBTC-IL MMM obtained both highest selectivity for CO_2/N_2 (27.1) and CO_2/CH_4 (29.3) with a high CO_2 permeability of 1101.6 Barrer.

However, without the present of IL, the 10 wt% CuBTC/6FDA-durene MMM displays a higher CO_2 permeability but lower CO_2/N_2 and CO_2/CH_4 selectivity, as shown in Figure 6-8b. As discussed before, obtaining favourable MOF/polymer interface is very challenging when incorporating micro-sized filler in polymer if not improving the MOF/polymer interaction. Therefore, the sacrifice of separation efficiency should be attributed to the existence of interfacial voids by the poor interaction between micron-sized CuBTC and polymer. In addition, the presence of IL on MOFs can enhance the carbon dioxide solubility of the membrane but without affecting that of N_2 and CH_4, thereby leading to higher value of selectivity in favour of CO_2.[33]

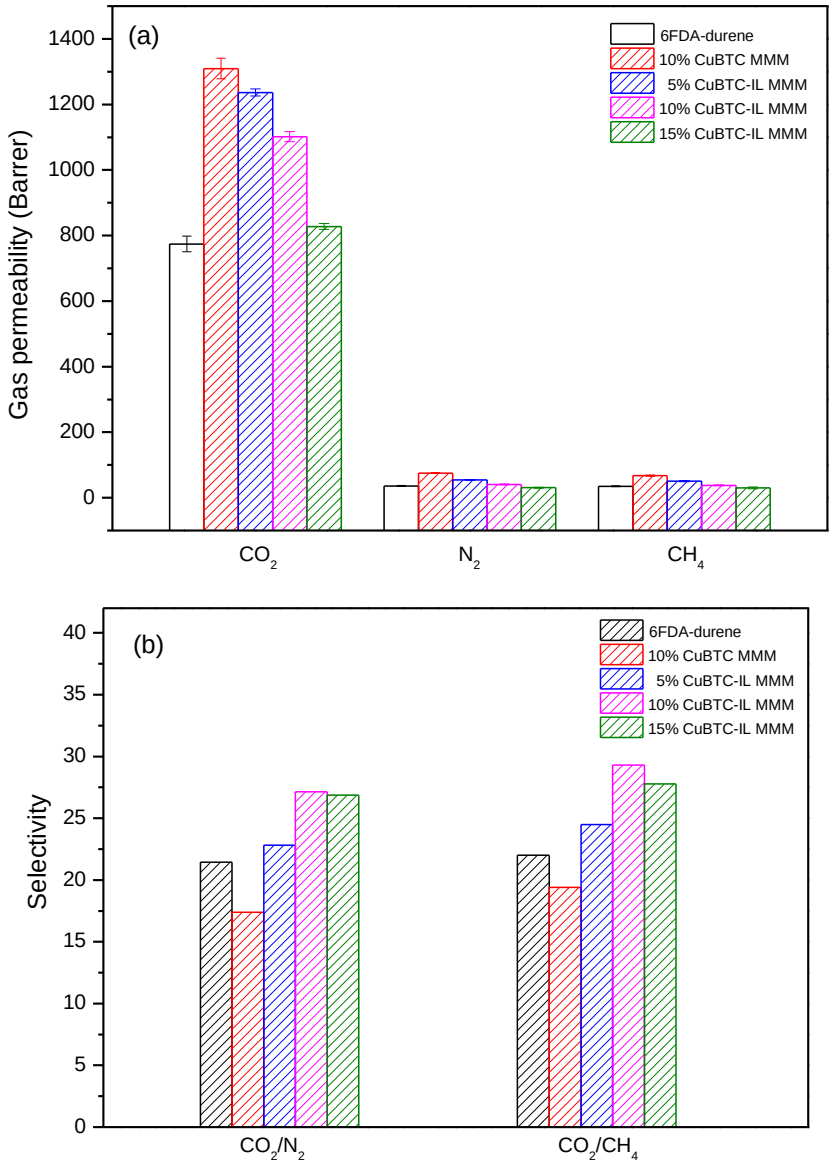

Figure 6-8 Gas permeability (a) and selectivity (b) of the pure 6FDA-durene membrane, CuBTC MMM and CuBTC-IL based MMMs

Table 6-1 Gas permeability and selectivity of MMM with mixing 10 wt% CuBTC and 20 wt% IL (25 ^{o}C, 2 atm feed gas pressure)

Permeability (Barrer)			Selectivity	
CO_2	N_2	CH_4	CO_2/N_2	CO_2/CH_4
145.0±4.7	8.1±0.87	7.4±0.89	17.9	19.6

In this work, the introduction of IL plays a critical role to heal the non-selective interfacial defects and improve CO_2 selectivity of the MMMs. By decorating IL on the surface of CuBTC, the ILs act as the wetting agent and binding material to eliminate the MOFs/polymer interface voids. The high compatibility and strong interaction between IL and polymer has been reported in the polymer/IL composite materials.[31] The imidazolium rings of the IL are expected to interact favourably through cation– π or π–π stacking with the aromatic rings of the polymer chains.[7, 25, 26] On the other hand, the interaction between CuBTC and IL (Figure 6-6) will provide satisfied affinity for IL to cover CuBTC surface as evidenced in Figure 6-4 and Figure 6-5. Therefore, with the aid of IL, the interfacial voids formed in CuBTC MMMs were significantly reduced due to the favourable MOF/IL and IL/polymer adhesion. Tomography focused ion beam scanning electron microscopy (FIB-SEM) was applied to access the filler/polymer interfacial contact in the CuBTC-IL MMM. The 10 wt% CuBTC-IL MMM sample with the best CO_2 separation performance was chosen. Figure 6-9 depicts the 3D surface-rendered view of the fillers and void volume in this CuBTC-IL MMM sample. Fillers with octahedral shape were identified, matched well with the CuBTC in the SEM images (Figure 6-4). The volume fractions of filler, polymer and void determined by image analysis are 8.35%, 91.65% and 0.0015%, respectively. The extremely small volume faction of voids confirms the contribution of IL in eliminating interfacial voids and enhancing adhesion between filler and polymer matrix.

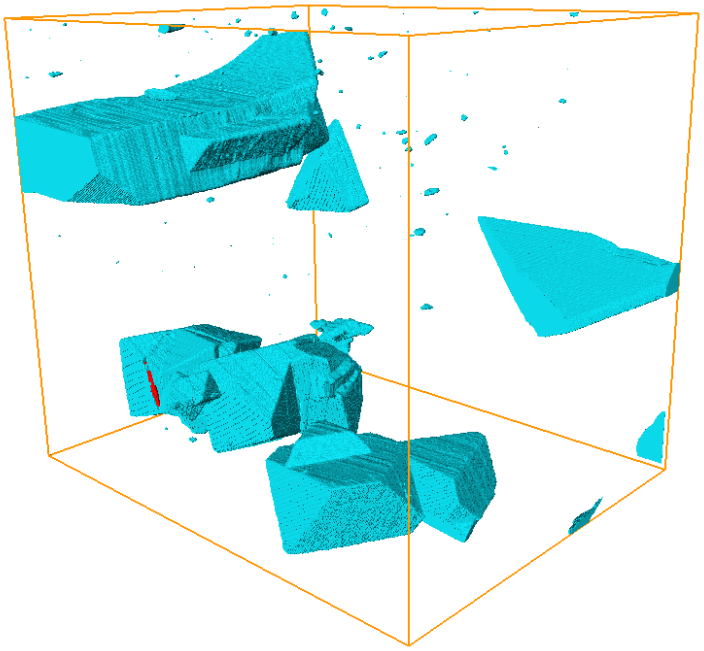

Figure 6-9 The corresponding surface-rendered view of the segmented FIB-SEM tomograms for CuBTC-IL MMM, filler appear in blue and voids in red.

The performance of our membranes for the CO_2/CH_4 gas pair is compared with other MMMs in the literature with respect to the Robeson's 2008 trade-off line[34] in Figure 6-10. All the CuBTC-IL/6FDA-durene MMMs present higher permeability and selectivity than that of pure 6FDA-durene membrane. Specifically, 10% CuBTC-IL/6FDA-durene MMM exhibit excellent CO_2 permeability (1101.6 Barrer) and good CO_2/CH_4 selectivity (29.3), clearly transcends the 2008 upper bound for polymer membrane. The as-synthesized CuBTC-IL/6FDA-durene MMMs show higher permeability and better selectivity than most of the reported MMMs containing MOFs, indicating potential for CO_2 separation such as biogas or field natural gas. Even though CuBTC may not be the best candidates for MOFs MMMs, the IL decoration method demonstrates the effectiveness in enhancing CO_2 permeability and selectivity and can be applied in wide-range of large sized fillers with better gas separation properties.

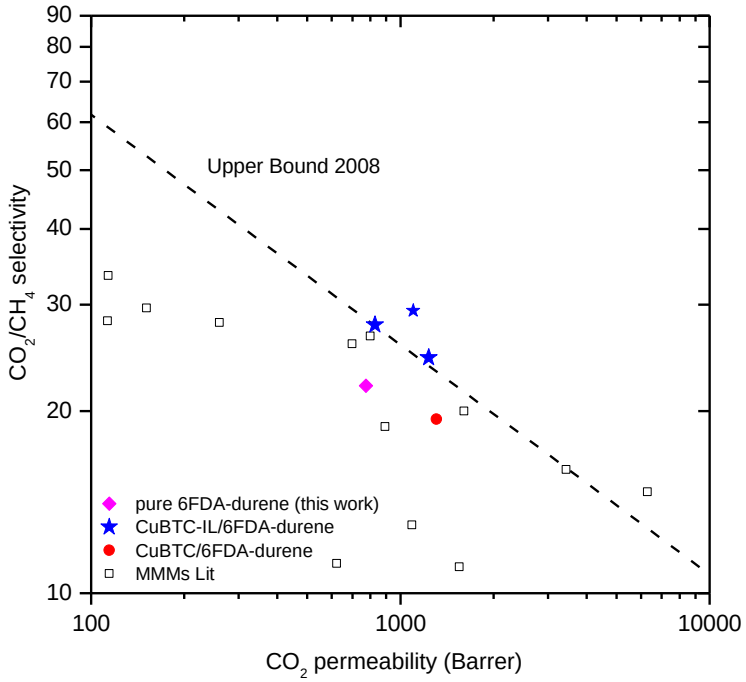

Figure 6-10 Gas separation performance of the CuBTC-IL MMMs for the CO_2/CH_4 gas pair with respect to 2008 Robeson trade-off line, compared with the compiled data on other MOFs based MMMs in literatures (Detailed citations of MMMs are presented in Appendix)

6.4 Conclusions

To eliminate the non-selective interfacial voids in MMMs containing micron sized fillers, in this study, thin layer of IL has been fabricated on one typical MOFs filler (CuBTC) for membrane fabrication. For minimizing the impact of free IL on membrane permeability, the amount of IL was specially controlled through the impregnation and washing process. This thin layer of IL acts as the MOFs/polymer interfacial binder to enhance the adhesion between micron-sized CuBTC and polymer by taking advantage of the favourable MOF/IL and IL/polymer interaction. With the incorporation of IL, the interfacial voids in CuBTC MMM were eliminated compared to the MMM with untreated CuBTC, leading to the significant improvement in CO_2 selectivity. The performance of 10% CuBTC-IL/6FDA-durene MMM clearly transcends the 2008 upper bound for polymer membrane. The strategy we shown here provides an efficient way to enhance the filler/polymer compatibility and further improve the gas separation efficiency, which can also be benefit to the application of large sized fillers with promising gas separation properties.

Reference

(1) Erucar, I., Yilmaz, G., Keskin, S., Recent Advances in Metal-Organic Framework-based Mixed Matrix Membranes. Chemistry an Asian Journal, 2013, 8, 1692-1704.

(2) Ferey, G., Hybrid Porous Solids: Past, Present, Future. Chemical Society Reviews, 2008, 37, 191-214.

(3) Li, J.-R., Sculley, J., Zhou, H.-C., Metal–Organic Frameworks for Separations. Chemical Reviews, 2012, 112, 869-932.

(4) Xin, Q., Ouyang, J., Liu, T., Li, Z., Li, Z., Liu, Y., Wang, S., Wu, H., Jiang, Z., Cao, X., Enhanced Interfacial Interaction and CO_2 Separation Performance of Mixed Matrix Membrane by Incorporating Polyethylenimine-Decorated Metal-Organic Frameworks. ACS Applied Materials & Interfaces, 2015, 7, 1065-1077.

(5) Denny, M. S., Jr., Cohen, S. M., In Situ Modification of Metal-Organic Frameworks in Mixed-Matrix Membranes. Angewandte Chemie International Edition, 2015, 54, 9029-9032.

(6) Anjum, M. W., Vermoortele, F., Khan, A. L., Bueken, B., De Vos, D. E., Vankelecom, I. F., Modulated UiO-66-Based Mixed-Matrix Membranes for CO_2 Separation. ACS Applied Materials & Interfaces, 2015, 7, 25193-25201.

(7) Venna, S. R., Lartey, M., Li, T., Spore, A., Kumar, S., Nulwala, H. B., Luebke, D. R., Rosi, N. L., Albenze, E., Fabrication of MMMs with Improved Gas Separation Properties Using Externally-Functionalized MOF Particles. Journal of Materials Chemistry A, 2015, 3, 5014-5022.

(8) Ge, L., Yang, Y., Wang, L., Zhou, W., De Marco, R., Chen, Z., Zou, J., Zhu, Z., High Activity Electrocatalysts from Metal–Organic Framework-Carbon Nanotube Templates for the Oxygen Reduction Reaction. Carbon, 2015, 82, 417-424.

(9) Rodenas, T., van Dalen, M., García-Pérez, E., Serra-Crespo, P., Zornoza, B., Kapteijn, F., Gascon, J., Visualizing MOF Mixed Matrix Membranes at the Nanoscale: Towards Structure-Performance Relationships in CO_2/CH_4 Separation Over NH_2-MIL-53(Al)@PI. Advanced Functional Materials, 2014, 24, 249-256.

(10) Song, Q. L., Nataraj, S. K., Roussenova, M. V., Tan, J. C., Hughes, D. J., Li, W., Bourgoin, P., Alam, M. A., Cheetham, A. K., Al-Muhtaseb, S. A., Sivaniah, E., Zeolitic Imidazolate Framework (ZIF-8) based Polymer Nanocomposite Membranes for Gas Separation. Energy & Environmental Science, 2012, 5, 8359-8369.

(11) Zhang, C., Dai, Y., Johnson, J. R., Karvan, O., Koros, W. J., High Performance ZIF-8/6FDA-DAM Mixed Matrix Membrane for Propylene/Propane Separations. Journal of Membrane Science, 2012, 389, 34-42.

(12) Bae, T.-H., Lee, J. S., Qiu, W., Koros, W. J., Jones, C. W., Nair, S., A High-Performance Gas-Separation Membrane Containing Submicrometer-Sized Metal–Organic Framework Crystals. Angewandte Chemie International Edition, 2010, 49, 9863-9866.

(13) Ge, L., Zhou, W., Rudolph, V., Zhu, Z. H., Mixed Matrix Membranes Incorporated with Size-Reduced Cu-BTC for Improved Gas Separation. Journal of Materials Chemistry A, 2013, 1, 6350-6358.

(14) Lin, R., Ge, L., Hou, L., Strounina, E., Rudolph, V., Zhu, Z., Mixed Matrix Membranes with Strengthened MOFs/Polymer Interfacial Interaction and Improved Membrane Performance. ACS Applied Materials & Interfaces, 2014, 6, 5609-5618.

(15) Dai, Z., Noble, R. D., Gin, D. L., Zhang, X., Deng, L., Combination of Ionic Liquids with Membrane Technology: A New Approach for CO_2 Separation. Journal of Membrane Science, 2016, 497, 1-20.

(16) Yang, Y., Shukla, P., Wang, S., Rudolph, V., Chen, X.-M., Zhu, Z., Significant Improvement of Surface Area and CO_2 Adsorption of Cu–BTC via Solvent Exchange Activation. RSC Advances, 2013, 3, 17065.

(17) Liu, Y., Wang, R., Chung, T.-S., Chemical Cross-Linking Modification of Polyimide Membranes for Gas Separation. Journal of Membrane Science, 2001, 189, 231-239.

(18) Wijenayake, S. N., Panapitiya, N. P., Versteeg, S. H., Nguyen, C. N., Goel, S., Balkus, K. J., Musselman, I. H., Ferraris, J. P., Surface Cross-Linking of ZIF-8/Polyimide Mixed Matrix Membranes (MMMs) for Gas Separation. Industrial & Engineering Chemistry Research, 2013, 52, 6991-7001.

(19) Mohshim, D. F., Mukhtar, H., Man, Z., The effect of Incorporating Ionic Liquid into Polyethersulfone-SAPO34 based Mixed Matrix Membrane on CO_2 Gas Separation Performance. Separation and Purification Technology, 2014, 135, 252-258.

(20) Rodenas, T., Luz, I., Prieto, G., Seoane, B., Miro, H., Corma, A., Kapteijn, F., Llabrés i Xamena, F. X., Gascon, J., Metal–Organic Framework Nanosheets in Polymer Composite Materials for Gas Separation. Nature Materials, 2015, 14, 48-55.

(21) Ge, L., Zhu, Z., Li, F., Liu, S., Wang, L., Tang, X., Rudolph, V., Investigation of Gas Permeability in Carbon Nanotube (CNT)−Polymer Matrix Membranes via Modifying CNTs with Functional Groups/Metals and Controlling Modification Location. The Journal of Physical Chemistry C, 2011, 115, 6661-6670.

(22) Seo, Y.-K., Hundal, G., Jang, I. T., Hwang, Y. K., Jun, C.-H., Chang, J.-S., Microwave Synthesis of Hybrid Inorganic–Organic Materials Including Porous $Cu_3(BTC)_2$ from Cu(II)-Trimesate Mixture. Microporous and Mesoporous Materials, 2009, 119, 331-337.

(23) Höfft, O., Bahr, S., Kempter, V., Investigations with Infrared Spectroscopy on Films of the Ionic Liquid [EMIM]Tf_2N. Langmuir, 2008, 24, 11562-11566.

(24) Talaty, E. R., Raja, S., Storhaug, V. J., Dölle, A., Carper, W. R., Raman and Infrared Spectra and ab Initio Calculations of C_{2-4}MIM Imidazolium Hexafluorophosphate Ionic Liquids. The Journal of Physical Chemistry B, 2004, 108, 13177-13184.

(25) Bak, B. M., Kim, S.-K., Park, H. S., Binder-Free, Self-Standing Films of Iron Oxide Nanoparticles Deposited on Ionic Liquid Functionalized Carbon Nanotubes for Lithium-Ion Battery Anodes. Materials Chemistry And Physics, 2014, 144, 396-401.

(26) Huang, Y., Xiao, Y., Huang, H., Liu, Z., Liu, D., Yang, Q., Zhong, C., Ionic Liquid Functionalized Multi-walled Carbon Nanotubes/Zeolitic Imidazolate Framework Hybrid Membranes for Efficient H_2/CO_2 Separation. Chemical Communications, 2015, 51, 17281-17284.

(27) Nik, O. G., Chen, X. Y., Kaliaguine, S., Functionalized Metal Organic Framework-Polyimide Mixed Matrix Membranes for CO_2/CH_4 Separation. Journal of Membrane Science, 2012, 413-414, 48-61.

(28) Lin, W.-H., Chung, T.-S., Gas Permeability, Diffusivity, Solubility, and Aging Characteristics of 6FDA-durene Polyimide Membranes. Journal of Membrane Science, 2001, 186, 183-193.

(29) Ahn, J., Chung, W.-J., Pinnau, I., Guiver, M. D., Polysulfone/silica Nanoparticle Mixed-Matrix Membranes for Gas Separation. Journal of Membrane Science, 2008, 314, 123-133.

(30) Aroon, M. A., Ismail, A. F., Matsuura, T., Montazer-Rahmati, M. M., Performance Studies of Mixed Matrix Membranes for Gas Separation: A review. Separation and Purification Technology, 2010, 75, 229-242.

(31) Kanehashi, S., Kishida, M., Kidesaki, T., Shindo, R., Sato, S., Miyakoshi, T., Nagai, K., CO_2 Separation Properties of a Glassy Aromatic Polyimide Composite Membranes Containing High-Content 1-Butyl-3-Methylimidazolium Bis(trifluoromethylsulfonyl)imide Ionic Liquid. Journal of Membrane Science, 2013, 430, 211-222.

(32) Shindo, R., Kishida, M., Sawa, H., Kidesaki, T., Sato, S., Kanehashi, S., Nagai, K., Characterization and Gas Permeation Properties of Polyimide/ZSM-5 Zeolite Composite Membranes Containing Ionic Liquid. Journal of Membrane Science, 2014, 454, 330-338.

(33) Vicent-Luna, J. M., Gutiérrez-Sevillano, J. J., Anta, J. A., Calero, S., Effect of Room-Temperature Ionic Liquids on CO_2 Separation by a Cu-BTC Metal–Organic Framework. The Journal of Physical Chemistry C, 2013, 117, 20762-20768.

(34) Robeson, L. M., The Upper Bound Revisited. Journal of Membrane Science, 2008, 320, 390-400.

Chapter 7 Conclusions and recommendations

7.1 Conclusions

This thesis outlines the development of novel MOF based mixed matrix membranes for gas separation with high permeability and selectivity. In particular, this thesis focuses on designing MMMs with eliminated filler/polymer interfacial defects for improving separation efficiency. Based on the studies in this thesis, the following conclusions could be drawn:

(1) The interaction between organic linkers in MOFs and polymer chains can be used to improve the adhesion between MOFs and polymer of target MMMs by selecting the proper MOFs/polymer couple. Through designing and controlling the interface interaction, the elimination of interfacial non-selective voids can be reached. The gas permeance and selectivity of MMMs are strongly dependent on the morphology of the membranes. A specific interaction between MOF Cd-6F and polymer 6FDA-ODA has been achieved by controlling the in-situ 6FDA-ODA polymerization procedure with the existence of Cd-6F. The enhanced adhesion between filler particles and polymer phase was observed. The MMM derived from in-situ polymerization displayed significant improvement in both gas permeance and CO_2 selectivity compared to pure polymer membrane.

(2) Introducing NH_2-MIL-101/CNT composite filler synthesized by confined growth of MOF on the external surface of CNTs can improve the NH_2-MIL-101 dispersion in the polymer phase and enhance the performance of MMM. The synthesized CNT-MIL fillers show good adhesion with the polymer matrix even at a high loading. MMMs containing the CNT-MIL composite displayed significant improvement in both CO_2 permeance and CO_2/CH_4 selectivity compared to pure polymer membrane. The combined performance of permeability and selectivity is above the Robeson upper bound.

(3) The method of confined growing MOFs on CNT can be extended to more applications of separating desired gas pair with proper MOFs selection. MMMs with ZIF-8/CNT composite filler display significant improvements in both C_3H_6 gas permeance and C_3H_6/C_3H_8 selectivity compared to pure polymer membranes. Tomographic FIB-SEM can be a powerful technique to quantitatively evaluate the spatial distribution of filler and the interfacial void space in the MMMs. The ZIF-8/CNT particles show good adhesion with the polymer in MMMs, with only 0.086% void volume fraction. The good ZIF-8 dispersion and filler/polymer interface lead to the effective C_3H_6 separation of the MMMs.

(4) The introduction of interfacial binding material which has favourable interaction with both filler and polymer can be an efficient way to eliminate the non-selective interfacial voids in MMMs and enhance CO_2 selectivity. The IL decoration on CuBTC enhances the MOF/polymer compatibility and

reduces the the interfacial voids in CuBTC MMM. The MMM with CuBTC-IL particles displayed much higher CO_2 selectivity than that of MMM with untreated CuBTC. The IL decoration method can be applied in developing MMMs with large size fillers which have outstanding gas separation properties.

In summary, MOFs based mixed matrix membranes show great potential to overcome the gas separation upper bound of pure polymer membranes. Selecting appropriate MOF/polymer pair to introduce the MOF/polymer interaction, confined growing MOF on other filler to improve the MOF dispersion, and applying binding material to enhanced the MOF/polymer adhesion are effective ways to fabricate void-free MMMs with high gas separation performance.

7.2 Recommendations for future work

For the future work, the following recommendations are made:

(1) The impact of water vapour in the gas separation process on filler/polymer interface can be further investigated. The water vapour can cause a reduction in the membrane gas separation performance due to competitive sorption and occupation of the membrane free volume.[1] Furthermore, the effect of water vapour in permeability of different gases, filler structure and the filler/polymer interaction need to be studied. Understanding the transport behaviour of water vapour in MMMs is necessary to fabricate MMMs with improved water resistance. As to the MOFs, the water resistance and thermal stability are the key issues that hinder their application in separating gases with water vapour, hence maintaining membrane structure integrity and material stability are required for the MOFs based MMMs development.

(2) Polymer can be modified through functionalization, crosslinking, grafting, etc, to control the interaction between polymer chains and MOFs. Compared to MOF modification, polymer modification is more various and more convenient. The contribution of functional groups in MOF/polymer interface and gas separation performance need to be studied. The packing and rigidity of the polymer chains o can also be designed and controlled, thus tailoring the diffusion rate of different gases molecular in MMMs and achieving the high gas selectivity.

(3) The mechanism of gas diffusion in MOF-based MMMs needs to be further investigated and the rate-limiting step of the gas separation process need to be distinguished. Understanding the gas permeation process can provide guidance methodology for materials selection and membrane modification to improve the membrane separation performance.

(4) The plasticization occurs when the polymer membrane used under high pressure of CO_2, the high concentration of CO_2 in the polymer increases free volume and mobility of the segments, resulting in the swelling of the polymer matrix and leading to a loss in gas selectivity.[2] The plasticization effect of MOFs based MMMs under higher pressure of CO_2 needs to be detailed investigated. The incorporation of MOF particles can restrict the mobility of the polymer chains therefore reducing the plasticization effect. The research on the effect of MOF structure type, MOF loading and MOF/polymer interaction on plasticization and derived membrane performance can give us some guidance to develop MOFs based MMMs for high pressure gas separation applications.

(5) Development of asymmetric membranes with MOFs by reducing effective membrane thickness with pore support can be the next step research. The studies in this thesis about designing and controlling MOF/polymer interaction and interface are critical to thin membrane technology, as the unselective diffusion through interfacial defects should be eliminated to ensure separation efficiency. At the same time, the permeability of membrane can be significantly enhanced by reducing bulk diffusion resistance.

(6) The application of MOFs based MMMs can be extended to other applications based on material selection and membrane structure design, such as desalination, pervaporation, organic vapour removal, etc.

References

(1) Chen, G. Q., Scholes, C. A., Doherty, C. M., Hill, A. J., Qiao, G. G., Kentish, S. E., Modeling of the Sorption and Transport Properties of Water Vapor in Polyimide Membranes. Journal of Membrane Science, 2012, 409-410, 96-104.

(2) Bos, A., Pünt, I. G. M., Wessling, M., Strathmann, H., CO_2-Induced Plasticization Phenomena in Glassy Polymers. Journal of Membrane Science, 1999, 155, 67-78.

Appendix

CO_2/CH_4 separation data for selected MOFs based MMMs reported in literature

MMMs	Loading (wt.%)	Pressure	Temperature (°C)	P_{CO2} (barrer)	P_{CO2}/P_{CH4}	Ref.
MOF-5/Matrimid	30	2 bar	35	20.2	44.7	[1]
Cu-BTC/PPO	40	2 bar	30	113.7	33.5	[2]
Cu-BTC/ODPA–TMPDA	40	2 bar	35	260	28	[3]
Cu-BTC/PDMS	30			2900	3.7	[4]
Fe-BTC/Matrimid	30	5 bar	35	13.5	30	[5]
MIL-53/Matrimid	37.5	2 bar	35	40.0	90.1	[6]
MIL-53/Matrimid	15	3 bar	35	12.43	51.8	[7]
NH_2-MIL-53/6FDA-ODA	32	10 bar	35	14.6	78	[8]
NH_2-MIL-53/ 6FDA-ODA-DAM(1/1)	10	150 psi	35	51.2	34.1	[9]
NH_2-MIL-53/ 6FDA-ODA-DAM(1/4)	15	150 psi	35	113	28.2	[9]
NH_2-MIL-101/6FDA-durene-SDA	10	3 bar	35	151	29.6	[10]
NH_2-MIL-101/ 6FDA-DSDA-durene-SDA	10	3 bar	35	70.9	41.6	[10]
ZIF-8/Pebax-2533	35	2 bar	25	1287	9.0	[11]
ZIF-8/Matrimid	50	2.7 bar	35	4.7	125	[12]
ZIF-8/6FDA-durene	20	10 bar	35	1090	12.96	[13]
ZIF-8/ 6FDA-durene-DABA(9/1)	20	10 bar	35	892	18.84	[13]
ZIF-8/ 6FDA-durene-DABA(7/3)	20	10 bar	35	698	25.84	[13]
ZIF-8/6FDA-durene	33.3	3.5 bar	35	1552	11.06	[14]
ZIF-90/6FDA-DAM	15	2 bar	25	800	26.6	[15]
UiO-66/6FDA-ODA	25	10 bar	35	50.4	46.1	[16]
NH_2−UiO-66−ABA /Matrimid 9725	30	9 bar	35	37.9	47.7	[17]
NH_2-MIL-53/6FDA-DAM-HAB(1/1)	10	150 psi	35	47.1	78.5	[18]
ZIF-8/PIM-1	43	1 bar	20	6300	14.7	[19]
ZIF-8/Matrimid	40	5 bar	35	45	43	[20]
ns-CuBDC/Matrimid	8.2	3 bar	25	4.09	78.7	[21]

Hollow ZIF-8/ PVC-g-POEM	30		35	623	11.2	[22]
NH_2-MIL-125(Ti)/PSF	30	3 bar	30	40	29.2	[23]
ZIF-71/6FDA-Durene	10	3.5 bar	35	1606	20	[24]
ZIF-71/6FDA-Durene	20	3.5 bar	35	3435	16	[24]
SWNT/PSF	10	4 bar	35	5.19	18.53	[25]
SWCNT/PDMS41	10	4 bar	35	191.30	5.21	[26]
MWCNTs/polyimide	1	15 bar	25	37.37	16.5	[27]
MWCNTs/PIM-1	3	2 bar	27	8250	9.34	[28]
MWCNTs/PVC	5	2 bar	25	11.48	52.18	[29]
MWCNTs/PVC-SBR	5	2 bar	25	16.31	62.73	[29]
MWCNTs/PBNPI	15	2 kg/cm^2	26	6.0	3.37	[30]
SBMA@CNT/Matrimid	10	2 bar	30	4.1	97	[31]
MWCNTs/PC-PEG	10	2 bar	25	20.32	35.64	[32]

References

(1) Perez, E. V., Balkus Jr, K. J., Ferraris, J. P., Musselman, I. H., Mixed-Matrix Membranes Containing MOF-5 for Gas Separations. Journal of Membrane Science, 2009, 328, 165-173.

(2) Ge, L., Zhou, W., Rudolph, V., Zhu, Z. H., Mixed Matrix Membranes Incorporated with Size-Reduced Cu-BTC for Improved Gas Separation. Journal of Materials Chemistry A, 2013, 1, 6350-6358.

(3) Duan, C., Jie, X., Liu, D., Cao, Y., Yuan, Q., Post-Treatment Effect on Gas Separation Property of Mixed Matrix Membranes Containing Metal Organic Frameworks. Journal of Membrane Science, 2014, 466, 92-102.

(4) Car, A., Stropnik, C., Peinemann, K.-V., Hybrid Membrane Materials with Different Metal-Organic Frameworks (MOFs) for Gas Separation. Desalination, 2006, 200, 424-426.

(5) Shahid, S., Nijmeijer, K., High Pressure Gas Separation Performance of Mixed-Matrix Polymer Membranes Containing Mesoporous Fe(BTC). Journal of Membrane Science, 2014, 459, 33-44.

(6) Hsieh, J. O., Balkus, K. J., Ferraris, J. P., Musselman, I. H., MIL-53 Frameworks in Mixed-Matrix Membranes. Microporous and Mesoporous Materials, 2014, 196, 165-174.

(7) Dorosti, F., Omidkhah, M., Abedini, R., Fabrication and characterization of Matrimid/MIL-53 mixed matrix membrane for CO_2/CH_4 separation. Chemical Engineering Research & Design, 2014, 92, 2439-2448.

(8) Chen, X. Y., Vinh-Thang, H., Rodrigue, D., Kaliaguine, S., Amine-Functionalized MIL-53 Metal-Organic Framework in Polyimide Mixed Matrix Membranes for CO_2/CH_4 Separation. Industrial &

Engineering Chemistry Research, 2012, 51, 6895-6906.

(9) Chen, X. Y., Hoang, V. T., Rodrigue, D., Kaliaguine, S., Optimization of Continuous Phase in Amino-Functionalized Metal-Organic Framework (MIL-53) based Co-Polyimide Mixed Matrix Membranes for CO_2/CH_4 Separation. RSC Advances, 2013, 3, 24266-24279.

(10) Seoane, B., Téllez, C., Coronas, J., Staudt, C., NH_2-MIL-53(Al) and NH_2-MIL-101(Al) in Sulfur-Containing Copolyimide Mixed Matrix Membranes for Gas Separation. Separation and Purification Technology, 2013, 111, 72-81.

(11) Nafisi, V., Hägg, M.-B., Development of dual layer of ZIF-8/PEBAX-2533 mixed matrix membrane for CO_2 capture. Journal of Membrane Science, 2014, 459, 244-255.

(12) Ordonez, M. J. C., Balkus Jr, K. J., Ferraris, J. P., Musselman, I. H., Molecular Sieving Realized with ZIF-8/Matrimid Mixed-Matrix Membranes. Journal of Membrane Science, 2010, 361, 28-37.

(13) Askari, M., Chung, T.-S., Natural Gas Purification and Olefin/Paraffin Separation Using Thermal Cross-Linkable Co-Polyimide/ZIF-8 Mixed Matrix Membranes. Journal of Membrane Science, 2013, 444, 173-183.

(14) Wijenayake, S. N., Panapitiya, N. P., Versteeg, S. H., Nguyen, C. N., Goel, S., Balkus, K. J., Musselman, I. H., Ferraris, J. P., Surface Cross-Linking of ZIF-8/Polyimide Mixed Matrix Membranes (MMMs) for Gas Separation. Industrial & Engineering Chemistry Research, 2013, 52, 6991-7001.

(15) Bae, T.-H., Lee, J. S., Qiu, W., Koros, W. J., Jones, C. W., Nair, S., A High-Performance Gas-Separation Membrane Containing Submicrometer-Sized Metal–Organic Framework Crystals. Angewandte Chemie International Edition, 2010, 49, 9863-9866.

(16) Nik, O. G., Chen, X. Y., Kaliaguine, S., Functionalized Metal Organic Framework-Polyimide Mixed Matrix Membranes for CO_2/CH_4 Separation. Journal of Membrane Science, 2012, 413-414, 48-61.

(17) Anjum, M. W., Vermoortele, F., Khan, A. L., Bueken, B., De Vos, D. E., Vankelecom, I. F., Modulated UiO-66-Based Mixed-Matrix Membranes for CO_2 Separation. ACS Applied Materials & Interfaces, 2015, 7, 25193-25201.

(18) Tien-Binh, N., Vinh-Thang, H., Chen, X. Y., Rodrigue, D., Kaliaguine, S., Polymer Functionalization to Enhance Interface Quality of Mixed Matrix Membranes for High CO_2/CH_4 Gas Separation. Journal of Materials Chemistry A, 2015, 3, 15202-15213.

(19) Bushell, A. F., Attfield, M. P., Mason, C. R., Budd, P. M., Yampolskii, Y., Starannikova, L., Rebrov, A., Bazzarelli, F., Bernardo, P., Carolus Jansen, J., Lanč, M., Friess, K., Shantarovich, V., Gustov, V., Isaeva, V., Gas Permeation Parameters of Mixed Matrix Membranes based on the Polymer of Intrinsic Microporosity PIM-1 and the Zeolitic Imidazolate Framework ZIF-8. Journal of

Membrane Science, 2013, 427, 48-62.
(20) Shahid, S., Nijmeijer, K., Nehache, S., Vankelecom, I., Deratani, A., Quemener, D., MOF-mixed matrix membranes: Precise dispersion of MOF particles with better compatibility via a particle fusion approach for enhanced gas separation properties. Journal of Membrane Science, 2015, 492, 21-31.
(21) Rodenas, T., Luz, I., Prieto, G., Seoane, B., Miro, H., Corma, A., Kapteijn, F., Llabrés i Xamena, F. X., Gascon, J., Metal–Organic Framework Nanosheets in Polymer Composite Materials for Gas Separation. Nature Materials, 2015, 14, 48-55.
(22) Hwang, S., Chi, W. S., Lee, S. J., Im, S. H., Kim, J. H., Kim, J., Hollow ZIF-8 Nanoparticles Improve the Permeability of Mixed Matrix Membranes for CO_2/CH_4 Gas Separation, in: Journal of Membrane Science, 2015, pp. 11-19.
(23) Guo, X., Huang, H., Ban, Y., Yang, Q., Xiao, Y., Li, Y., Yang, W., Zhong, C., Mixed Matrix Membranes Incorporated with Amine-Functionalized Titanium-based Metal-Organic Framework for CO_2/CH_4 separation. Journal of Membrane Science, 2015, 478, 130-139.
(24) Japip, S., Wang, H., Xiao, Y., Shung Chung, T., Highly Permeable Zeolitic Imidazolate Framework (ZIF)-71 Nano-Particles Enhanced Polyimide Membranes for Gas Separation. Journal of Membrane Science, 2014, 467, 162-174.
(25) Kim, S., Chen, L., Johnson, J. K., Marand, E., Polysulfone and Functionalized Carbon Nanotube Mixed Matrix Membranes for Gas Separation: Theory and Experiment. Journal of Membrane Science, 2007, 294, 147-158.
(26) Kim, S., Pechar, T. W., Marand, E., Poly(imide siloxane) and Carbon Nanotube Mixed Matrix Membranes for Gas Separation. Desalination, 2006, 192, 330-339.
(27) Aroon, M. A., Ismail, A. F., Montazer-Rahmati, M. M., Matsuura, T., Effect of Chitosan as a Functionalization Agent on the Performance and Separation Properties of Polyimide/Multi-Walled Carbon Nanotubes Mixed Matrix Flat Sheet Membranes. Journal of Membrane Science, 2010, 364, 309-317.
(28) Khan, M., Filiz, V., Bengtson, G., Shishatskiy, S., Rahman, M., Abetz, V., Functionalized Carbon Nanotubes Mixed Matrix Membranes of Polymers of Intrinsic Microporosity for Gas Separation. Nanoscale Research Letters, 2012, 7, 1-12.
(29) Rajabi, Z., Moghadassi, A. R., Hosseini, S. M., Mohammadi, M., Preparation and Characterization of Polyvinylchloride based Mixed Matrix Membrane Filled with Multi Walled Carbon Nano Tubes for Carbon Dioxide Separation. Journal Of Industrial And Engineering Chemistry, 2013, 19, 347-352.
(30) Weng, T.-H., Tseng, H.-H., Wey, M.-Y., Preparation and Characterization of Multi-Walled Carbon Nanotube/PBNPI Nanocomposite Membrane for H_2/CH_4 Separation. International Journal

Of Hydrogen Energy, 2009, 34, 8707-8715.
(31) Liu, Y., Peng, D., He, G., Wang, S., Li, Y., Wu, H., Jiang, Z., Enhanced CO2 Permeability of Membranes by Incorporating Polyzwitterion@CNT Composite Particles into Polyimide Matrix. ACS Applied Materials & Interfaces, 2014, 6, 13051-13060.
(32) Moghadassi, A. R., Rajabi, Z., Hosseini, S. M., Mohammadi, M., Preparation and Characterization of Polycarbonate-Blend-Raw/Functionalized Multi-Walled Carbon Nano Tubes Mixed Matrix Membrane for CO_2 Separation. Separation Science and Technology, 2013, 48, 1261-1271.